Reliability Analysis of Railway Concrete Bridges using Expert Judgment Studies

S. Aggarwal

TU Delft

Reliability Analysis of Railway Concrete Bridges using Expert Judgment Studies

by

S. Aggarwal

to obtain the degree of Master of Science
at the Delft University of Technology,
to be defended publicly on 18th December 2018, 13.00 .

Student number: 4626710

Thesis committee:	Dr. ir. O. Morales-Nápoles,	TU Delft,Supervisor & Chairman
	Dr. ir. M. A. N. Hendriks,	TU Delft
	Ir. G. Leontaris,	TU Delft

TU Delft

Abstract

New railway bridges for high-speed trains are being built in a many countries around the world. In addition to the construction of new bridges, existing bridges are ageing. These two factors make the assessment of railway bridges essential. The bridges are designed considering certain predefined reliability criteria to account for the variability in load and resistance. However, for the assessment of these bridges, a probabilistic analysis of the structure in the presence of uncertainties is recommended. This thesis presents a probabilistic analysis of a railway bridge based on a case study of a newly constructed bridge. In the analysis performed, uncertainties in concrete material properties are incorporated. Given the unavailability of measured data in the location of bridge construction, expert judgment elicitation is carried out to estimate for the uncertainties in loading conditions of a train. Further, these uncertainties are incorporated in a finite element analysis to estimate the bridge response in the form of shear force and bending moment. The variables corresponding to the maximum shear force and the maximum bending moment, as well as the loading conditions and the material properties, are then merged into a Non-Parametric Bayesian Network. Conditionalization of the developed Bayesian networks is carried out to draw inferences on the bridge response when evidence on load or material properties is known. It is shown that expert judgment elicitation can be applied for risk assessment of railway bridges. Further, the developed Non-Parametric Bayesian network can be used to estimate and update the probability of failure. Improvements to this study can be made by updating the probability of failure in the event of an earthquake.

Acknowledgement

I would like to thank my supervisor Dr. Oswaldo Morales-Nápoles for his support and for providing me with all the resources that were needed during this thesis work. His enthusiasm while discussing a problem statement motivated me to take up this project and successfully carry it to the end. His daily supervision helped me during each stage of this thesis project. I am truly glad to have a supervisor like him.

I would also like to thank my committee member, Dr. Max Hendriks for answering my questions related to the modelling of the structure. I am also thankful to him for assessing my work and evaluating my report.I am thankful to George Leontaris, who is also my committee member for helping me understand the concept of Expert Judgment Studies, and also providing me with his MATLAB code for deeper analysis.

I would like to thank Dr. David Delgado from the Universidad Autónoma del Estado de México (UAMEx) for his guidance and support right from the beginning of the thesis. His contribution in also conducting the Expert Judgment is extremely valuable to me. I am also thankful to Miguel Lugo from UAMEx for the information he shared with me that helped me structure my thesis and also for sharing the results of his experimental work that has been used in this thesis.

ProRail has generously provided the Weight-in Motion data which is also used in this research. I would like to thank Juliette van Driel and Maurice van Olderen, both working at ProRail, for their efforts of supplying the data to me. I would like to thank Thijs Roeleveld and Joost Houtenbos , both working at Ricardo Rail for helping me in reaching out to ProRail.

Moreover, I would like to thank Dr. K. Anupam, for his constant guidance and support at TU Delft. His encouragement kept me motivated and confidence in my endeavours at TU Delft.

I am also grateful to my friends Akshay, Prajakta, Rucha, Nilaya, Arjun, Ajinkya, Kshiteej, Srinidhi for supporting me throughout the two years of my masters at TU Delft. Furthermore, I would like to thank friends in India, Rahul, Sargam, and Shobhit for their constant encouragement.

Most importantly, I would like to thank my parents and my sister for supporting me in all the situations. Their trust has always motivated me to give my best performance.

Contents

1 Introduction

1.1. General Overview

The growth of economies and increase in population calls for improvement in the transportation infrastructure in the world. In response to this growing need, many major developing economies in the world are building railway infrastructure for high-speed trains. Several countries are also introducing rail passenger trains on long span bridges. Moreover, there is a need to ensure safety concerning the superstructure and substructure of ageing bridges. The rapidly changing needs of the economy and the constant requirement to ensure safety is making reliability assessment of bridges under railway loading essential.

For design of bridges, the design codes incorporate certain factors to account for safety which are applied to loads as well as resistance models. These factors of safety are defined to account for variability in the applied loads and resistance offered by the structure. However, to perform a reliability assessment of the bridge is a probabilistic analysis in the presence of uncertainties is recommended. This comprehensive approach gives the structural engineer a deeper insight into the factors influencing structural reliability.

For the reliability of a railway bridge, trainloads can be treated as moving loads on the bridge. However, to derive the uncertainty in the train loads, a reliable source of measured data is required. However, such data does not exist for all railway systems in the world, and only a few countries have made recent progress in measuring the axle load data for railway systems. Unavailability of measured data for different variables is a limitation in civil engineering due to cost or technical difficulties. To overcome this limitation, a structural approach, called *Structured Expert Judgment* has been proposed by several researchers with the aim of treating expert opinion as scientific data. In this research, this methodology is introduced for probabilistic analysis in structural mechanics.

Nowadays, with advanced computational tools available, Finite Element (FE) Analysis of different bridge configurations can be performed. FE approach also offers the advantage of assessing the most critical section in the structure more thoroughly. Usually, a simply supported bridge is modelled to perform bridge reliability. Hence in this research, a simply supported bridge is modelled to perform further reliability assessment.

1.2. Aim of the Research

This research intends to perform a probability analysis of a concrete bridge under railway axle load and material uncertainty using expert judgment studies.

In order to fulfill the aim of the research, the following objectives and research questions are defined as follows:

- Expert Judgment studies
  - What are the results of the expert judgment elicitation to estimate the axle load uncertainty in a train running at a velocity of 160km/h?
  - What is the level of similarity between expert judgment elicitation performed in Mexico to the axle load measurements in the Netherlands?
- Finite Element Modeling of the bridge
  - How to model a simply supported bridge using a finite element methodology to perform computationally efficient large number of simulations for reliability analysis?
- Probabilistic Analysis of the bridge
  - How to develop a Non-Parametric Bayesian Network for a simply supported bridge model with load and material uncertainty?
  - What are the effects of conditionalization on the bridge response ?
  - What is the probability of failure of the bridge?

1.3. Research Methodology

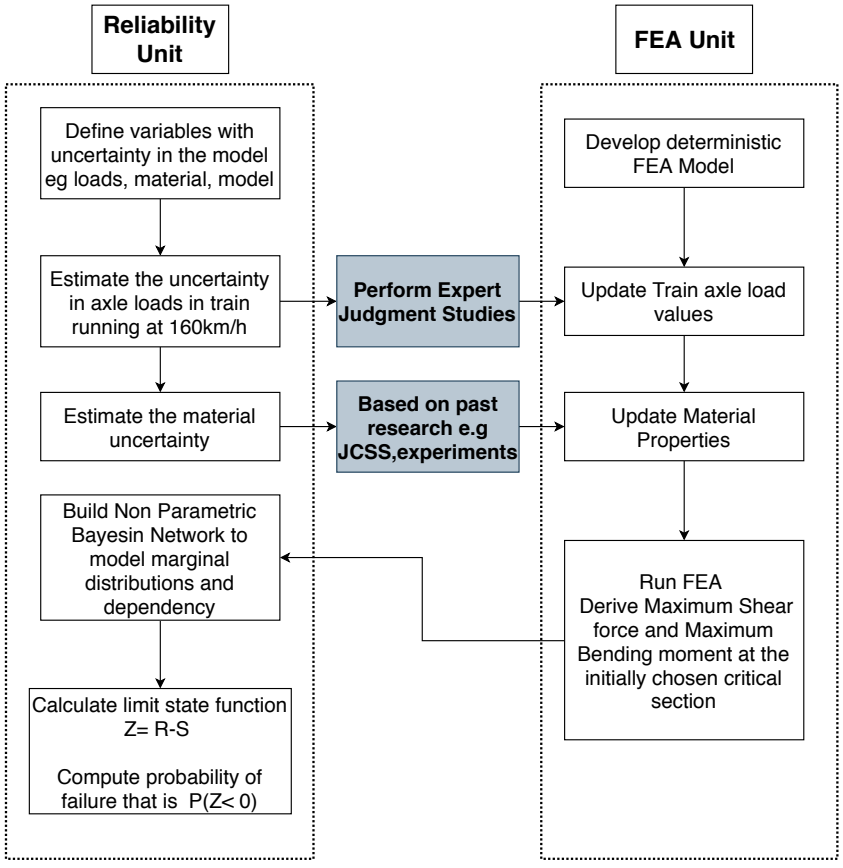

Figure 1.1: Research Methodology

1.4. Thesis outline

This thesis is structured such that there is a comprehensive understanding and description of the research objective and questions.

- Chapter 1 discusses the general overview, research objective and questions and the overall methodology followed
- Chapter 2 contains necessary background information on material uncertainty, expert judgment studies, finite element modelling of the bridge, and lastly existing guidelines on finite element reliability analysis.
- Chapter 3 gives a detailed description of the expert judgment methodology and results elicited in this research.Appendix B contain necessary questionnaire for the understanding of this chapter.
- Chapter 4 presents a description of the case study of the bridge considered in this research. Finite element modelling details of the bridge are also discussed in this chapter
- In chapter 5, a probabilistic analysis of the bridge is presented using NPBN
- The final chapter 6 closes this research with conclusions and recommendations

2

Literature Review

This chapter gives a background information on existing models and available understanding on the different components used in this research. In section 2.1,the uncertainty modelling in a structural system is described. section 2.2 discusses the concrete bridge modelling techniques proposed by researchers over the years. In section 2.3, available literature on a combined study of reliability methods and finite element modelling is presented. The last section, section 2.4, summarizes the findings from the literature and its application in this research.

2.1. Modeling of Load and Resistance Uncertainty

To assess the reliability of a structural system, a probabilistic analysis is performed. For probabilistic analysis of existing structures, knowledge of the load and resistance models is required. To model the uncertainties involved in material properties, dimensions, and methods of analysis (discussed in section 2.3), resistance can be treated as a random variable [65]. Furthermore, the basic load combinations of any structural analysis include dead load, live load and dynamic load (ignoring environmental loads, additional loads due to deformations, etc). This research discusses only the first two types of combinations since the dynamic load analysis can be avoided, for the given speed and bridge configuration. The following section presents the available literature on some of the methodologies that can be used to develop statistical models for these load and resistance components.

2.1.1. Load Uncertainty: Discussing the application of Expert Judgment Studies

Live load on a railway bridge comprises of a range of forces produced by moving vehicles. Usually, the static and dynamic components of the live loads are modelled separately. Several parameters including the span length, truck weight, axle loads, shaft configuration, position of the vehicle on the bridge (transverse and longitudinal), beam spacing, and the stiffness of structural members (slab and girders) influence the effect of the load on the bridge. These parameters primarily influence the static load of the vehicle on the bridge. Parameters influencing the dynamic component of the vehicular loads are not considered because the speed of the train is less than 200km/h and therefore according to the Eurocode 2004, the dynamic component can be neglected. One of the techniques of estimating uncertainty in the static load components is measuring Weight-in Motion (WiM) using sensors (described in Appendix D). In the event of unavailability a similar data recorded by sensors, this research proposes using Expert Judgment (EJ) studies to estimate load uncertainties. Detailed description of the methodology is presented in chapter 3. The following section presents the background information on EJ studies, or in other words EJ elicitation.

Expert Judgment Elicitation has been practiced by engineers, scientists and decision makers over the past many years. They often come across situations when no relevant data is available due to cost, technical difficulties or the uniqueness of the situation. In such situations, expert opinion can be treated as one of the alternate source of data to model parameter uncertainties [22][45][81]. One of the earliest study that formalized EJ was performed by Commission et al.[19] for risk assessment of nuclear power plants. Most of the data used for the first extensive risk evaluation of chemical installations (Canvey Island 1978) came from expert judgments. Over the course of the years, the method

for elicitation and aggregation of individual experts' assessments improved and formalized. The first attempt of a structured and well-thought procedure for the whole expert elicitation process was done for the NUREG 1150 study (USNRC 1990) Cooke. Seven years later, guidance on uncertainty and use of experts (USNRC 1997) was published during which a study on expert judgment and accident consequence uncertainty analysis [30] began. The latter study led to the publication of *Procedures guide on structured expert judgment*[20]. In [21], Cooke mentioned about the development of a 'practical model with a transparent mathematical foundation' for expert judgment elicitation and aggregation, and also presented case studies of past EJ studies. Details of the models presented by Cooke are described later.

According to Clemen and Winkler [17], there are two available approaches for elicitation and aggregation of individual experts' assessment namely, behavioural and mathematical approaches. In mathematical approach, a single 'combined' assessment per variable is constructed by applying procedures or analytical models operating on the individual assessments. On the contrary, in behavioural aggregation, experts interact with the aim of achieving group consensus. The most popular behavioural methods are the Delphi technique and the Nominal Group. As reported by Ouchi [68], one of the disadvantages of behavioural methods is that there are no formal rules to reconcile differences when experts are unable to come to a consensus. Cooke points out that experts become overconfident during group interaction leading to more extreme probability estimates. Generally, mathematical approaches are perceived to give more accurate results in aggregating expert opinions [17]. In this research, the Cook's method which is based on mathematical approach is used.

In Delft University of Technology, several studies representing more than 80,000 elicited questions have been performed with the aim of developing methods and tools to support the formal application of expert judgment. Applications were made in a variety of sectors, such as nuclear applications, the chemical and gas industries, toxicity of chemicals, external effects (pollution, waste disposal sites, inundation, volcano eruptions), aerospace sector and aviation sector, the occupational sector, the health sector, and the banking sector [31]. The techniques as developed can be applied to give quantitative assessments or qualitative and comparative assessments. From quantitative assessments, nominal values of parameters can be derived for practical applications. From qualitative and comparative assessments, ranking of variables can be derived.

Expert Judgment elicitation is performed for estimation of 'uncertainty' and 'dependence'. The methodologies to elicit uncertainty is different, though based on similar techniques, from methodologies to elicit dependence. 'Uncertainty' can be defined as something that is not known or certain. One of the ways to become certain is by observation. Dependence in a probabilistic sense can be defined as the influence of event A on event B. More details on dependence is given in section 3.1.2. For an uncertainty or dependence model to be robust, a structured approach to eliciting variables of interest is recommended [45]. This is referred to as Structured Expert Judgment (SEJ). SEJ formally refers to the deliberate effort to subject the entire process of elicitation to transparent methodological rules, with the goal of treating expert judgments as scientific data in a formal decision process. More details about SEJ can be found in [41], [62], and [21].

Eliciting Uncertainty

In [22], Cooke and Goossens discuss four models for combining expert opinion for uncertainty elicitation; Bayesian Combination of expert assessments; Non-Bayesian combination of expert distributions; Linear Opinion pools; Performance based weighting – the classical model. The Classical model [21] is easy to apply, easy to explain and does not use equal weighting (see chapter 3). Hereafter all the discussion is based on the classical model since it is used in this research for eliciting uncertainty. The Classical Model, a performance based weights use two quantitative measures of competency : Calibration and Information [5]. Calibration measures the statistical likelihood that an expert's assessment corresponds to those of experimentally measured values. Information measures the degree to which an expert's uncertainty distribution is concentrated that is how far are the 5th and 95th quantile assessments. Seed variables are used to measure the calibration and information. Seed variables are based on data available from experiments or measurements (refer Appendix B for more details). A closed source software EXCALIBUR [1] has been used for the analysis and aggregation of expert judgments for majority of past studies. Recently, a number of cross validation studies have been conducted using Eggstaff's MATLAB code [24] [18]. In a recent research development at Delft, Leontaris and

[1] EXCALIBUR is freely available at http://www.lighttwist.net/wp/excalibur

Morales-Nápoles developed a MATLAB toolbox, called ANDURIL[2], that consists of different functions and supports the majority of the features of EXCALIBUR. This toolbox facilitates higher accessibility to researchers of the current methods and gives them an opportunity to explore different approaches or extensions to current methods.

Eliciting Dependence
According to [81], there are three approaches for dependence modelling. The first approach is applicable to Bayesian (belief) Networks (BNs), copulas, parameterised families of multivariate distributions and Bayes Linear methods, in which the dependence between stochastic variables are modelled directly. In the second approach, auxiliary variables which are not a part of the model variables, are also included for the ease of quantification. The third approach, uncertainties are assessed on some output variables to calibrate uncertainties on the randomly distributed variables. Overall, there is limited guidance on eliciting dependencies [81], however some progress has been made on BNs (chapter 3). Therefore in this research, BNs have been used and discussed hereafter. To elicit the dependence structure between variables, methods have been proposed to derive rank correlations between variables [20] [17]. Most of the proposed methods are attached to bivariate dependencies. According to them, The experts are either asked for dependencies directly or indirectly (e.g. a conditional probability of exceedance, a probability of concordance, a probability of discordance). Though it is not decisive, however, few previous experimental results indicate that obtaining bivariate dependence by using the direct method is more accurate [17].

The process of eliciting multivariate dependence is more complex than that for bivariate dependence. Hence a flexible modeling tool is favoured to elicit multivariate dependence. Non-parametric Bayesian network (NPBN) is one of such tools to represent multivariate dis- tributions.Hanea et al. [33] has discussed few applications of NPBN for dependence modeling. NPBNs are quantified in terms of univariate marginal distributions, rank correlations, and conditional rank correlations. The univariate marginal distributions can be elicited from experts using the methods described in earlier section, including the classical method, in the event of unavailability of relevant data. To elicit dependence under such a situation, rank correlations and conditional rank correlations can be assessed from experts [33]. Similar to bivariate dependence, the experts can be asked for rank correlations directly or indirectly. In one of the previous studies, conditional probabilities of exceedance was elicited [56] and in the other, ratios of rank correlations were elicited [61]. It is still inconclusive whether the experts can more accurately estimate conditional rank correlations through estimates of conditional probabilities of exceedance or through directly estimating bivariate rank correlation coefficients. Another interesting topic of discussion is the measure of 'calibration' or accuracy of experts multivariate dependence assessments. To the best of the author's knowledge, there is currently only method of estimating calibration score, for multivariate assessments [58]. The proposed method calculates the calibration score, *dCal* by using the *Hellinger distance* (see chapter 3 for more details). Whether some other measures of distance in Gaussian distribution, including those given by [4], have similar characteristics to those of *dCal* is subject to future research.

2.1.2. Material Uncertainty

The inputs required for the resistance model in a probabilistic assessment of a structure are usually material uncertainties and geometrical uncertainties. Factors influencing the material uncertainties, that is, concrete uncertainties for this research, along with various methodologies proposed in the past to model them are discussed here.

Uncertainties in concrete properties are reported in the literature by several researchers Rackwitz[73], Caspeele [15], Vrouwenvelder [80],etc. and the Probabilistic Model Code developed by Joint Committee on Structural Safety summarized most findings. The deviation in material properties can be related to variability in the following [84] - Concrete composition (ratio of water and cement); material properties of cement, aggregate, purification of water. Other factors including operating conditions (mixing technology, transportation, curing, etc.); testing norms; maintenance conditions and environmental factors also influence the concrete material properties [84].

In general, in a probabilistic risk assessment of a structure, uncertainties in strength of materials are represented by models in terms of probability distributions e.g. Gaussian distribution. According to

[2]Available at https://github.com/ElsevierSoftwareX/SOFTX_2018_39

Rackwitz [73], the uncertainties in strength of materials can be broadly classified into two types - the first accounts for spatial or time-dependent variations in material properties in a given structure and can be modelled using random field approach as proposed in Probabilistic Model Code [44]; the second type of uncertainty neglects in-homogeneity and is expressed in terms of probability distribution. Usually, the latter type of uncertainty is preferred for advanced probabilistic analysis and for assurance of structural reliability. It is noted here that in this research, only the second type of uncertainty is considered.

In order to quantify the concrete uncertainties, one of the first probabilistic model is reported by Mirza et al. [55] based on experiments in United States, Canada and Europe. Later on, in [84], Wiśniewski et al. reviewed the existing probabilistic models for concrete according to which the model proposed by Joint Committee of Structural Safety [44] is considered to be very comprehensive. Assessment of material uncertainty, should ideally be made from experimental tests on large number of samples. However, in reality, only limited amount of results from experiments can be reported [26]. Compressive strength f_{co} of standard specimens (defined for cylinder of 300mm height and 150mm diameter) is considered as a reference property of concrete when tested according to standard conditions and aging period of 28 days (See ISO/DIS 2736 and ISO 3893). Other properties of concrete can be related to this reference strength according to [8] and are summarized in Table 2.1 .

Table 2.1: Concrete input values related to reference strength

	f_c (Mpa)	f_{ct} (Mpa)	E_c (Mpa)	ν
mean	f_{ck} +Δf	$0.3f_{ck}^{2/3}$	$E_{c0}(f_{cm}/10)^{1/3}$	0.15
cov	15%	20%	8%	-
distribution	lognormal	lognormal	lognormal	-

From Table 2.1, the mean values of of concrete properties can be computed based on the mean value of concrete compressive strength. However, the coefficient of variation and the distribution type for other properties of concrete are not computed from the properties of compressive strength. Therefore, even though the concrete properties are highly inter-correlated [84], they are not full dependent, that is, $\rho_{fc,Ec} \neq 1$. There is not enough literature evidence on the correlation between the properties of concrete, however, $\rho \sim 0.85 - 0.90$ is considered in this research.

2.2. Finite Element Modelling of Bridge

In this section, literature concerning the concrete slab-box girders-column arrangement is elaborated. The first part discusses the guidelines proposed by *Sustainable Bridges* project carried out in Europe. The second part of the section explains the methodologies proposed in the past for numerical modeling of the bridge.

Guidelines proposed by Sustainable Bridges project

In order to fullfil the present and future demands on improved capacities for the passenger and freight traffic on the European railway network, a project called *Sustainable Bridges* was launched. The intention of the project was to develop a toolbox of new systems and methods for assessment, strengthening and monitoring of the European railway bridges [11]. Certain guidelines on modelling and assessment of load and resistance are given in [74], [14], [72]. These guidelines have been adopted in this research for modeling the geometry of the bridge and hence has been elaborated as follows.

Table 2.2: Suitability of models for the analysis of global effects (usually longitudinal analysis of the bridge deck)

Longitudnal Configuration	Initial Assessment	Intermediate Assessment	Enhanced Assessment
Beams*	beam	beam, grillage	beam, grillage, FEM
Frames	2-D frame	2-D or 3-D frame	3-D frame, FEM
Arches	2-D frame	2-D or 3-D frame	3-D frame, FEM
Trusses	2-D frame	2-D or 3-D frame	3-D frame, FEM

Note: * this includes box girders, slabs, slab on beams, trough bridges, etc.

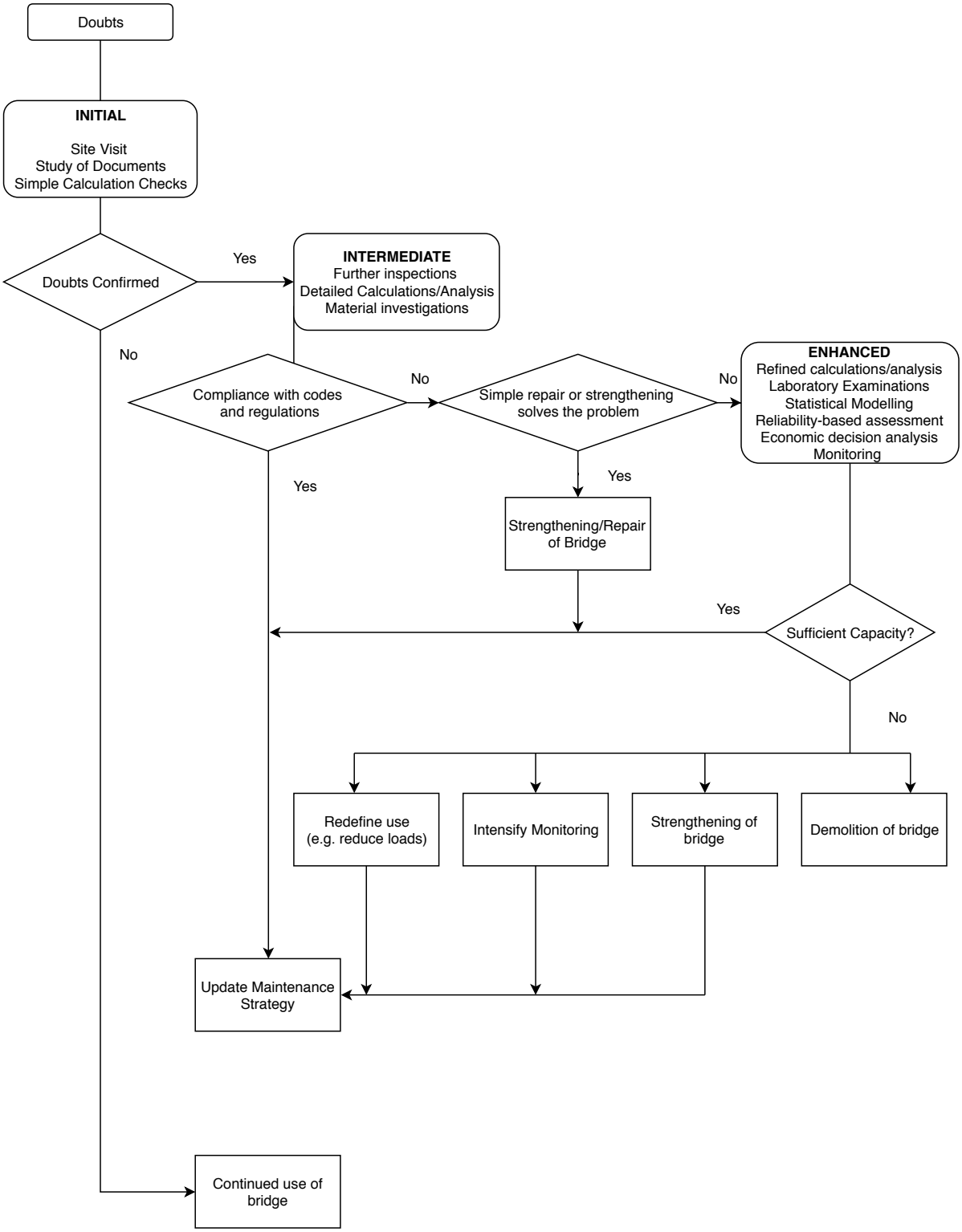

Figure 2.1: Flow diagram for reassessment of existing bridges [29]

The structural analysis of the bridge is performed to determinate the internal forces, moments, shear stresses, strains and deformations. Material resistance is considered to perform capacity checks with respect to cross-sectional forces and moments under dead and live loads. The modeling of the bridge geometry can be idealized based on the methodologies explained above. For idealizations on material geometry, four different methods (According to CEN2004a and CEN2004b) can be adopted:

- Linear elastic analysis - Can be used for the verification of Serviceability Limit State(SLS) as well as Ultimate Limit State (ULS).
- Linear elastic analysis with limited redistribution - Can be used for the verification of ULS. It gives a more realistic distribution of stresses than Linear Elastic analysis. It can be used for probabilistic approaches.
- Plastic analysis - It is an efficient method for verification for all bridge types in ULS.
- Non-linear analysis - It takes into account both material (cracking, buckling, etc.) and geometric non-linearity. The method can be used for all bridge types in SLS as well as ULS.

As reported in [13], there are many levels of modelling complexity for trains moving over the bridges, depending on the assumptions made (Linear, Non-linear, Plastic) and the simplifications considered . In addition to these complexities, the dynamic effects of high-speed railway lines play an important role in the total load effects developed in the structure during a vehicle passage [13].At present, Eurocode 1 2004 contains the design requirements related to the dynamics of railway bridges. According to the Eurocode 2004, it is not always necessary to perform a dynamic analysis. Section 6.4.4 of Eurocode 1, part 2 provides the criteria to determine whether a static or a dynamic analysis is required. As stated earlier, according to the Eurocode requirements, a dynamic analysis is not necessary.

Numerical Modeling of the Bridge

The equation of motion of a bridge modelled in FE under a series of time-varying forces can be expressed by

$$[M_b]\ddot{u}_b + [C_b]\dot{u}_b + [K_b]u_b = f_b \tag{2.1}$$

where

$[M_b]$ = global mass matrix,kg

$[C_b]$ = global damping matrix,Ns/m

$[K_b]$ = global stiffness matrix,N/m

$[\ddot{u}_b]$ = nodal acceleration matrix, m/s^2

$[\dot{u}_b]$ = nodal velocity matrix, m/s

$[u_b]$ = nodal bridge displacements and rotations, m/s^2

$[f_b]$ = interaction forces between the train and the bridge acting on each bridge node at time t

The matrices, $[M_b]$, $[C_b]$ and $[K_b]$ in Equation 2.1 depend on the type and number of elements used in modelling the bridge deck and columns. FE packages like ABAQUS, LS-DIANA,ANSYS, NASTRAN, etc. could be used to construct these models. According to [9], ABAQUS [39] has the capability to represent the behavior of a realistic structure and to predict deflections, strains, and stresses while minimizing unnecessary complexities. These advantages along with those mentioned in Table 2.6 are the reasons for favouring ABAQUS in this research. More details on basic concepts of FE methodology is given in Appendix C.

There are four generally accepted techniques of FE modeling of bridge - (a) 1D Beam model; (b) 2D Plate modeling (c) 2D grillage model [83] (d) 3D FE model. The 1D beam model is an approximate analysis model according to Aashto[2] to consider in-plane shear and bending moment. For bridges with long spans, the whole bridge can be considered to be a 1D beam model. This method can be adopted for determining the shear force and longitudinal moments. The dead loads can be approximated by the corresponding mass density and geometry. However, live loads are maximized by loads' lateral position and girder influence lines, which are called live load envelopes. Many bridge codes,treat the longitudinal and transverse effects of wheel loads as uncoupled phenomena for the ease of design. The design live-load moment due to train loads is first estimated by obtaining the maximum train moment on a single girder. This maximum single girder moment is then multiplied by a factor to obtain the design moment. This factor is referred as the live-load distribution factor [7].

Grillage bridge models (see Figure 2.2) have been used by bridge engineers for many years. This method was pioneered by Lightfoot and Sawko [52]. It is easy to comprehend and use, relatively inexpensive and has given accurate results in the past for a wide variety of bridge types [32]. In *Bridge Deck Behaviour* [32], guidelines of modelling diverse bridge types have been given. The general idea of this methodology is to represent the deck by an equivalent grillage of beams. A grillage mesh can be seen as a skeleton mesh of 1-D beams in 'x' and 'y' directions. In Figure 2.2, an example of the model is shown where M_x is bending moment about x axis for beam oriented along x and similarly M_y is bending moment about y axis for beam oriented along y. The girders are modelled as longitudinal beams (in Figure 2.2 along x direction) with longitudinal stiffness and the traverse beams (in Figure 2.2 along y direction) are modelled to introduce transverse stiffness. Ideally, the grillage mesh generated should be such that the internal forces, moments and vertical deflections in any grillage beam should be equal to the resultant of the stresses on the cross section of the part of the slab the beam represents [32]. Despite its wide usage, grillage modelling has certain drawbacks. The internal forces are not continuous at grillage nodes,hence it is difficult to ensure the same twisting curvature in two perpendicular directions (k_{xy}=k_{yx}). Other aspects which are ignored by the grillage method are effects of construction sequence, reinforcement modelling, analysis of secondary effects, in-plane effects and nonlinear response of deck [69].

Plate bridge models (see Figure 2.3) have been investigated by several researchers [67] [48] [38],][85] [12] [29]. These models are based on the Kirchhoff plate theory. The Kirchhoff plate theory assumes out of plane strains to be negligible. Kinematic, constitutive and equilibrium equations can be used for every plate element to calculate the moments which are shown in Figure 2.3 as M_x, M_y and M_{xy} acting on each face, and also to calculate shear Q_x, Q_y as shown in Figure 2.3.It is noted here that the

moments and shear forces are functions of the nodal vertical displacement and stiffness properties of the plate.

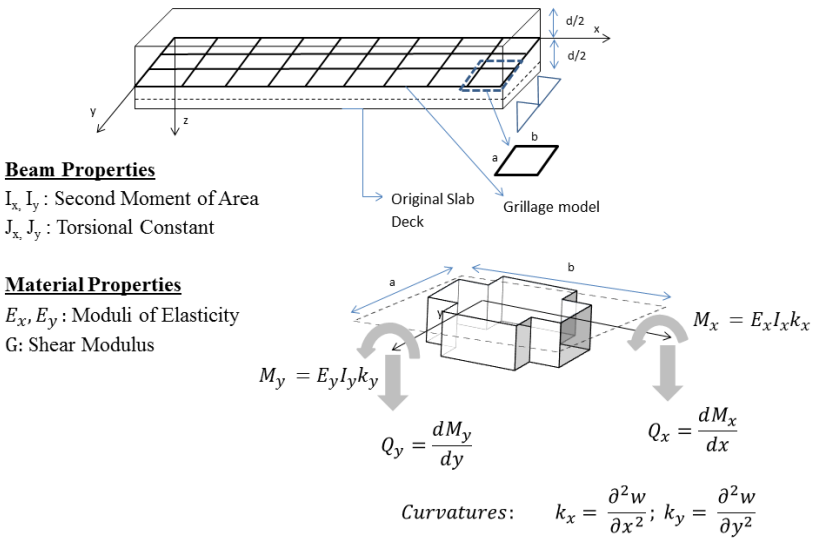

Figure 2.2: Grillage model of a bridge deck [29]

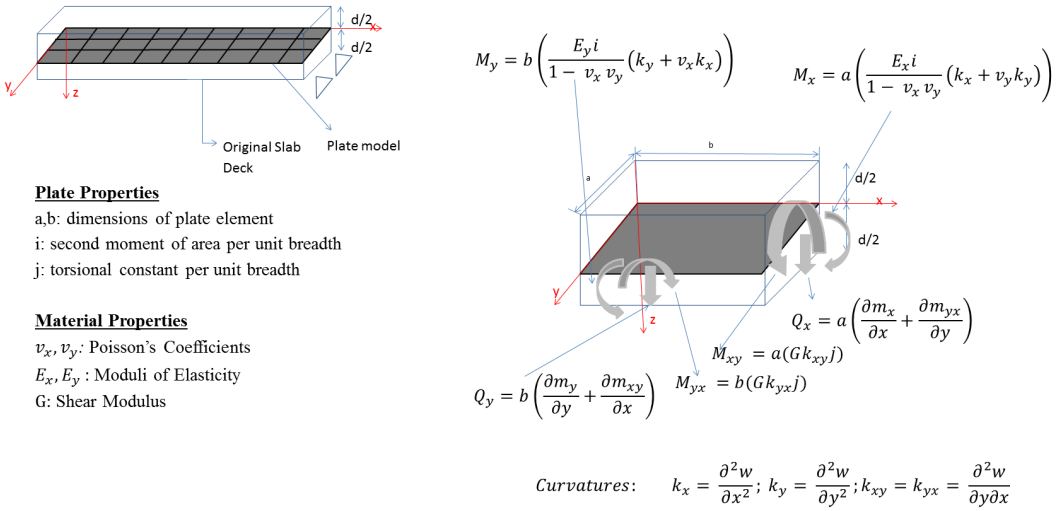

Figure 2.3: Plate model of a bridge deck [29]

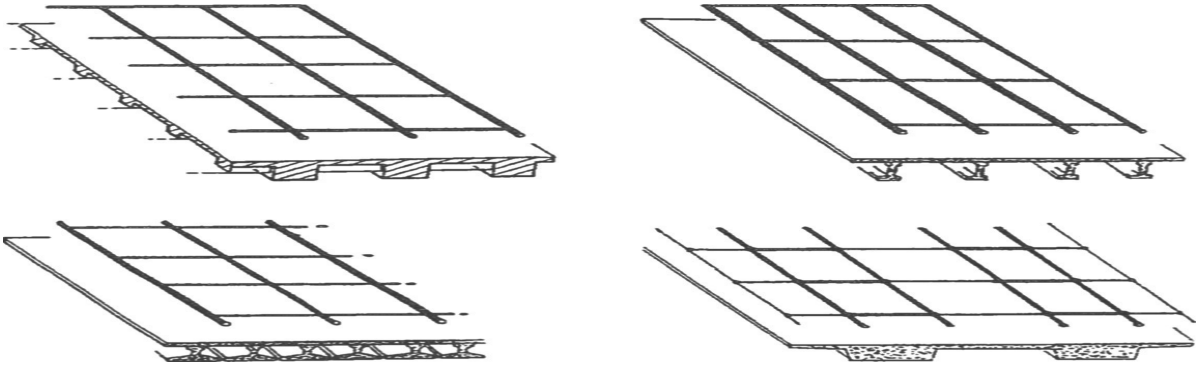

Figure 2.4: 2-D grillage meshes [32]

2.3. Finite Element Reliability Assessment

In order to predict the failure of a structure, uncertainty in material properties, applied loads, dimensions, etc. should be taken into account[78]. Based on the above section, it is clear that advances in FEA make it applicable to complex problems like bridges. To factor uncertainties in FEA it is recommended to perform probabilistic finite element analysis (PFEA), which is often termed as finite element reliability analysis (FERA) ([35] 2004, 2006,2007).

What is Finite Element Reliability Analysis?

The term finite element reliability analysis refers to a method which accounts for uncertainties in geometry, material properties and applied loads in a finite element model [6]. Such uncertainties should be modelled as random or stochastic fields. It is a perception that in some structures, the response sensitivity of the structures is associated with material properties or geometry of the structure. Therefore, even small uncertainties in these properties can effect the structural reliability. The underlying assumption in a structural reliability problem is that the structural is either in safe state or failure state.The boundary between these two states is known as the limit-state surface.

In finite element reliability analysis, the the problem is defined in terms of a set of random model variables x and a finite element model defined by response vector $u = u(x)$ for a given realization of x for k components. A set of continuous and differentiable limit-state function can be defined as $z_i(u(x)), i = 1, 2, ..., k$ where $z_i \leq 0$ indicates failure for the i^{th} component of the structural system. The failure domain is defined as the union of the component events such that the probability of failure is $P(\cup_{i=1}^{k} z_i) \leq 0$ [36]. To obtain these results by first order reliability method(FORM) and second order reliability method (SORM) (See Appendix A), a 'design point' has to be determined [23] on the limit-state failure surface. Finding the design point poses a constrained optimization problem. In the context of finite element reliability analysis, this means computing the finite element response sensitivities with respect to the model parameters [35].

System vs Member level assessment

Safety assessment of a bridge can be performed at two levels, system level or member level. In **member level assessment**, it is assumed that the failure of a member implies failure of the structural system. However, failure of one of the component/members of the bridge may or may not mean the collapse of the whole structure. This is because, most bridges consist of a system of interconnected components and members. Therefore, the reliability of a single member may or may not be representative for the whole bridge. Hence a **system level assessment** should also be performed. Since the research is performed in Europe, the safety assessment guidelines written in Eurocode are followed. The safety rules in the Eurocode [43] are based on a member level. Additionally, the partial factors provided in the Eurocode, are based on linear relation between the loads and the corresponding internal forces in the members.

Levels of approximation

Over the last few decades, the design codes have become increasingly complex, and are however still not sufficient to assess the existing structures. One of the recommended strategies to overcome this limitation is the use of levels-of-approximation(LoA) approach. This approach is recommended by

Muttoni and Ruiz [63] in the *fib* Model Code [8]. In this approach, a hypothesis is made depending on the level of the accuracy required. This hypothesis is based on the application of the use of the theories related to physical parameters in the structural system. In cases, where the required accuracy is not very high, a safe hypothesis can be adopted for simple and quick analysis. If the degree of accuracy is not sufficient for a given analysis, for example, design of complex structures, assessment of existing structures, etc., then the hypothesis can be refined for better estimates of the response.

In the Netherlands, the LoA approach is followed for the assessment of existing slab bridges. These levels are further elaborated as follows:

- Level of Approximation 1 : It is also called in Quick Scan method (Vergoossen et al., 2013). The results of shear stress is in the form of Unity Check that is the ratio of design shear stress over design shear capacity [50]. This method is similar to performing hand calculations based on design codes.
- Level of Approximation 2: In this level of approximation, a linear finite element model is analyzed to determine the shear stress distribution [50].
- Level of Approximation 3: To achieve higher accuracy and results closer to reality, non-linear finite element models are built and analyzed to determine the structural behaviour under applied loads. [50].
- Level of Approximation 4: Though the results of LoA 3 are generally sufficient, however in cases where estimation of structural capacity influences economic costs for example, strengthening in existing bridges, more refined analysis is required. For such analysis, LoA 4 is adopted [50].

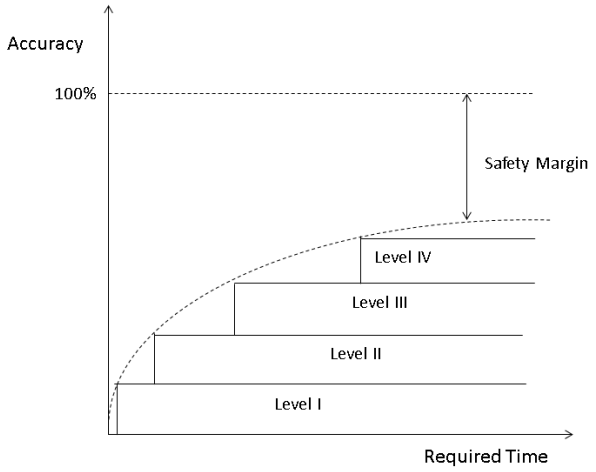

Figure 2.5: Representation of the increasing Levels of Approximation,[63]

In this research, a probability of failure of the structure (P_f) due to bending failure is estimated using probabilistic techniques. Although the above mentioned levels of approximation are defined for shear stress, they are extended for bending moment stress for this research.

Review on existing reliability-based methods

To assess the probability of failure of a bridge member in shear or bending, probability density functions of the applied loads, resistance models and material models have to be taken into account. In Probabilistic Model Code, developed by the Joint Committee on Structural Safety [44], recommendations on the probabilistic density functions for a reinforced concrete solid slab as well prestressed concrete are

given. These functions differ slightly from those given by Nowak and Szerszen [65]. In [49], Lantsoght et al. proposed that the probability density function of the resistance model of beam failing in shear is different from the case of concrete solid slab bridges subjected to concentrated wheel loads due to transverse load redistribution. Lantsoght et al. found that a conservative approximation of a resistance model can be made based on a lognormal distribution. In this research, this recommendation has been adopted and the material resistance model is based on lognormal distribution. More details on the material uncertainties is given in section 2.1.2.

Different geographies in the world prescribe different reliability index (See Appendix A) for the assessment of existing structures. These values are listed in Table 2.3. The target reliability values in Table 2.3 are prescribed for a reference period of one year at member level for ULS. In the Netherlands, Dutch Guidelines for the Assessment of Existing Bridges (RBK) have been developed. The reliability levels in RBK are from NEN-EN 1990:2003 [27] and NEN 8700:2011 [1], and are shown in Table 2.4. Moreover, Steenbergen et al. performed highway bridge assessment under full probabilistic analysis and derived partial safety factors for shear force assessment for given reliability indices (see Table 2.4). To the best of author's knowledge, such a study, however, has not been performed for railway bridges.

Table 2.3: Target reliability index different countries and International Bodies at member level for ULS [74]

Country	Canada	USA	Denmark	Europe	JCSS	ISO
(Reference)	(CAN/ CSA-S6-00, 2000 [16])	(AASHTO 1994 [66]); (AASHTO 2003 [3])	(NKB,1978)[64]; (Verjdirektor-atet 2003)[25]	(EN 1990, 2001)[27]	(JCSS, 2001) [44]	(ISO, 1999)[54]
Design	3.75	3.75	4.2	4.7	4.2	4.7
Assessment	3.25	2.5	4.2	4.3	-	4.7

Table 2.4: Different reliability levels for assessment of existing structures given in the Guideline for existing bridges (RBK)

Reliability level	β	Reference period
RBK Design	4.3	100 years
RBK Reconstruction	3.6	30 years
RBK Usage	3.3	30 years
RBK Disapproval	3.1	15 years

Note: All considered values are for Consequences Class 3 (highway bridges) built under the regulations for construction of 2003 or earlier

Over past few years, there is increased interest in reliability-based methods for bridges. Schlune et al.[75] showed that for beams subjected to combined shear and bending, the required reliability level (given in NEN-EN 1992-1-1:2005) is not achieved. Encouraged by similar findings, reliability-based methods for assessment of existing bridges also have been developed in different geographies. In Switzerland, a systems-level safety evaluation combined with nonlinear finite element analysis was developed [71]. In the United States,existing reinforced concrete bridges were also studied for shear capacity based on a probabilistic analysis [40]. Furthermore, reliability analysis for existing bridges under seismic events have also been studied following the 2011 Virginia earthquake [46]. Procedures on linking non-destructive testing results with probabilistic analysis methods have been developed in Germany [10] .

Based on the review of existing models and research in reliability-based assessment of existing bridges, variation in the safety philosophy is observed. For the design of new bridge, the uncertainty in structural resistance is associated with material uncertainty; geometrical uncertainty and method of analysis (level of approximation) [65]. For the assessment of an existing bridge, according to the ideology followed in the Netherlands, the geometric properties are not treated as random since the structure has already been built [76], and the geometrical uncertainties are ignored. On the contrary, in North America [79],the uncertainty on the geometric properties is fully modelled.

Existing software and limitations
The purpose of this section is to describe the existing computational tools available to perform reliability analysis in finite element framework. To the best of author's knowledge there are limited software platforms available that include in its interface both finite element method and reliability analysis. There are currently two available alternatives listed as below:

- Combine a general purpose FE analysis software, e.g., ABAQUS, with an existing reliability platform, e.g., NESSUS/ISIGHT
- Using object oriented programming language e.g. Tcl, to write one's own FEA program, e.g., OpenSees

The advantages and disadvantages between the two given alternatives are listed in Table 2.5.

Table 2.5: Comparison between the two computational approaches to perform FERA [6]

Software	Advantages	Disadvantage
FEA Software e.g. ABAQUS	- Ease of Use - Graphical User interface	-License Cost -Linking between various platforms e.g. ABAQUS with ISIGHT or ABAQUS with Matlab
FEA program e.g. Opensees	-Flexibility to program different reliability algorithm e.g. FORM, SORM	-Knowledge of advanced programming

In FE program approach, there is currently one popular open source option, OpenSEES, that combines FE analysis and probabilistic methodology. Further documentation on the program can be found online[3]. However, there are many commercial general purpose software available for FE analysis. During the past decades, these software have undergone improvements to apply the best known models describing behaviour of materials, structural elements etc. into numerical finite element code. The most popular commercial software along their main for nonlinear analysis of the structures are given in Table 2.6. This serves as a guideline for this research to favour ABAQUS amongst available FEA software.

Table 2.6: FEA software and their features for non-linear analysis

FEM Software	Features related to nonlinear modelling				
	Non linearity of steel	Non linearity of concrete	Tension stiffening	Time dependent effects	Buckling
ATENA	yes	yes	yes	yes	yes
DIANA	yes	yes	yes	yes	yes
ABAQUS	yes	yes	yes	yes	yes
ANSYS	yes	yes	yes	yes	yes
NASTRAN	yes	Limited	Limited	yes	Limited
PERMAS	yes	Limited	Limited	yes	Limited
SOLVIA	yes	yes	yes	Limited	yes
LUSAS	yes	yes	yes	yes	yes
TDV	yes	yes	Limited	yes	yes

[3] http://opensees.berkeley.edu/

2.4. Conclusions

The key findings from the literature review reported is summarized as follows. To perform a probabilistic assessment on a structure, load and resistance models can be built using random distributions of variables. In the unavailability of measured data, expert judgment studies can be performed. In addition, the expert judgment elicitation can be performed for eliciting both uncertainty and dependence following a structured approach. However, the methodologies for assessing the expert performance are different. Further, factors influencing material uncertainty are widely studied and a log-normal distribution for concrete properties has been proposed.

The finite element modeling of a concrete bridge can be performed with four approaches - 1D Beam model, 2D plate Model, 2D grillage Model, 3D FE model. 1D beam model is the least accurate and computationally most favourable approach. 3D model on the contrary is computationally most intensive and also most accurate. An favourable level of accuracy can be achieved using 2D plate model or 2D grillage model. Further, depending on the level of approximation which can be accepted for the analysis, a suitable modelling technique can be chosen. It is observed that there is a variation in the safety philosophy followed by different countries and codes. Furthermore, all countries do not treat all properties of the bridges as uncertain variables.

Finite element reliability analysis of a bridge required computational tools that can combine reliability analysis with finite element framework. FEA programming and combining FE software with a reliability platform, are two approaches that are available currently to perform a FERA.

3

Expert Judgment Elicitation

Expert Judgment study is undertaken to elicit uncertainty and dependency for variables for which measured or historical data is unavailable. In this section, the methodology of the structured expert judgment is explained, followed by a discussion on the elicited variables. Thereafter, quantification of expert opinion based on performance measures is discussed. The expert judgment questionnaire developed for this research is given in Appendix B.

3.1. The Methodology

Expert Judgment Elicitation is not a new practice in science and technology. Further, to treat expert opinion as reliable and robust data, a formal, a structured approach is followed. This is known as Structured Expert Judgment. As introduced in chapter 2, there are different techniques to quantify uncertainty and dependency. In this study, uncertainty is estimated using the Cooke's Classical Model which is described in section 3.1.1. Dependence elicitation and quantification technique is explained in section 3.1.2.

3.1.1. Eliciting Uncertainty

The Classical Model used in this research assesses uncertainty in the form of probability distributions. The differentiating feature of the Classical Model is that it combines the expert opinion based on a performance-based weighted-average model. In order to assess the experts' performance, two measures, calibration and information scores are used. Detailed explanation is provided in subsequent sections.

At TU Delft, an approach to implement Structured Expert Judgment using the Classical Model has been developed which is discussed as follows [5]:

- Multiple experts are selected. According to Cooke and Goossens [22], the minimum number of experts to be assessed is four. The number of experts in this research is 7.
- Experts are individually asked questions regarding the uncertainty over the result of possible measurements or observations. The variables over which uncertainty is elicited is within the domain of expertise of the experts. These variables are called the **target variables**. The experts give their subjective uncertainty distribution in predefined quantiles in a continuous range. Typically, 5^{th} , 50^{th} and 95^{th} quantiles are elicited.
- The experts are asked for their opinions on uncertainty over variables, the true values of which are known or will be known to the analyst but remains unknown to the experts at the moment of elicitation. These variables are called the **seed variables**.
- The experts are treated as statistical hypothesis and are scored based on their calibration and information. The calibration score of each expert is derived using expert's belief on seed variables.
- A different weight is assigned to each expert based on the calibration score provided he/she has a score higher than a threshold value. A combination of expert assessment is prepared using weighted average pooling.

The Classical Model :A brief description

In continuance of the approach to implementing the Classical Model described above, this section defines the basic tools which are used in the Classical Model to measure and combine the experts' assessment.

Calibration

In simple terms, calibration measures the extent to which an experts' assessment is representative of the uncertainty in the variables. Thus, calibration questions are used to define an indicator to assess the validity of the hypothesis that an expert's uncertainty assessment will represent true value for unknowns. Expert Calibration is done from expert opinion on the seed variables described above. Assuming there are E experts, $e = 1 \dots E$, and each of them answers N seed variables and N_1 target variables. Both seed and target variables are assessed for three quantiles that are 5^{th}, 50^{th} and 95^{th}. More quantiles can also be assessed from each expert, however, in this research study only these three quantiles are considered. Thus, for each question there are $j = 1 \dots 4$ interquantile bins which in this case are $(0; 0.05], (0.05; 0.5], (0.5; 0.95], (0.95; 1.00)$. the probability vector p is:

$$p = \begin{pmatrix} 0.05 \\ 0.45 \\ 0.45 \\ 0.05 \end{pmatrix} \tag{3.1}$$

The empirical version of p for expert e, is given by $s(e) = (s1 \dots s4)$. For N seed variables, there are $x = x_i \dots x_N$ true realizations. Each of these realisations must be in one of the quantile bins assessed by the expert. Then, for an expert e, $s_j(e)$ is equal to the number of realisations of seed variables falling in the jth inter-quantile assessed by expert e divided by the total number of seed variables.

$$s_1(e) = \frac{Number\ of\ realizations \leq 5^{th}\ quantile}{N} \tag{3.2}$$

$$s_2(e) = \frac{5^{th}\ quantile < Number\ of\ realizations \leq 50^{th}\ quantile}{N} \tag{3.3}$$

$$s_3(e) = \frac{50th\ quantile < Number\ of \leq 95^{th}}{N} \tag{3.4}$$

$$s_4(e) = \frac{Number\ of\ realizations \geq 95^{th}\ quantile}{N} \tag{3.5}$$

The experts exhibit their uncertainty assessment skill by the agreement of their vector $s_j(e)$ with the vector p. Only assessing the true value of the seed variables is not enough. To be a good uncertainty assessor, one's assessment should capture the true value in one's different quantile bins.The relative information between p and $s(e)$ is given by

$$I(s(e)|p) = \sum_{j=1\dots4} \{s_i \cdot \ln \frac{s_j(e)}{p_j}\} \tag{3.6}$$

where

$I(s(e)|p) =$ relative information of distribution $s(e)$ with respect to p,$I(s(e)|p)$ is χ^2-distributed with 3 degrees of freedom in this case

If $s_j(e)$ is equal to p_j, then the natural logarithm will produce a value of 0, implying no relative information by between the expert's uncertainty assessment and probability vector p. It means that if one believed p then learns s, one would be surprised or disagree with the outcome.

Experts' assessments are treated as statistical hypotheses. The null hypothesis for each expert H_0 is that the inter quantile interval containing the true value for each variable is drawn independently from the vector p .

The calibration score is given by

$$C_e = P\{2NI(s(e)|p \geq r|H_0\} \tag{3.7}$$

where

C_e = Calibration score of expert, e

r = percentile of interest in the χ^2 distribution of interest

The calibration score $C(e)$ is the probability that a deviation at least as large as r could be observed on N realisations if H_0 were true. r is evaluated from $2NI(s(e)|p)$ for the data corresponding to a particular expert. An expert whose data for seed variables tests this hypothesis as completely true gets a score of 1. Therefore, the calibration score is defined in a range of $[0, 1]$ with 1 being the highest score and 0 being the lowest score. Scores close to zero indicate that it is unlikely that the expert probabilities are correct. Usually, the minimum score at which an expert's contribution is included is 0.05.

Information

Information score measures the degree to which the uncertainty distribution is spread out. The degree of concentration of the distribution is measured relative to a background measure which, in the Classical Model, is uniform or log-uniform distribution. To establish a uniform background measure, first an intrinsic range of $I = [q_5, q_{95}]$ is chosen such that q_5 is the least valued 5^{th} percentile of all experts uncertainties for a variable and q_{95} is the highest valued 95^{th} percentile of all experts uncertainties for a variable. While estimating q_5 and q_{95} for seed variables, the values of true realizations are also taken into consideration. This intrinsic range [q_5,q_{95}] is modified to a new wider range $I* = [q_l, q_h]$ where :

$$q_l = q_5 - k * (q_{95} - q_5)/100 \tag{3.8}$$

$$q_h = q_{95} + k * (q_{95} - q_5)/100 \tag{3.9}$$

A value of k is chosen by the analyst such that the range is neither too broad nor too narrow. In this research k=10% is chosen which is recommended by Cooke. Then, the information score is estimated as the average relative information with respect to the background measure of distribution $I*$. The Information score is computed per expert as

$$I_e = \frac{1}{N}\sum_{i=1}^{N}[\ln q_{h_i} - q_{l_i} + p_1 ln\frac{p_1}{q_{5,i} - q_{l,i}} + \cdots + p_4 ln\frac{p_4}{q_{h,i} - q_{95,i}}] \tag{3.10}$$

In Equation 3.10, background measure is applied as uniformly distributed. For a log-uniformly distributed background measure, the log of $q_{,i}$ would be used instead of $q_{,i}$. It is observed that the information score is not dependent on the realisations (other than being used when calculating the intrinsic range) and hence information score may also be computed for the target variables. This approach is commonly followed in the classical model and is implemented in EXCALIBUR[1].

Combined Score

A combination of the expert's uncertainty distributions is called *Decision Maker (DM)*. Each expert is given a weight based on their performance on assessment of the seed variables. This method of combination is called the performance-based weighed pooling or the *performance based DM*. Here, the performance score is calculated as the combined score which is the product of the calibration score and information score. Expert with higher score contributes more to the DM. Therefore, the decision maker is influenced by an expert who can better estimate the uncertainties in his/her field of expertise. It is important to note that statistical accuracy dominates informativeness, that is, a poor calibration score cannot be compensated by high information score. The weight of an expert is given by

$$w_\alpha(e) = Ind_\alpha(C_e) * C_e * I_e \tag{3.11}$$

where

Ind_α = indicator function

C_e = calibration score

I_e = information score

$w_\alpha(e)$ = weight of expert

[1]Originally developed at TU Delft, used for application of *Cooke's Classical model*, Lighttwist Software maintains EXCALIBUR now

Ind_α denotes an indicator function for the minimum threshold value (typically 0.05) of calibration score. This indicator facilitates selection of experts based on their expertise. If the expert score exceeds α, only then the expert is assigned a weight. In a linear pooling of item i for all experts, with the total number of experts E, let the decision maker assessment be denoted by $(DM_\alpha(x))$, then Equation 3.12 shows the weighted average method of calculating $DM_\alpha(x)$.

$$DM_\alpha(i) = \sum_E w_\alpha(e).f_{e,i} / \sum_E w_\alpha(e) \tag{3.12}$$

where

$f_{e,i}$ = expert e's probability density function for item i

In the performance-based DM, the value of α is chosen such that the calibration score of the DM is maximised. The weights in a *performance based DM* are constructed by a strictly proper scoring rule in an appropriate asymptotic sense, that is, experts receive their maximal expected long-run weight by stating their true belief.

The following methods can determine the DM weights:

- *Global Weight* : This method of weighing uses weights which are based on the performance of each expert. The weight for each expert remains the same for all items.
- *Equal Weight* : Weights are not based on experts performance, and every expert receives the same weight, $w_e = 1/N_E$, where N is the number of experts.
- *Item Weight* : Each item can have a different set of weights. It is based on the information score of all experts per item.

The *equal weight DM* system gives equal weights to all experts. Such a combination often gives unreasonably large confidence bounds when assessments are pooled together. The *item weight DM* system recognises the differential expertise of experts with respect to seed variables. If an expert has less knowledge about an item then choosing quantiles that are spread further apart which lowers the information score for that item. The global and item weight DM can further be optimised by numerical iteration on the calibration and information scores. As an alternative, the minimum allowable calibration score α could be increased.

Besides different methods of weighing, the classical method recommends two methods of scaling - uniform and logarithmic. It is recommended by Cooke to use logarithmic scaling when a range of values to be elicited for variables or its true realisation (in case of seed variables) spans over three orders of magnitude. In the case of log-uniform scaling, the experts' assessment are converted to log values, and the background measure for information score is also taken to be log-uniform. The scoring and combining principles in logarithmic scaling is the same as that of uniform scaling.

3.1.2. Eliciting Dependence

Two quantities A and B are independent if beliefs about A do not change when given information about B.In statistical sense,

$$P(A|B) = \frac{P(A \cap B)}{P(B)} \tag{3.13}$$

where

$P(A|B)$ = probability of occurrence of A given occurrence of B. If A and B are independent, then $P(A|B)$ = $P(A)$

$P(A \cap B)$ = probability of occurrence of both A and B

$P(B)$ = probability of occurrence of B

The theoretical background of the concepts applied in this section is given in section 5.1.

Bayesian Networks Bayesian Networks(BNs), which are popularly also known as Bayesian Belief Networks, Causal nets, graphical probability networks or simply BBN is an approach for graphical modelling of problems relating to uncertainty and probabilistic assessments. A detailed description of BNs is given in section 5.1.

Example : Consider the Figure 3.1 which consists of four variables with conditional correlations. During the elicitation, the experts are asked for certain probabilities :

Suppose X_2 is observed to be greater than its respective median value, what is the probability that X_1 is also observed to be greater than its median value .

Question 1: $P_1 = P(F_{X_1}(X_1) > 0.5 | F_{X_2}(X_2) > 0.5)$

Suppose X_2, X_3 are observed to be higher than their respective median value, what is the probability that X_1 is also observed to be higher than its median value

Question 2: $P_1 = P(F_{X_1}(X_1) > 0.5 | F_{X_2}(X_2) > 0.5, F_{X_3}(X_3) > 0.5)$

Suppose X_2, X_3,X_4 are observed to be higher than their respective median value, what is the probability that X_1 is also observed to be higher than its median value

Question 3: $P_1 = P(F_{X_1}(X_1) > 0.5 | F_{X_2}(X_2) > 0.5, F_{X_3}(X_3) > 0.5, F_{X_4}(X_4) > 0.5)$

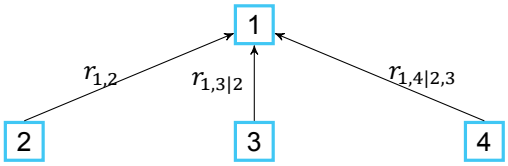

Figure 3.1: Bayesian Network with conditional rank correlations [56]

To calculate the exceedance probability P_1, double integral of the bivariate standard normal density function $\phi(u, v, \rho_{u,v})$ is taken. The computed exceedence probability is a function of $\rho_{u,v}$. The probability estimated by the expert for question 1 is given by this exceedence probability. Corresponding to the expert's probability, product moment correlation $\rho_{u,v}$ can be obtained (see Figure 3.2). Further, using the relation given by Equation 5.17, the $\rho_{1,2}$ can be then converted to the rank correlation, $r_{1,2}$

To estimate the rank correlation correlations $r_{1,2|3}$ and $r_{1,2|3,4}$, a repeated inverse integral of the distribution of the form $\phi(u, w, v, \rho_{u,w}, \rho_{u,v|w})$ has to be taken. This would give $\rho_{1,2|3}$ which can be converted to $1, 2|3$ for a normal copula using the same relation given in Equation 5.16 and Equation 5.17.

In the unavailability of historical data, these correlations are obtained from Expert Judgment elicitation. Elicitation of expert's beliefs about dependence between multiple variables is carried out with the aim of obtaining quantitative assessments. When eliciting dependence from the experts, the analyst drafts the elicitation based on a pre-determined multivariate stochastic model.

At this stage the expert has given probabilities as an answer to the questions, these probabilities have to be 'converted' to rank correlations as explained above.

Calibration of Expert's Dependence Estimates

This section is explained based on the technique given by [82] to compute expert calibration score of dependence elicitation. Similar to Cooke's method, it is also based on linear pooling of assessment using equal weights and global weights.

Considered the BN shown in Figure 3.3. The aim is to fill the correlation matrix Equation 3.15 using expert assessment. In Equation 3.15, a correlation matrix is given where each item represents a dependence between the row and column variables. For example, $r_{2,3}$ represents the rank correlation between X2 and X3. Since the correlations are direction independent, $r_{2,3}$=$r_{3,2}$.The variables $X1$, $X2$, $X3$, $X4$ are shown in Figure 3.3 using nodes and arcs. Based on the theory in section 5.1, it can be deduced that $\rho_{1,3|2} = 0$, $\rho_{1,4|2,3} = 0$. Using the Equation 3.14, and substituting $\rho_{1,3|2} = 0$, $\rho_{1,3}$ is computed. similarly, other partial correlation coefficients can be calculated. ρ is then converted to rank correlation (r), as described in the above section. More detail about conditional and unconditional correlations is given in section 5.1.

$$\rho_{1,3|2} = \frac{\rho_{1,3} - \rho_{1,2} * \rho_{2,3}}{\sqrt{(1 - \rho_{1,2}^2)(1 - \rho_{2,3}^2)}} \tag{3.14}$$

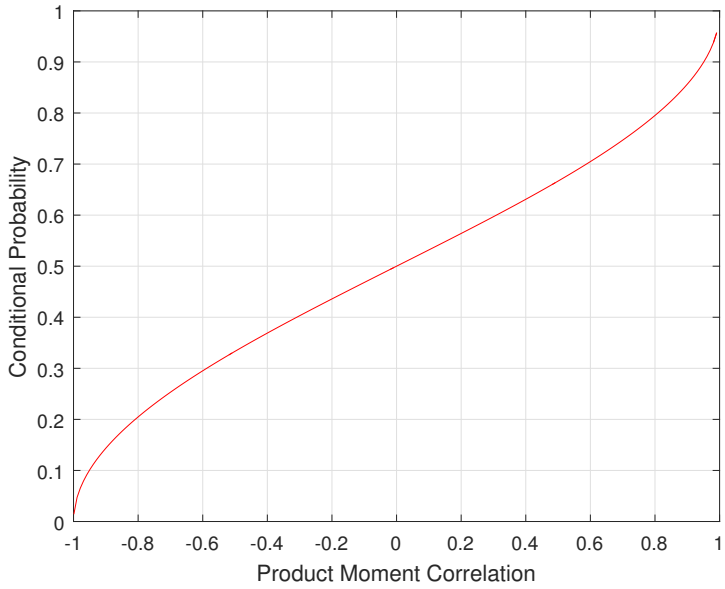

Figure 3.2: Expert's conditional probability assessment as a function of the rank correlation coefficient [81]

$$\sum c = \begin{array}{c} \begin{matrix} X1 & X2 & X3 & X4 \end{matrix} \\ \begin{pmatrix} 1 & r_{1,2} & r_{1,3} & r_{1,4} \\ r_{2,1} & 1 & r_{2,3} & r_{2,4} \\ r_{3,1} & r_{3,2} & 1 & r_{3,4} \\ r_{4,1} & r_{4,2} & r_{4,3} & 1 \end{pmatrix} \end{array} \begin{matrix} X_1 \\ X2 \\ X3 \\ X4 \end{matrix} \tag{3.15}$$

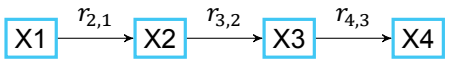

Figure 3.3: Correlation matrix and Bayesian Network with unconditional rank correlations between seed variables

In [57] propose the *Hellinger distance* to assess the experts' performance for multivariate dependence assessment. in [59] a technique is proposed to assess whether experts can approximate the dependence structure of a NPBN under the normal copula assumption to a desired level of accuracy. For Gaussian copulas the *Hellinger distance H* is defined as:

$$H(\sum_C, \sum_E) = \sqrt{1 - \frac{det(\sum_C)^{1/4} det(\sum_E)^{1/4}}{(1/2 det(\sum_C) + 1/2 det(\sum_E))^{1/2}}} \tag{3.16}$$

where

$\sum_C$ = Correlation matrix of seed variables

$\sum_E$ = Correlation matrix of expert elicitation of seed variables

The d-calibration score can then be defined as beginequation

$$D = 1 - H(\sum_C, \sum_E) \tag{3.17}$$

The d-calibration score is defined in the range of $[0, 1]$ with 1 being the perfect score. If the score is equal to 0, then it implies that either at least two seed variables are linearly dependent and the expert

does not assess this or the other way round. Combining the expert assessment by linear pooling is defined according to Equation 3.18.

$$\Sigma_R = \sum_{i}^{E} (W(i) * \Sigma_T(i)) \tag{3.18}$$

where

Σ_R = Resulting target correlation matrix
$W(i)$ = Weight of expert i,$W(e) = 1/E$ for equal weighting system
Σ_T = Target Correlation matrix
E = Number of experts

3.2. Elicited Variables

Bridge structural response is usually strongly correlated to the applied load. The applied load in the form of individual axle load of the train can be measured using a weigh-in-motion (WiM) system. No WiM is installed on the bridge under consideration; hence, individual axle loads are elicited using expert judgment. The train under consideration is 97.8m long with five cars. Each car of the train has four axles with one wheel on either side. The axle load is the total of the individual wheel load. The expert judgment elicitation is performed under the assumption that the axle load distribution in all four axles respectively, will be equal in each of the five cars. Four variables, load in axle 1 (*Axl1*), load in axle2 (*Axl2*), load in axle 3 (*Axl3*) and load in axle 4 (*Axl4*), are assessed by the experts.

The axle load model for road WiM described by Morales-Nápoles et al. [60] establishes a dependency between individual axle loads. It is assumed that the rail WiM behaves similar to road WiM. Therefore, load in each axle is correlated to load in another axle in the train. Therefore, to include axle load dependency in the statistical model, a correlation between the axle loads is elicited using expert judgment.

3.3. The Elicitation

For this research, seven experts participate in assessing variable uncertainty and dependence based on the methodologies described in section 3.1. Since this research was a pilot study, all experts are not necessarily experts in railway engineering. All the experts, however belong to the civil engineering community. First, the experts are given an in-person workshop to explain the methodology and the goals of elicitation. To familiarize the experts with the tone of the questions, a training expert judgment exercise is carried out. Following the training session, personal assessment of experts is performed in approximately one hour. To maintain fairness and neutrality, the facilitator of the expert judgment workshop is present at all times. The expert judgment questionnaire prepared are included in Appendix B.

To elicit uncertainty in variables, four target variables and eight calibration variables are chosen. The four target variables are the variables to be assessed, *Axl1*, *Axl2*, *Axl3*, *Axl4*. In general, using twelve or more seed questions is recommended for expert judgment elicitation. However, due to the lack of relevant data on which seed questions can be framed, this research is limited to using eight seed questions eliciting assessment on eight seed variables only. These eight seed variables can be segmented into two groups. The first consisting of questions concerning the maximum weight measured by a WiM system installed on a highway in the Netherlands in a certain time frame. The second group consists of questions concerning the mean axle load measured by a WiM system installed on rail tracks in the Netherlands. These variables are related to the axle load distribution in moving vehicles and are thus associated with the target variables. To elicit dependence in variables, four target dependencies and three calibration dependencies are chosen. The dependencies are elicited based on conditional (exceedance)probabilities. The conditional probability is transformed into a rank correlation coefficient (to build Bayesian Network) under the assumption of normal copula densities of variables, using the relation as shown in Figure 3.2.

3.4. Results and Discussions

Uncertainty and dependence elicitation were performed in this thesis, based on *Classical Model* and *conditional probabilities technique*. This section discusses the analysis of the elicitation and explains the results observed.

3.4.1. Uncertainty

Seed Variables

Figure 3.4 and Figure 3.5 present the results obtained for all the seed variables. In the figures, experts' assessment for 5^{th}, 50^{th} and 95^{th} percentile are marked with solid markers. The true value is shown with a dark blue marker. Equal weight assessment is also shown on these graphs, which will be discussed later in the section.

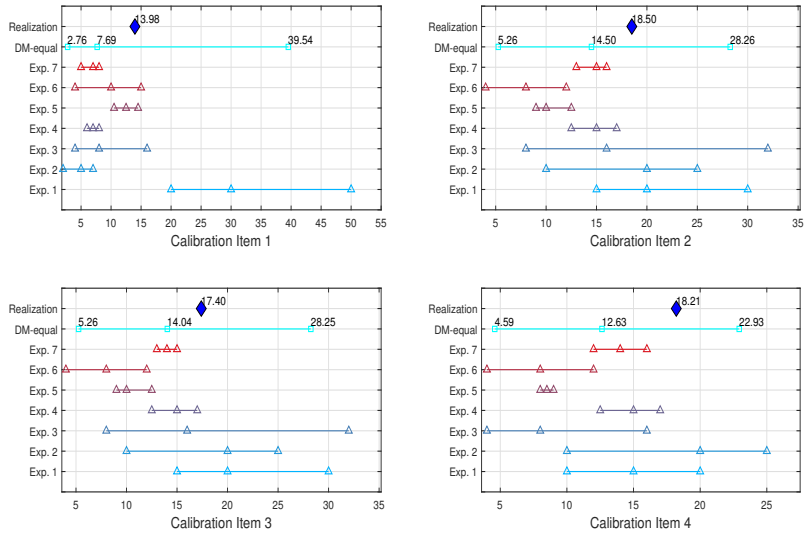

Figure 3.4: Uncertainty distributions of the experts for seed question 1 to 4 - maximum axle load in Axle 1 to Axle 4 in four-axle vehicle

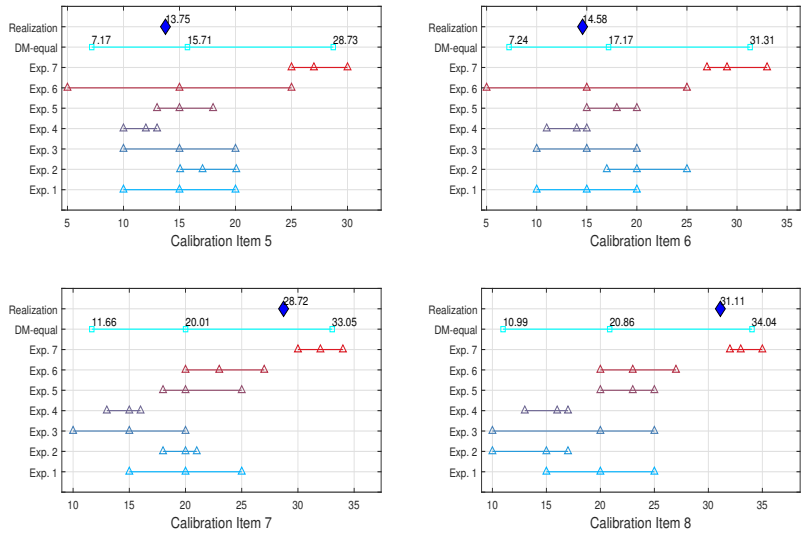

Figure 3.5: Uncertainty distributions of the experts for seed question 5 to 8 - mean and maximum axle load in trains near Schiedam and Zeist

Target Variables

The general observations on the target variable elicitation of the Expert Judgment study follows:

- Most experts have a smaller interval width for all target variables as compared to the that of seed variables.
- All experts give similar target variable distribution for target variable 2 and 3. Target variable 2 is the axle load distribution in axle 2 and target variable 3 is the axle load distribution in axle 3.

Figure 3.6 presents the results for target variable 1 and 2. In the figures, the bar limits are 5^{th}, 50^{th} and 95^{th} percentile.

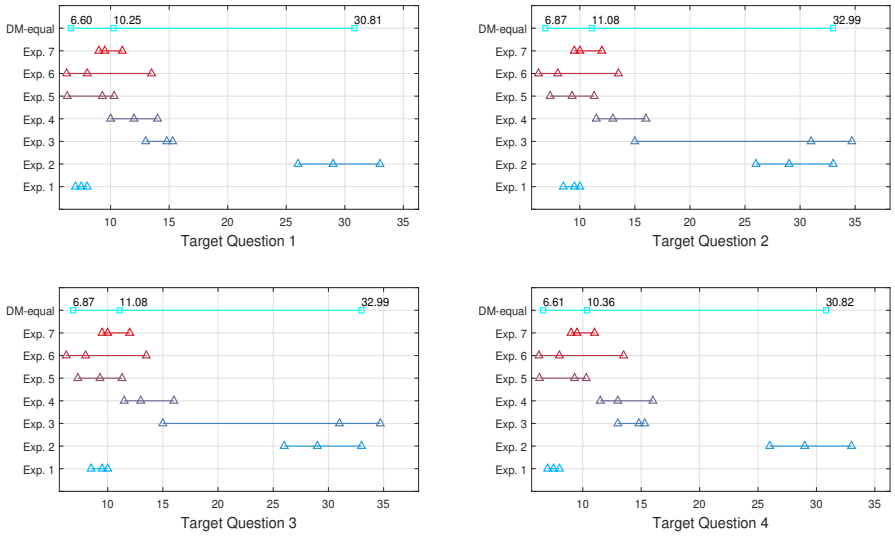

Figure 3.6: Uncertainty distributions of the experts for all target variable 1

Table 3.1: Calibration, Information and combined score for all experts

Experts	Calibration	Information score all variables	Information score seed variables	Total Score
Expert 1	8.76E-02	1.47	1.17	1.03E-01
Expert 2	2.53E-04	1.41	1.44	3.65E-04
Expert 3	3.44E-02	1.17	0.83	2.85E-02
Expert 4	3.59E-08	1.64	1.98	7.10E-08
Expert 5	6.63E-05	1.76	1.97	1.31E-04
Expert 6	1.44E-04	0.74	0.95	1.37E-04
Expert 7	4.97E-08	1.96	2.29	1.14E-07

Table 3.2: Calibration and Information score for Decision Makers
EW: Equal Weight ; IW: Item Weight ; 0.02: significance value of 0.02; op=optimized; GW : Global weight

	Calibration	Information score for seed variables
DM_EW	2.86E-01	0.18
DM_IW_0.02	6.69E-02	0.84
DM_IW_op	8.76E-02	1.17
DM_GW_0.02	6.69E-02	0.82
DM_GW_op	8.76E-02	1.17
DM_GW	6.69E-02	0.73

Calibration for uncertainty
Each expert contributes to the overall decision making based on their closeness to the true value in a statistical sense using information scores and calibration scores, described in section 3.1.

The scores of all seven experts are presented in Table 3.1. The calibration score is defined in the range of $[0, 1]$ with 1 being the highest score and 0 being the lowest score. Usually, the minimum score at which an expert's contribution is counted is 0.05. The information score is measured relative to a background measure and hence can be greater than 1. For the same reason, the information score can be calculated for the target variables as well. The total score also called the combined score of the expert is the product of the calibration score and information score. The detailed description of calibration, information and combined score is given in section 3.1.1.

In the Table 3.1, the information score when both target and seed variables are considered is close to the information score for only seed variables. This supports the assumption that the expert assesses the target variables and seed variables with similar uncertainty. For expert 1, both the calibration and information scores are very high. For Expert 4, 5 and 7, the calibration score is very low, and this lowers their total score despite a good information score. Expert 2, 3 and 6 have better calibration scores compared to experts 4, 5 and 7 with similar information scores hence have a higher total score.

Decision Maker
To arrive at a resulting uncertainty distribution for target variables, the expert uncertainties are combined. The Decision Maker (*DM*) combines the expert distributions by using a weighting system (see Equation 3.1.1. The selection of the weighting system is made by the analyst. The different weighting system considered in this research are Global Weights (*GW*), Equal Weights (*EW*), and Item Weights. (*IW*).

The goal of the DM is to maximise the calibration and information score. The analyst accepts the DM with the highest calibration and information score. In Table 3.2, all DM system have calibration scores higher than 0.05; hence all of them are acceptable. Global weight and Item weight are rejected because they are either equal to or lower than the calibration score of a single expert (Expert 1). Therefore, DM_EW is the chosen Decision Maker for resulting uncertainty distributions. In Figure 3.7, the confidence interval for both GW (without optimisation) and EW are spread out. Expert 2 - Expert7 have calibration score less than 0.05; hence the analyst chooses Decision maker with an equal weighting

system in order to choose the decision maker with highest calibration score.

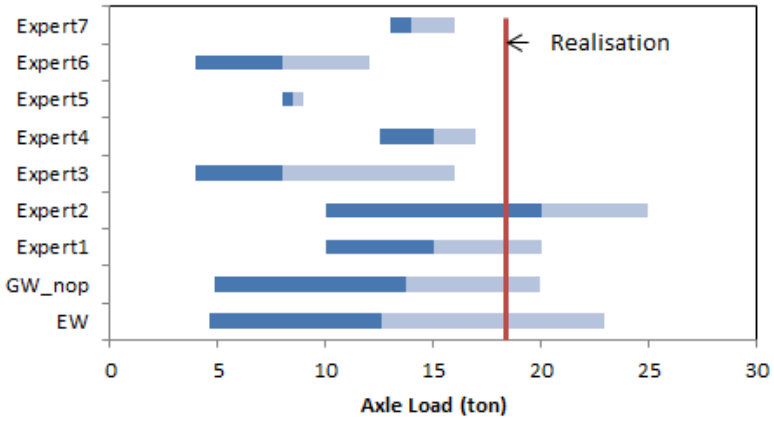

Figure 3.7: Uncertainty distributions for experts, equal weight DM and global weight DM for seed question 4
EW: Equal Weight ; GW_{nop} : Global Weight without optimization

Resulting Distributions

The probability distribution for target variables is estimated from the equal weighting Decision maker. The DM provides with the 5th, 50th and 95th quantiles for the four target variables. The 0th and 100th percentile is extrapolated to using the k=10% overshoot rule (section 3.1).

The resulting quantiles are presented in Figure 3.8. Based on these distributions, random values can be retrieved using random sampling using a Monte-Carlo approach.

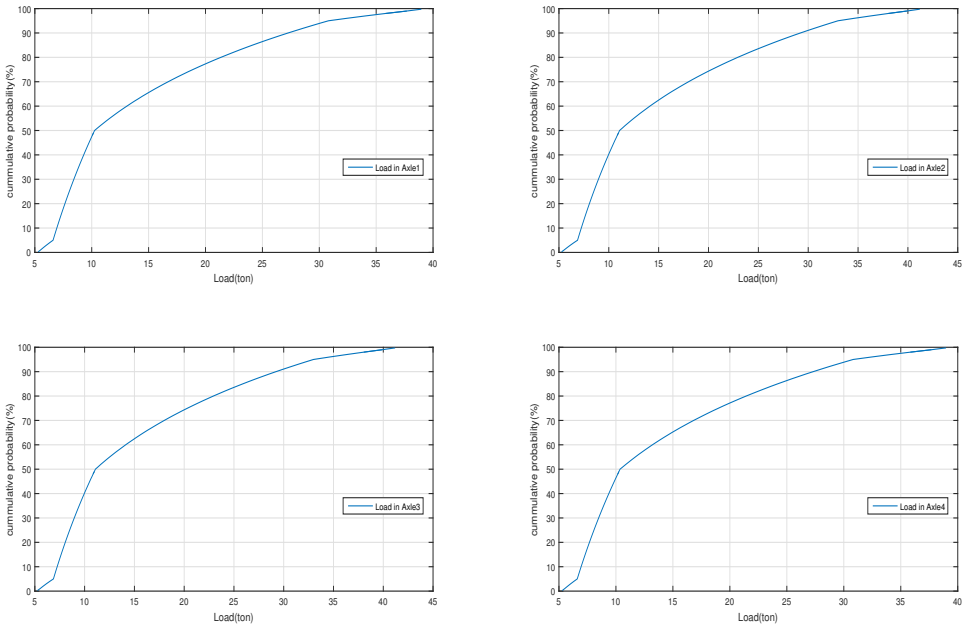

Figure 3.8: Cummulative probability distribution from EJ elicitation on uncertainty

3.4.2. Dependence

To obtain, the dependencies(described in section 5.1 and section 3.1.2) between the four variables, *Axl1*, *Axl2*, *Axl3* and *Axl4*, experts were asked to assess the conditional probabilities between seed variables and target variables. The framing of the questions is of the following form [82]:

"Consider the pair of variables, X and Y. Suppose that Y has been observed to be above its median value. Knowing this information, what is the probability that X also lies above its median value"

Following the description above, the definition of X and Y in this research is presented in Table 3.3. The axle load in seed variables is associated with the WiM system installed on highways in the Netherlands. The axle load in target variables is associated with loads carries by train axles.

Table 3.3: X and Y definition for elicitation of dependence for seed and target variables

Seed Variables (Load in ton)			Target Variables (Load in ton)		
	X	Y		X	Y
Question 1	Axle 1	Axle 2	Question 1	Axle 1	Axle 2
Question 2	Axle 2	Axle 3	Question 2	Axle 2	Axle 3
Question 3	Axle 3	Axle 4	Question 3	Axle 3	Axle 4
			Question 4	Axle 4	Axle 1

Table 3.4: Conditional probability assessment of all experts and realisations

	Seed Variables			Target Variables			
	Q1	Q2	Q3	Q1	Q2	Q3	Q4
Expert 1	60%	80%	85%	60%	80%	80%	40%
Expert 2	80%	85%	90%	80%	80%	80%	60%
Expert 3	10%	40%	10%	20%	30%	30%	20%
Expert 4	60%	80%	90%	60%	70%	70%	50%
Expert 5	65%	70%	60%	70%	75%	75%	40%
Expert 6	50%	60%	70%	70%	75%	80%	85%
Expert 7	40%	70%	80%	85%	76%	85%	72%
Realisation	68.03%	71.09%	90.79%				

In Table 3.4, expert's beliefs about dependencies between seed and target variables are presented. Comparing the results in Table 3.4 to Figure 3.2, it can be concluded that other than Expert 3, all experts assess a positive correlation between seed variables. The true values or realisations also match the experts' beliefs. Expert 3 believes that both seed and target variables are negatively correlated. All other experts think that the dependencies are related to the position of the axle and hence are positively correlated; however each expert assesses different probabilities.

Calibration for dependence

The experts are given a calibration score through d-calibration score [58] which uses *Hellinger distance* (section 3.1.2). More details about the methodology are presented in Figure 3.1.2.

$$\Sigma c = \begin{array}{c} \begin{matrix} axle1 & axle2 & axle3 & axle4 \end{matrix} \\ \begin{pmatrix} 1 & r_{1,2} & r_{1,3} & r_{1,4} \\ r_{2,1} & 1 & r_{2,3} & r_{2,4} \\ r_{3,1} & r_{3,2} & 1 & r_{3,4} \\ r_{4,1} & r_{4,2} & r_{4,3} & 1 \end{pmatrix} \end{array} \begin{matrix} axle1 \\ axle2 \\ axle3 \\ axle4 \end{matrix} \tag{3.19}$$

The symmetrical rank correlation matrices for all experts (E1,..,E7) are presented in Equation 3.20 to Equation 3.26, represented by $\sum_{Ei} c$ for each expert *i*. The correlation matrix of true values or realisations of the seed variables in given in Equation 3.29.

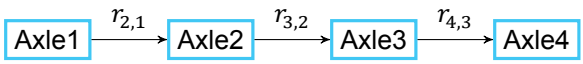

Figure 3.9: Bayesian Network with unconditional rank correlations between seed variables

$$\Sigma_{E_1}c = \begin{pmatrix} 1 & 0.31 & 0.25 & 0.23 \\ 0.31 & 1 & 0.81 & 0.72 \\ 0.25 & 0.81 & 1 & 0.89 \\ 0.23 & 0.72 & 0.89 & 1 \end{pmatrix} \tag{3.20}$$

$$\Sigma_{E_2}c = \begin{pmatrix} 1 & 0.81 & 0.72 & 0.69 \\ 0.81 & 1 & 0.89 & 0.85 \\ 0.72 & 0.89 & 1 & 0.95 \\ 0.69 & 0.85 & 0.95 & 1 \end{pmatrix} \tag{3.21}$$

$$\Sigma_{E_3}c = \begin{pmatrix} 1 & -0.95 & 0.3 & -0.28 \\ -0.95 & 1 & -0.31 & 0.3 \\ 0.3 & -0.31 & 1 & -0.95 \\ -0.28 & 0.3 & -0.95 & 1 \end{pmatrix} \tag{3.22}$$

$$\Sigma_{E_4}c = \begin{pmatrix} 1 & 0.31 & 0.25 & 0.24 \\ 0.31 & 1 & 0.81 & 0.77 \\ 0.25 & 0.81 & 1 & 0.95 \\ 0.24 & 0.77 & 0.95 & 1 \end{pmatrix} \tag{3.23}$$

$$\Sigma_{E_5}c = \begin{pmatrix} 1 & 0.45 & 0.27 & 0.09 \\ 0.45 & 1 & 0.59 & 0.19 \\ 0.27 & 0.59 & 1 & 0.31 \\ 0.09 & 0.19 & 0.31 & 1 \end{pmatrix} \tag{3.24}$$

$$\Sigma_{E_6}c = \begin{pmatrix} 1 & 1.2E-08 & 3.87E-09 & 2.34E-09 \\ 1.2E-08 & 1 & 0.31 & 0.19 \\ 3.87E-09 & 0.31 & 1 & 0.59 \\ 2.34E-09 & 0.19 & 0.59 & 1 \end{pmatrix} \tag{3.25}$$

$$\Sigma_{E_7}c = \begin{pmatrix} 1 & -0.31 & -0.19 & -0.15 \\ -0.31 & 1 & 0.59 & 0.48 \\ -0.19 & 0.59 & 1 & 0.81 \\ -0.15 & 0.48 & 0.81 & 1 \end{pmatrix} \tag{3.26}$$

The d-calibration score lies in the range $[0, 1]$, where 0 is the worst score, and 1 is the best score. If the d-calibration scores lie below a threshold value, then the expert is given a 0 score. Based on the individual d-calibration score, each expert's contribution to the total score is calculated and then assigned a weight. This method is followed in the global weight system of combining experts' assessment. In equal weight system, each expert is assigned the same weight irrespective of the d-calibration score. In Table 3.5, the resulting d-calibration score for the different weighing methods considered in this research is presented. It is observed that the global weighing system has a better d-calibration score. The objective is to maximise the calibration score. Therefore global weights are used in this research.

Table 3.5: d-calibration score for combination of experts

	d-calibration score
Equal weights	0.4521
Global weights	0.7925

The maximum calibration threshold for global weights is 0.6950. In Table 3.6, a d-calibration score of each expert is listed. It is observed that only Expert 4 has a score higher than the optimum threshold and hence gets a weight of 1. Comparison of Equation 3.29 and Equation 3.27 supports that combination using equal weighing system, only $r_{4,2}$ and $r_{3,2}$ is close to realization values. This observation can be attributed to the low degree of correlation, though positive, between seed variables assessed by most experts. Hence, even though, only one expert contributes to the pooling of assessments in the global weighing is acceptable.

The influence of ignoring the minimum threshold is also studied. It is observed that when the assessment of expert 4 is combined with that of expert 1, who has the second highest d-calibration score (and also just misses the minimum threshold value), the d-calibration score of the decision maker is

Table 3.6: d-calibration score and weight of experts

	d-calibration score	weights
Expert 1	0.6943	0
Expert 2	0.6328	0
Expert 3	0.0864	0
Expert 4	0.7925	1
Expert 5	0.4277	0
Expert 6	0.4599	0
Expert 7	0.5414	0

0.72. This is an interesting point of analysis, whether to choose a decision maker with only one expert, or a decision maker with combination of two experts' assessment with a slightly lower d-calibration score.

$$\Sigma_{EW}c = \begin{pmatrix} 1.00 & 0.09 & 0.23 & 0.12 \\ 0.09 & 1.00 & 0.53 & 0.5 \\ 0.23 & 0.53 & 1.00 & 0.51 \\ 0.12 & 0.5 & 0.51 & 1.00 \end{pmatrix} \tag{3.27}$$

$$\Sigma_{GW}c = \begin{pmatrix} 1 & 0.31 & 0.25 & 0.24 \\ 0.31 & 1 & 0.81 & 0.77 \\ 0.25 & 0.81 & 1 & 0.95 \\ 0.24 & 0.77 & 0.95 & 1 \end{pmatrix} \tag{3.28}$$

$$\Sigma_{realisation}c = \begin{pmatrix} 1 & 0.54 & 0.34 & 0.32 \\ 0.54 & 1 & 0.62 & 0.59 \\ 0.34 & 0.62 & 1 & 0.96 \\ 0.32 & 0.59 & 0.96 & 1 \end{pmatrix} \tag{3.29}$$

Resulting correlation matrix

To estimate the combined target dependencies based on a combination of expert assessment, linear pooling of expert assessment of specific dependencies is performed. In this research, global weighing is chosen. Only expert 4 contributes to the target correlation matrix since no other expert carries weight (see Table 3.6). The resulting target correlation matrix is shown in Equation 3.30. In the elicitation of dependencies in seed variables (built on WiM for highway vehicles), it is assumed that that $r_{4,1|2,3} = 0$, hence exceedance probabilities are not elicited between axle 4 and axle 1. However for target variables (loads in train axles), it is assumed that every $n = 1 \ldots N$ car has $j = 1 \ldots 4$ axles, and distribution of every j^{th} axle of all N cars is the same. Therefore, according to the EJ analyst, load in axle 4 of car *n* is not independent of load in axle 1 of car *n+1*, which mathematically means $r_{4,1} \neq 0$. This is represented in the Bayesian network shown in Figure 3.10. In the resulting matrix, post combination of expert assessment, the resulting correlation between load in axle 1 and 4, $r_{4,1}$=0.0 that is load in axle 4 and axle 1 are unconditionally independent according to the assessment by the experts.

$$\Sigma_{result}c = \begin{pmatrix} 1 & 0.31 & 0.19 & 0 \\ 0.31 & 1 & 0.59 & 0.35 \\ 0.19 & 0.59 & 1 & 0.59 \\ 0 & 0.35 & 0.59 & 1 \end{pmatrix} \tag{3.30}$$

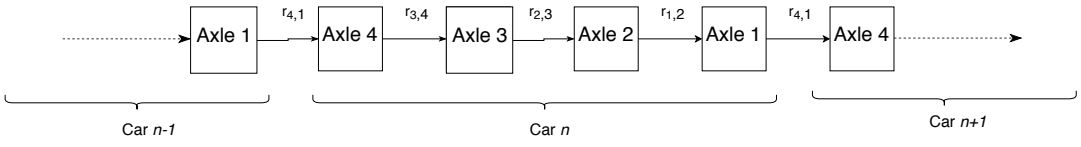

Figure 3.10: Bayesian Network with unconditional rank correlations between target variables

3.5. Measured Data vs Expert Judgment elicitation

In the Netherlands, railway weight-in motion data is measured at 45 sites on Dutch Railway network. More details about the technology and the type of data collected is provided in Appendix D. A comparative study is performed between the results of the expert judgment elicitation and the measured data. In Figure 3.11 and Figure 3.12, the comparison of the cumulative distribution function of axle loads is shown. It can be seen that the experts have a lower estimation for the lower bound of the axle loads distribution and a higher estimation of the higher bound of the axle load distribution. Further, since the comparison is done between two different countries, therefore, there may be difference in loading conditions and track conditions. On comparing the correlation matrix, it can be observed that the expert assessment of dependency between axle loads is significantly different from the measured data. On further analysis, it was inferred that the calibration questions and target questions for Expert Judgment elicitation did not implicitly state that dependency between axle 4 of car $n+1$ and axle 1 of car$n$ is asked. Further, the calibration questions for the dependency elicitation was based on data from WiM on highway vehicles. Therefore, the difference in the dependence between axle loads, other than due to the difference in locations, may be because of the data used for calibration questions.

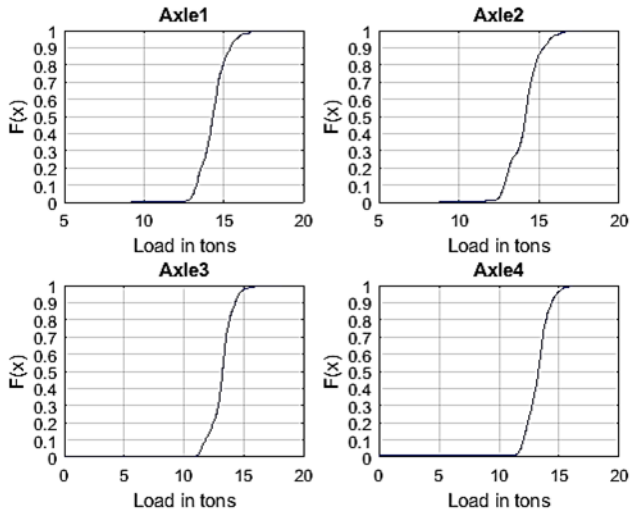

Figure 3.11: Cummulative distribution function of axle loads in tons measured with Rail WiM in Netherlands

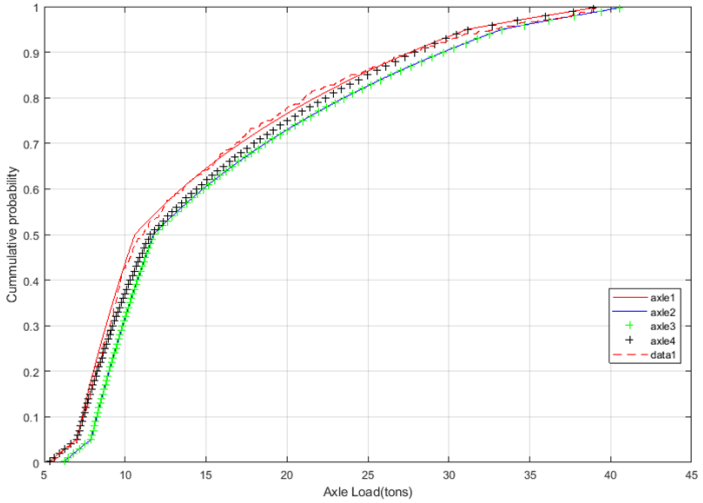

Figure 3.12: Cummulative distribution function of axle loads in tons elicited from experts

	Axle1	Axle2	Axle3	Axle4
Axle1	1,00	0,84	0,88	0,79
Axle2	0,84	1,00	0,82	0,91
Axle3	0,88	0,82	1,00	0,83
Axle4	0,79	0,91	0,83	1,00

(a) Correlation matrix between axle loads for measured data

	Axle1	Axle2	Axle3	Axle4
Axle1	1,00	0,31	0,19	0,00
Axle2	0,31	1,00	0,59	0,35
Axle3	0,19	0,59	1,00	0,59
Axle4	0,00	0,35	0,59	1,00

(b) Correlation matrix between axle loads for elicited dependency

Figure 3.13: Comparison of correlation matrix between elicited dependency and measured data

3.6. Conclusions

The expert judgment elicitation is carried out for both uncertainty and dependence since there is no historical data available on axle load distribution in trains. The elicitation of uncertainty and dependence is carried out independently. This is because expert calibration may not be the same for uncertainty and dependence. In this research, equal weighting is chosen for combining expert assessment for uncertainty, however, for dependence, global weights are used.

For elicitation of uncertainty, seven experts are assessed. It can be observed, that the response to seed variables based on railway WiM is more accurate than highway WiM. However, if seed variables only based on railway WiM are chosen, then there are too few variables to assess on. Therefore, equal weights are chosen based on the overall high calibration score with all seed variables. The calibration could be improved if the seed variables are based on railway WiM since it is more reflective of the expert's field of expertise.

For elicitation of dependence, three seeds variables are used. The seeds are only based on the highway WiM, since highway WiM data was the only reliable data available. Also, this research majorly highlights the application of the technique in structural engineering; hence further improvement can be made in selecting seed variables for dependence. It is observed that of the experts is very accurate in assessing dependencies and hence is given a weight of 1 in a global weighing system.

4

The Case Study

In this research, a railway concrete girder is assessed for failure under bending. The loads that are applied on the bridge are the self weight and the live loads in the form of railway axle loads. The bridge assessment is performed under uncertainties in load and material strength. As stated before, the load uncertainties are elicited from the Expert Judgment (chapter 3) and material uncertainties are modelled from experimental tests performed in past research [53]. In order to assess the influence of these uncertainties on the bridge response, a finite element analysis of the bridge is performed. For every finite element analysis (FEA), the load and material properties are deterministic, which are sampled through Monte Carlo simulations (see section A.4). This chapter discusses the geometry of the model, and finite element techniques adopted in this research. Further, the application of ABAQUS CAE in performing FEA are discussed.

4.1. Simply supported model with plain concrete

According to the recommendations available in the literature (section 2.2), the modelling methodology in finite element depends on the level of assessment to be performed for the analysis. In order to perform the analysis at the level of assessment II, a linear finite element model is an acceptable approximation for determining shear stress distribution. In this research, the same assumption is extended to determine the bending stress distribution as well. Hence, in this study, a LoA II analysis is performed using a simply supported plain concrete beam.

As a reference, the geometry of the concrete girder and deck modelled is similar to that of the new interurban bridge between the Mexico and Toluca which has a total span of 57.7km. The train which is proposed to be running on this bridge has a 300,000 passenger capacity and will be running at a speed of 160km/h. The bridge girder which has clear span of 33m and is simply supported over the columns of the bridge is chosen for the analysis in the research. In Figure 4.1, the section of the bridge girder is presented. The longitudinal beams of the bridge are double box girders. The height of the girder is 2.2 m and depth of the girder varies across the span due to non-prismatic sections used.

In this study, the bridge is modelled as a simply supported concrete beam. First, an equivalent rectangular beam section is considered. The equivalent section is derived by equating the area of cross section and moment about major axis. Figure 4.2 shows the actual cross section profile of real bridge and derived equivalent rectangular section of bridge.

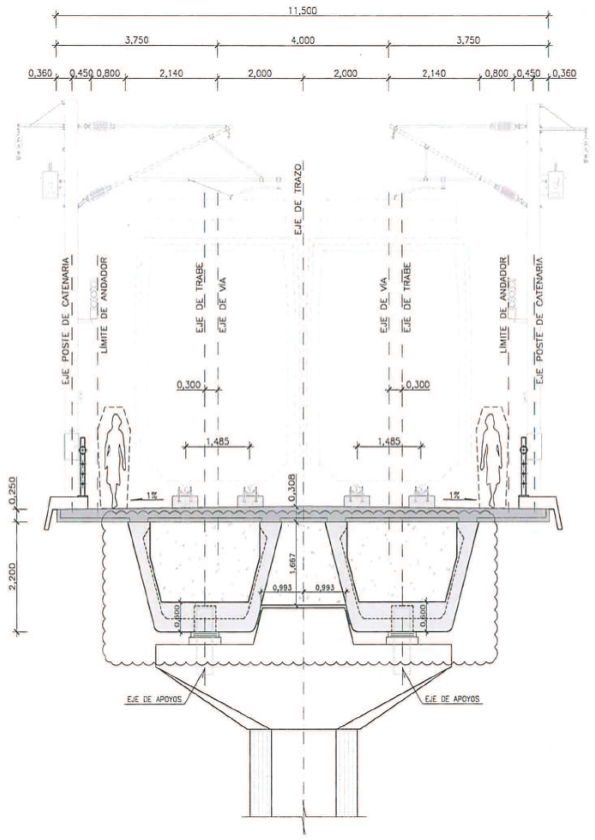

Figure 4.1: Elevation of cross section of bridge girder

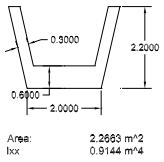

(a) Cross section of the beam profile in the real bridge

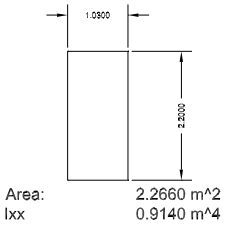

(b) Cross Section of equivalent profile

Figure 4.2: Simply supported beam model

The finite element analysis is performed using 2-noded beam element, B21 in x and y plane. As guided by past researchers (see chapter 2), for the initial assessment of the bridge, a linear elastic analysis is performed on the simply supported beam. The sketch of the beam is shown in Figure 4.3.

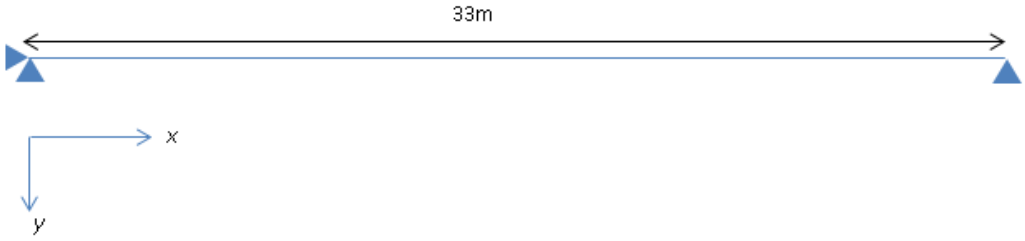

Figure 4.3: Simply supported model sketch

Table 4.1: FEM input of simply supported model

	1D Model
Analysis Type	Linear Elastic
Element Type	B21
Degree of Freedom/element	6
Interpolation scheme	Linear
Integration scheme	Implicit
Non-Linear Geometry Effects	No
Total Number of Elements	66
Total number of nodes	67
Element size	0.5m

Table 4.2: Characteristics of the FEM Model

	Span Length	Height of section	Width of section	Material Type	Material Model
2D Analysis	33m	2.2m	1.03m	Plain Concrete	Linear Elastic Isotropic

In the following section, brief description on the FE environment of ABAQUS CAE is discussed which is used in this research to model the bridge.

4.2. ABAQUS FE System

To create and analyze the bridge, Finite Element Analysis is performed using ABAQUS finite element software. There are two ways to perform pre-processing of the model. First, ABAQUS/CAE, which is a graphical and interactive interface, where the individual components can be modelled as parts. The second way is to write the input file manually using ABAQUS keywords. The input file gives higher flexibility to the user however, one has to learn the exact syntax. Model geometry, material properties, connections and boundary conditions are defined in the input file. For this research, first the model is defined in ABAQUS/CAE. The input file is generated by CAE environment. For further analysis, changes are made to the already generated input file directly.

In this research, a moving load analysis has been performed to analyze the bridge behaviour under moving train load. To model the moving load, different force time amplitude curves are defined for each node in the script file. A matlab code is written to generate different amplitude curves and calculate the time steps such that at each time step, the load is exactly at a particular node. To perform, a probabilistic assessment of the bridge, different samples of load combination is generated using data elicited from experts (refer chapter 3). To run the script for each sample of the load combination, a python script is written, which generates a different input file for each sample. For example, if 500 samples of load combinations (Axle load 1, Axle Load 2, Axle Load 3, Axle Load 4) are created, the python script generates 500 input files for each load combination.

Since the analysis performed in this study is linear elastic, a fixed time increment can be used. ABAQUS/Viewer, is a post processing system where the user can see the results in a graphical user interface.

4.3. Modeling of moving Load

As stated in chapter 2, train loads have a static and a dynamic component when acting on the bridge. The dynamic component ($m \cdot \ddot{a}$) which takes into account the dynamic amplification factor due to train bridge interaction is ignored in this study. Uncertainty in the static component ($m \cdot \dot{g}$) is elicited using expert judgment studies as described in chapter 3. The next step is to model the loads on the bridge such that at $t = 0s$, the train is one time increment behind entering the bridge and at $t = t_{last}$, the train crosses the bridge completely. To perform the finite element analysis with the modelling the moving load (at a speed of 160km/h), it is assumed that the train loads being applied exactly at nodal position at each time increment will give approximately accurate results. Equation 4.1, Equation 4.2 and Equation 4.3

give the equations to calculate the total time,time increment and number of increments for the train passage. In Equation 4.2, it is assumed that the nodal distance is equal between all nodes on beam, and the nodal distance is smaller than the smallest inter-axle spacing.

$$Time_{total} = \frac{(length_{bridge} + distance_{axl1-axle_{end}})}{velocity_{train}} \tag{4.1}$$

$$Time_{increment} = \frac{nodaldistance}{velocity_{train}} \tag{4.2}$$

$$numberofincrements = \frac{Time_{total}}{Time_{increment}} \tag{4.3}$$

4.4. Results and Discussion

This section discusses the results of one of the simulations performed. The values of Youngs modulus(Ec), mass density (wc), and axle loads, axle1, axle2, axle3, axle4 are sampled using Monte Carlo simulations, which is discussed in the next chapter. The variables are treated as deterministic in simulation 1 and the values are listed in Table 4.3.

Table 4.3: Deterministic values for random variables for simulation 1

Property	Deterministic Value for simulation 1
Youngs Modulus (Ec) (MPa)	31926
Mass density (kg/m^3)	2345
Axle Load 1(kN)	61.64
Axle Load 2(kN)	211.40
Axle Load 3(kN)	132.20
Axle Load 4(kN)	191.88

All the results in the following sections are based on simulation 1 using values listed in Table 4.3.

4.4.1. Concentrated force

In Figure 4.4, the rendered beam profile is shown at different time steps representing the concentrated force distribution as the axle load moves on the bridge. At Step 0 it can be seen that there is not concentrated force on the bridge and hence the train has not entered the bridge. At time step 1, the first axle of the train is at the first node of the beam. The maginitude of vertical force in axle 1 for this simulation is 61.64kN. The time increment is given such that the axle forces are always acting on nodal position. At time step 27, all four axles of the first car are acting on the bridge. Further, at time step 64, first two cars of the five car train is on the bridge. After this time step, the first axle of the first car leaves the bridge. It can also be observed, that the concentrated force of axle 1 of first car is equal to that of axle 1 of second car and similarly for axle2, axle 3 and axle4. This is because of the assumption for this simulation that the load in every $j = 1 \cdot 4$ axle of $n = 1 \cdot 5$ car of the train is equal. The results of this simulation are presented as BN-I in the next chapter.

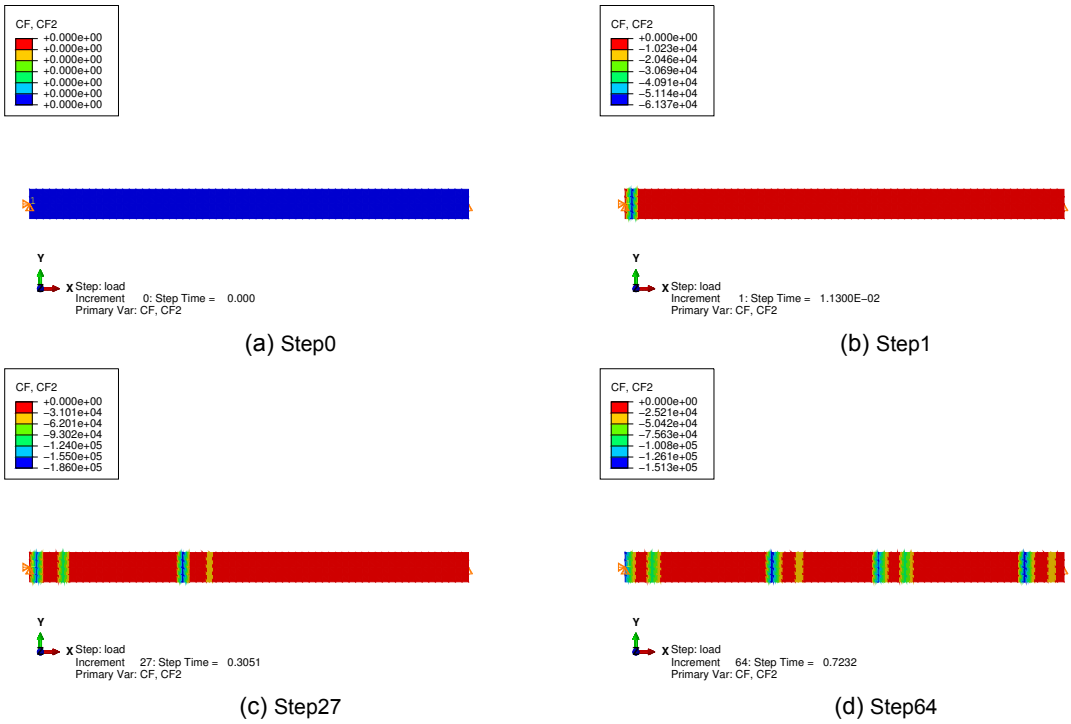

(a) Step0 (b) Step1

(c) Step27 (d) Step64

Figure 4.4: Concentrated force for simulation1 in undeformed rendered beam profile

4.4.2. Shear Force

In Figure 4.5, the shear force distribution in the rendered beam profile is shown. At time step 0, since there is no axle load and only self weight is acting on the bridge, the shear force distribution is maximum and equal in magnitude at the supports. However at time step1, as the train axle is over bridge node1 Figure 4.5(b), the shear force is higher at node 1. As the train moves over the bridge, the shear force changes and increases at both supports, though it remains unequal at both ends. When all four axles of the first two cars are on the bridge, the shear force at element 66 (which connects node 66 and 67) is higher than element 1.

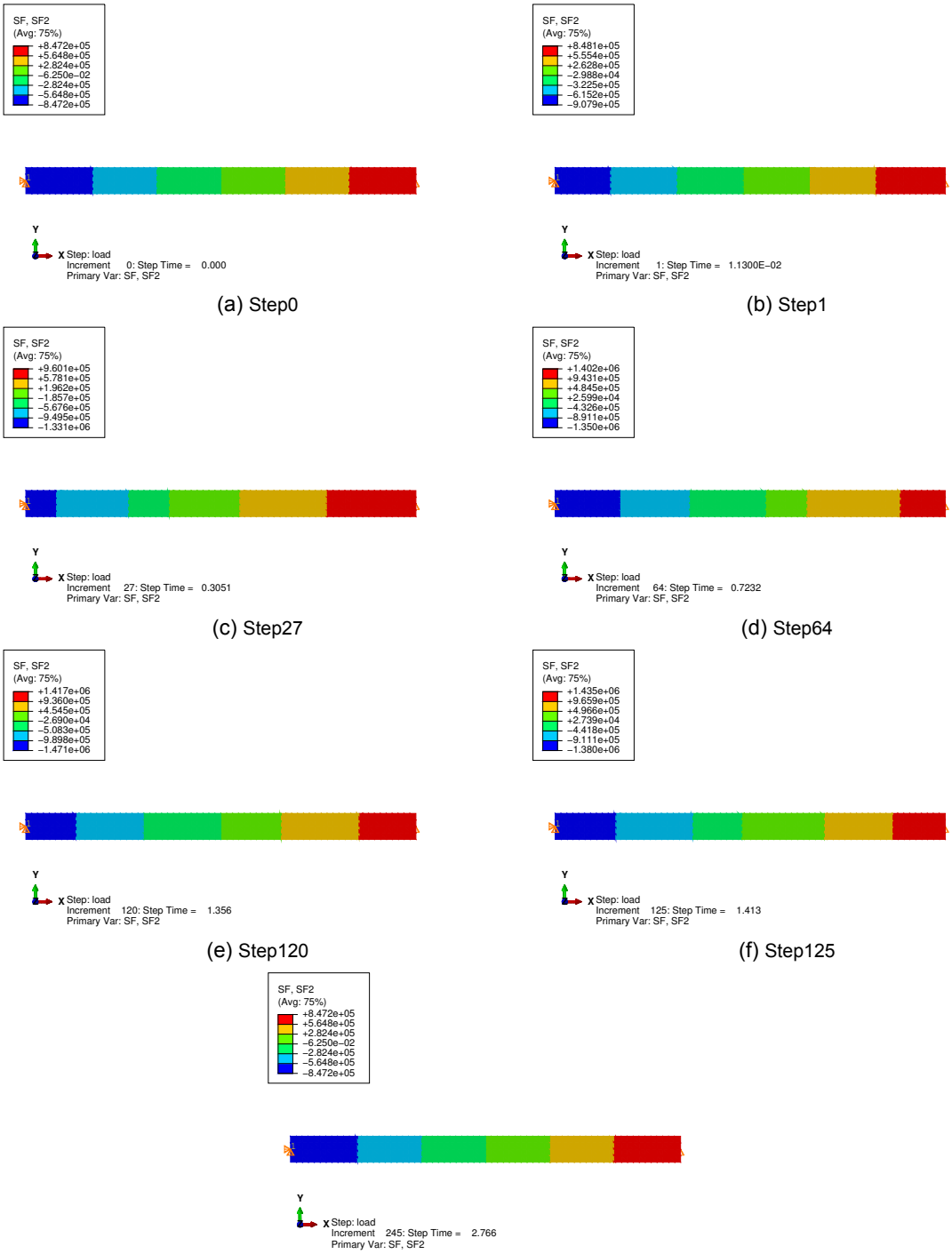

Figure 4.5: Shear force distribution for simulation1 in undeformed rendered beam profile

4.4.3. Bending moment

In Figure 4.6, the bending moment distribution in the rendered beam profile is shown. Bending moment is always maximum at the mid span or the region near the mid span in the beam. The bending stresses in a prestressed beam are mainly carried by the longitudinal reinforcement or prestressed tendon.

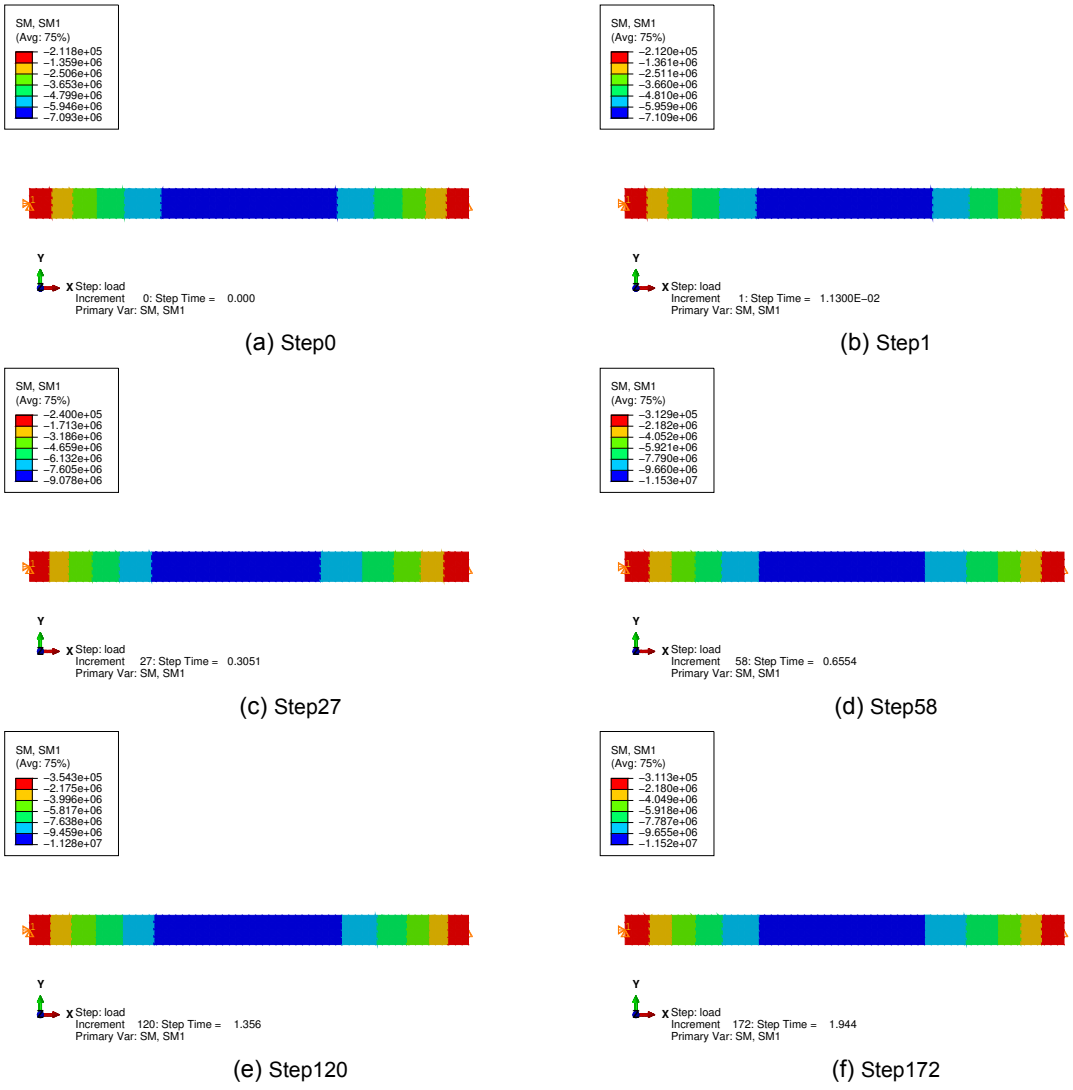

Figure 4.6: Bending moment distribution for simulation1 in undeformed rendered beam profile

4.4.4. Beam stress

The beam behavaiour is as according to expectations, that is compressive at the top and tensile at the bottom. The bending stresses are equal in compression and tension as seen from Figure 4.7. The shear stress observed in Figure 4.8, is critical at the end supports. It can also be observed that the shear stress increases as the more train axle get introduced on the beam

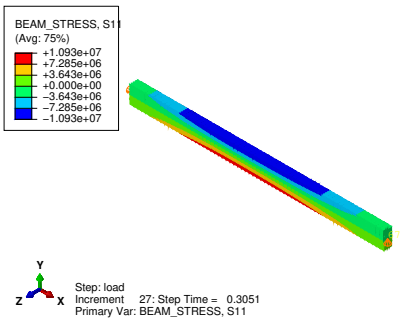

(a) Step27

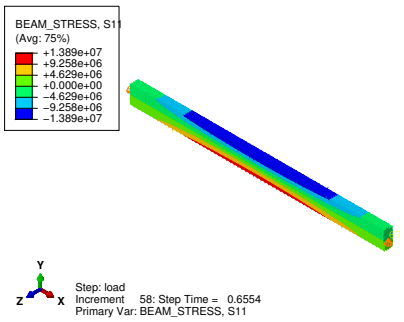

(b) Step58

Figure 4.7: Horizontal Stress (S11) distribution for simulation1 in undeformed rendered beam profile

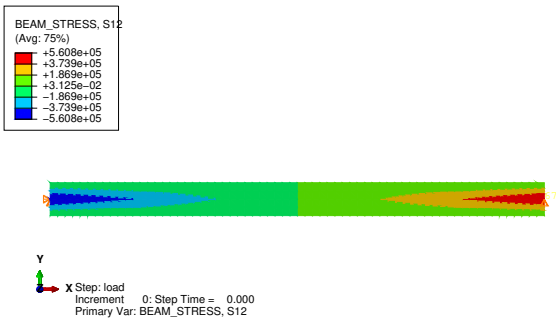

(a) Step0

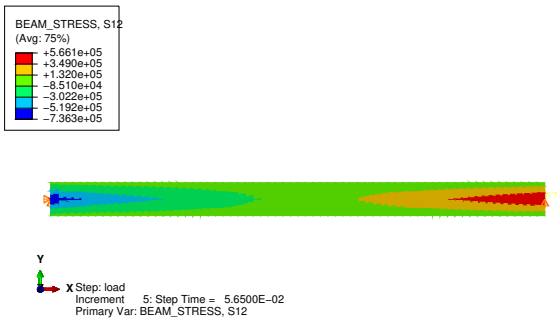

(b) Step5

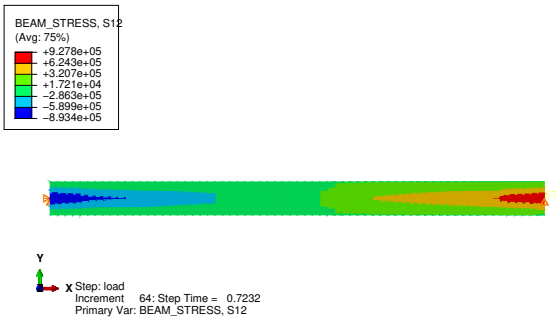

(c) Step64

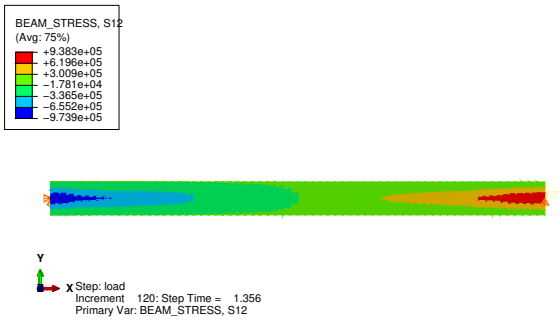

(d) Step120

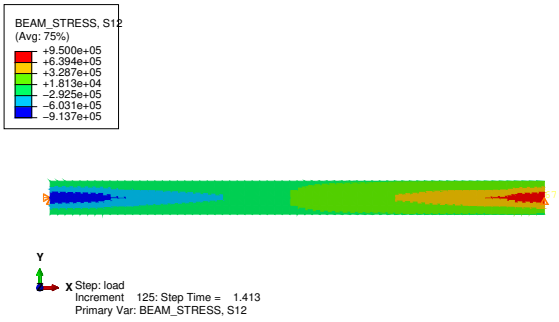

(e) Step125

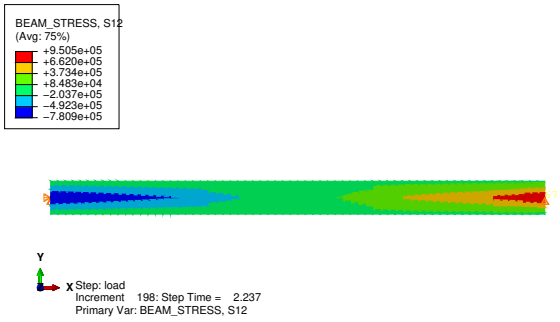

(f) Step198

Figure 4.8: Shear stress(S12) distribution simulation1 in undeformed rendered beam profile

5

Probabilistic Analysis

This chapter provides the details of the probabilistic assessment of the bridge. In the first part of the chapter, sampling using Monte-Carlo simulation is discussed. The second section of the chapter discusses the methodology to model moving load on the bridge. This is followed by determining the time steps at which maximum bending moment or shear force at critical sections is observed. The next section discusses the Non-Parametric Bayesian Network (NPBN) for the concrete simply supported beam, which described in chapter 4. Finally, the probability of failure under shear is discussed.

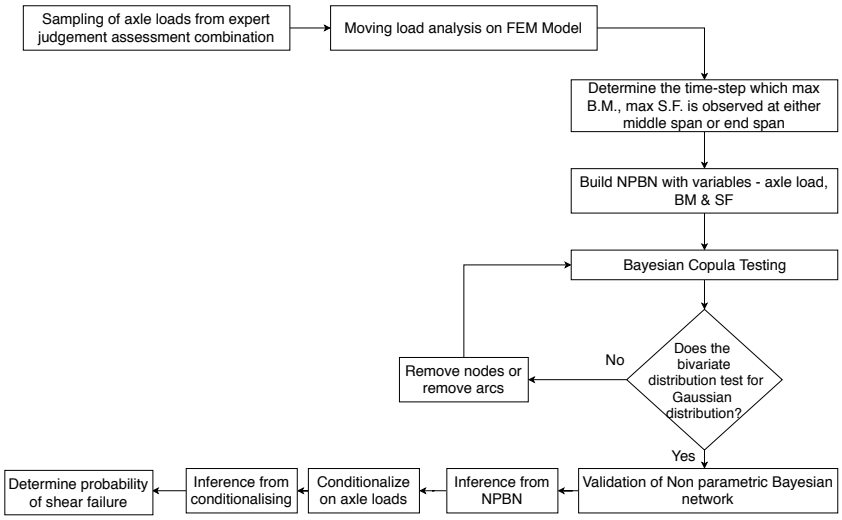

Figure 5.1: Representation of steps followed for probabilistic analysis of simply supported concrete beam

5.1. Theoretical background of Bayesian Network and Conditional Probability

Bayesian Networks, which are popularly also known as Bayesian Belief Networks, Causal nets, graphical probability networks or simply BN is an approach for graphical modeling of problems relating to uncertainty and probabilistic assessments. More formally, they can be defined as directed acyclic graphs (DAGs) comprising of nodes and arcs. The nodes in a BN represent univariate random variables and the dependency relations between these nodes are represented by arcs. BNs, because of their property to represent probabilistic distributions and dependence between variables is a useful tool to represent multi-dimensional probabilistic analysis. Furthermore,Bayesian network helps the analyst to draw statistical conclusions which can be made based on probability calculus and Bayes theorem. The graphical interface offered by Bayesian network is considered as its qualitative advantage, and the numerical analysis aspect can be treated as its quantitative advantage. More details about Bayesian Networks are explained in the following sections.

5.2. Probability and Statistics

As stated before, the Bayesian networks represent univariate distribution and dependencies between variables. These two concepts mainly represent the probability and statistical background of the BNs.

Dependence

Two quantities A and B are independent if beliefs about A do not change when given information about B.In statistical sense,

$$P(A|B) = \frac{P(A \cap B)}{P(B)} \tag{5.1}$$

where

$P(A|B) =$ probability of occurrence of A given occurrence of B. If A and B are independent, then $P(A|B)$ = $P(A)$

$P(A \cap B) =$ probability of occurrence of both A and B

$P(B) =$ probability of occurrence of B

The same definition can be extended to two jointly distributed continuous random variables X and Y (continuous because only continuous variables are dealt with in this research). The conditional density of X in presence of Y can be defines as the probability distribution of X when Y is equal to a particular value, or in mathematical expression can be given by $f_x(X|Y = y)$.

$$f(X,Y) = f_X(X|Y)f_Y(Y) = f_Y(Y|X)f_X(X) \tag{5.2}$$

The equation Equation 5.2 is based on the *Bayes' Theorem* according to which if $f_X(X) \neq 0$ and $f_Y(Y) \neq 0$ then :

$$f_X(X|Y) = f_Y(Y|X)f_X(X)/f_Y(Y) \tag{5.3}$$

$$f_Y(Y|X) = f_X(X|Y)f_Y(Y)/f_X(X) \tag{5.4}$$

Bayes' Rule is central to the understanding of the probability calculus perfomed in Bayesian Networks. The theorem in the context of distributions is explained further. Assuming we have two variables X and Y. These two variables are continuous and their joint distribution is given by $f(X,Y) = f_X(X|Y)f_Y(Y)$. Now, we have an observation for $X = x$, post which we would like to calculate $f_Y(Y|X = x)$ that is understand how would our belief change about Y when given information of $X = x$. In order to understand this, the terms *prior distribution* and *posterior distribution* are explained. The former term refers to the initial distribution obtained before any extra information is added. The latter term refers to the revised distribution using the additional information later obtained. Therefore, $f_Y(Y)$ is the prior distribution for Y and $f_Y(Y|X = x)$ is the posterior distribution for Y. According tp the Bayes' rule, $f_Y(Y|X = x)$ can be obtained by multiplying $f_Y(Y)$ with$f_X(X = x|Y)/f_X(X)$. Here $f_X(X = x|Y)$ can be written as the likelihood for Y given $X = x$ that is $L(Y|X = x)$. Hence, the posterior distribution can be expressed in terms of prior distribution and likelihood. This principle is used to conditionalise the Bayesian Network that is to derive posterior distribution after getting additional information regarding a variable or a set of variables.

The concept explained above can be extended to a set of n variables $(X_1, X_2, X_3 \cdots X_n)$ based on the chain rule given by:

$$f(X_1, X_2, X_3 \cdots X_n) = f(X_n|X_1, X_2, X_3 \cdots X_{n-1})f(X_{n-1}|X_1, X_2, X_3 \cdots X_{n-2}) \cdots f(X_1) \tag{5.5}$$

As mentioned before, the arcs in a BN represent dependence between variables. To quantify this dependence, there are few statistical measures available which are discussed below:

- Pearson's Product-moment correlation coefficient
  It can be defined between two variables X and Y in terms of covariance and standard deviation.

$$\rho_{X,Y} = \frac{cov(X,Y)}{\sigma_X \sigma_Y} = \frac{E(X \cdot Y) - E(X)E(Y)}{\sqrt{var(X) \cdot var(Y)}} \tag{5.6}$$

where

$E(X)$ = Expectation of variable X

$E(Y)$ = Expectation of variable Y

σ_X = standard deviation of X

σ_Y = standard deviation of Y

The Pearson's product-moment correlation coefficient hereafter referred to as product-moment correlation coefficient is defined in the interval [-1,1]. For $\rho \geq 0$, the variables X and Y are positively correlated, for $\rho \leq 0$, the variables X and Y are negatively correlated and for $\rho = 0$, the variables X and Y are independent. Positive correlation can be simply understood as a linear relation between X and Y with positive slope and similarly negative correlation can be understood as a linear relation with negative slope.

Though relatively straight-forward to compute, the product-moment correlation coefficient has certain drawbacks in uncertainty analysis. First, it is mainly defined for finite expectations and variance values of X and Y. Second, it is not invariant under non linear increasing transformations.

- Spearman rank correlation
  To overcome the difficulties in modelling dependencies using product-moment correlation coefficient, Spearman (1904) introduced the Spearman rank correlation.

$$r(X,Y) = \rho(F_X(x), F_Y(y)) \tag{5.7}$$

where

$r(X,Y)$ = Rank correlation

F_X = cumulative distribution functions for X

F_Y = cumulative distribution functions for Y

To compute the rank correlation, we simply substitute the values with their ranks. For example, we have K samples of vectors X and Y, then the distribution $(x_1, x_2 \cdots x_K)$ and $(y_1, y_2 \cdots y_K)$ can be converted to ranks $(x_1^{'}, x_2^{'} \cdots x_K^{'})$ and $(y_1^{'}, y_2^{'} \cdots y_K^{'})$ respectively. The sample rank correlation is computed Equation 5.8

$$r = \frac{\sum_i (x_i^{'} - x)(y_i^{'} - \bar{y})}{\sqrt{\sum_i (x_i^{'} - x)^2 (y_i^{'} - \bar{y})^2}} \tag{5.8}$$

where

$\bar{x}$ = mean of $(x_1, x_2 \cdots x_K)$

$\bar{x}$ = mean of $(y_1^{'}, y_2^{'} \cdots y_K^{'})$

Alternatively, the rank correlation can also be defined in terms of product moment correlation as given in Equation 5.17 for a normal copula (which will be elaborated upon later).

- Partial Correlation
  The partial correlation can be defined in terms of partial regression coefficients and can be computed similarly to partial regression coefficients.

$$\rho_{12;3,\cdots,n} = \frac{\rho_{12;3,\cdots,n-1} - \rho_{1n;3,\cdots,n-1}\rho_{2n;3,\cdots,n-1}}{\sqrt{1 - \rho^2{}_{1n;3,\cdots,n-1}}\sqrt{1 - \rho^2{}_{2n;3,\cdots,n-1}}} \tag{5.9}$$

5.3. Basics of Bayesian Network

A Bayesian Network as stated before consists of a set of variables $X = \{X_1, \cdots, X_n\}$ and dependencies between them. The directed acylic graphs (DAGs) represented a dependence structure of variables. Discrete BNs, continuous BNs and hybrid BNs are the three types of BNs for discrete variables, continuous variables and both types of variables respectively. Complete description of the approach can be found in [70]. A directed un-acylic graph of variables X_1, X_2 and X_3 is shown in Figure 5.2. The concept of parent and child in a Bayesian network is explained though this figure. variable X_2 is a child of variable X_1 and X_1 is a child of X_3 and similarly X_3 is a child of X_1. Further, X_1 is a parent to variables X_2 and X_3 and X_2 are parents to X_1 and X_3 respectively.

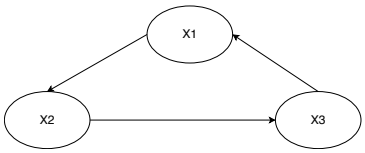

Figure 5.2: directed un-acyclic graph of X1,X2,X3

In Figure 5.3(a), it is seen that X_1 influences X_2 and X_2 influences X_3, however X_1 does not directly influence X_3. Therefore, if value of X_2 is known, X_1 and X_3 are completely separated. This concept is known as *d-separation* in which X_1 has not influence on X_3. In Figure 5.3(b), the children $X_2, X_3 and X_4$ are d-separated if X_1 is known. The third case is interesting, where the child node X_1 has three parents X_2,X_3 and X_4. If information about X_1 is known, $X_2, X_3 and X_4$ are dependent.

Thus a BN is constructed first by identifying the relevant variables which are non-deterministic in nature. The model builder then arranges them as nodes and arcs and the arcs representing dependencies must be quantified by the model builder. Given the parents of a particular node, the child node variables is conditionally independent of its ancestors. Hence mathematically expressing, let each variables be associated with a conditional probability function of the variable given its parents $f_{X_i|Pa(X_i)}$ then the joint probability can be written as:

$$f x_i, \cdots, x_n = \Pi_{i=1}^{n} f_{X_i|Pa(X_i)}(x_i|x_{Pa(x_i)}) \tag{5.10}$$

if

$Pa(X_i) = 0$ then $f_{X_i|Pa(X_i)} = f_{x_i}$

In Equation 5.10, if variable X_i has no parents, then the variable is independent at all times.

In order to explain Non Parametric Bayesian Network (NPBN), first the concept of Copulas will be introduced since the NPBNs are based on bivariate copulas.

5.4. Copulas

In simple terms, copula can be understood as a distribution on the unit square such that its marginal distributions are uniform. The dependence structure of associated random variables are included in a copula. According to R.B. Nelson, a copula is a function C from $[0,1]^2$ to $[0,1]$.

In two dimensions, joint distribution of two variables X and Y defined in terms of the function C as :

$$F_{X,Y}(x,y) = C(F_X(x), F_Y(y)) \tag{5.11}$$

where

$F_{X,Y}$ = joint distribution of (X,Y)

$F_X(x)$ = marginal density of X

$F_Y(y)$ = marginal density of Y

In this research, only Gaussian or normal copula is used.The terms normal and Gaussian in the content of copulas and joint distributions are interchangeable.

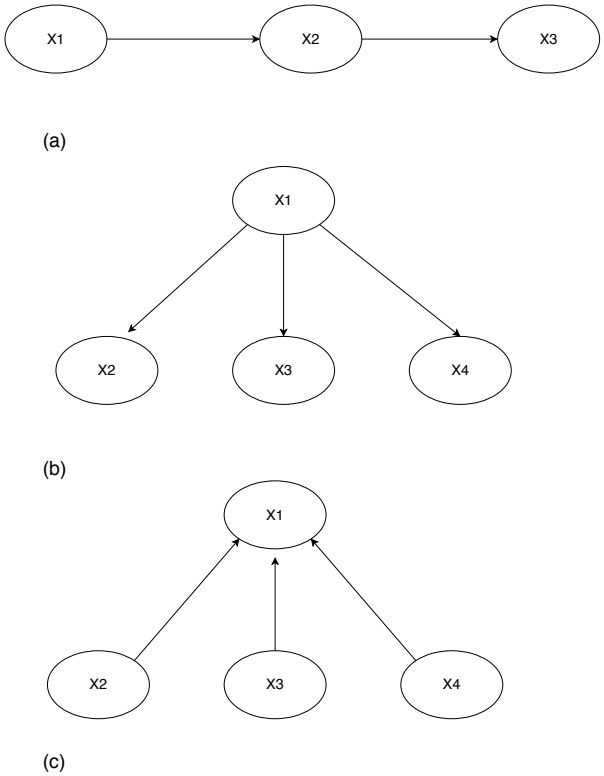

Figure 5.3: Different types of directed acyclic graphs (a)Serial Connection (b)Diverging Connection (c)converging Connection

Gaussian Copula

A multivariate normal distribution is used to build a Gaussian copula using the probability integral transform.

$$C_{\sum}(u) = \Phi_{\sum}(\Phi^{-}1(u_1), \cdots, \Phi^{-}1(u_d)); \mathrm{u} \in [0,1]^d \tag{5.12}$$

where

$\Phi^{-}1 =$ inverse commutative distribution function of standard normal

$\Phi_{\sum} =$ joint commutative distribution function of multivariate normal distribution with mean vector zero and covariance matrix equal to the correlation matrix $\sum$

For a bivariate copula, the Gaussian copula is expressed as:

$$C_{\rho}(u, v) = \Phi_{\rho}(\Phi^{-}1(u), \Phi^{-}1(v)) \tag{5.13}$$

where

$u, v \in [0,1]^d$

$\rho =$ product moment correlation between X and Y

A covariance matrix for a bivariate copula is given by :

$$\sum = \begin{pmatrix} 1 & \rho \\ \rho & 1 \end{pmatrix} \tag{5.14}$$

Further, the conditional product moment correlation is equal to partial correlation for joint normal variables [33] (refer Equation 5.15 and Equation 5.16).

$$\rho_{XY;Z} = \rho_{XY|Z} \tag{5.15}$$

For a normal copula,

$$\rho_{1,2|3} = \frac{\rho_{1,2} - \rho_{1,3}\rho_{2,3}}{\sqrt{1-\rho^2{}_{1,3}}\sqrt{1-\rho^2{}_{2,3}}} \tag{5.16}$$

$$\rho = 2 * sin(r * \pi/6) \tag{5.17}$$

where

$\rho =$ product moment correlation

$r =$ Spearman's Rank correlation

For a normal copula, a relation between product moment correlation and Spearman's rank correlation can be established according to Equation 5.17.

5.5. Non Parametric Bayesian Network

In a continuous NPBN, the nodes are linked with a continuous invertible distribution function. The influence of a parent on a child node is given by a (conditional) one parameter copula. This parameter characterises association between variables and can be for example Spearman's rank correlation r or Kendall's tau. The arcs of the NPBN is assigned conditional copulas/rank correlations. For each variable X_i with m parents $X_k = Pa_1(X_i), \cdots, X_l = Pa_m(X_i)$ associate the arc $Pa_j(X_i) -> X_i, j = 1, \cdots, m$ with rank correlation:

$$r(X_i, pa_j(X_i)), j = 1 \tag{5.18}$$

$$r(X_i, pa_j(X_i)|pa_1(X_i), \cdots, pa_{j-1}(X_i)), j = 2, \cdots, m \tag{5.19}$$

The order in Equation 5.19 is not unique and there can be a different order of the labelled variables. According to Hanea et al. given a continuous NPBN on n variables, the joint distribution of the variables is uniquely determined. Furthermore, the arcs of a NPBN can be assigned any number $\in [-1, 1]$. The rank correlations will be realized using bivariate (conditional) copulas.

5.6. Monte Carlo simulation

In simple terms, computational algorithms that rely on repeated random sampling to obtain numerical results can be broadly termed as Monte Carlo methods[1]. The main concept is to use randomness to solve problems that are uncertain. There are majorly three problem types where Monte Carlo methods can be applied: numerical integration, optimisation,and producing random samples from a probability distribution. In this research, in order to generate samples from the probability distribution of axle loads, which is elicited using expert judgment studies (see chapter 3), Monte Carlo simulation is performed. For more details on this methodology see Appendix A.

In order to perform Monte Carlo simulations, MATLAB functions are used in this research. At first, the command *copularnd* is used to generate 1000 random samples from Gaussian copula of variables whose correlation matrix is given by *R*. In Equation 5.20, ρ_{EJ} denotes the rank correlation matrix between the four variables (axle1, axle2, axle3, axle4) as elicited from the expert judgment studies. After the Monte Carlo simulations, the rank correlation between the same variables is given in Equation 5.21 where $\rho_{sampling}$ denotes the rank correlation matrix of the samples generated.

$$\rho_{EJ} = \begin{pmatrix} 1 & 0.31 & 0.19 & 0 \\ 0.31 & 1 & 0.59 & 0.35 \\ 0.19 & 0.59 & 1 & 0.59 \\ 0 & 0.35 & 0.59 & 1 \end{pmatrix} \tag{5.20}$$

$$\rho_{sampling1000} = \begin{pmatrix} 1 & 0.34 & 0.15 & -0.03 \\ 0.34 & 1 & 0.57 & 0.30 \\ 0.15 & 0.57 & 1 & 0.53 \\ -0.03 & 0.30 & 0.53 & 1 \end{pmatrix} \tag{5.21}$$

[1] source : Wikipedia

For the purpose of comparison, a samples of 10000 values is extracted using Monte Carlo simulations. The obtained correlation matrix is given in Equation 5.22.

$$\rho_{sampling10000} = \begin{pmatrix} 1 & 0.30 & 0.20 & 0.01 \\ 0.30 & 1 & 0.59 & 0.34 \\ 0.2 & 0.59 & 1 & 0.59 \\ 0.01 & 0.34 & 0.59 & 1 \end{pmatrix} \tag{5.22}$$

When performing Monte Carlo simulations, it is to be noted that a large number of samples should be generated so that the sample distribution mirrors the probabilistic distribution from which it is generated. In this research, due to the constraints in computational resources, the number of samples is restricted to 1000 even though we observe a slight deviation between $\rho_{EJ} and \rho_{sampling1000}$. However, a higher number of samples, e.g. to the order of 10^4 is recommended for future analysis.

5.7. Concrete uncertainty

As introduced before in chapter 2, uncertainty in the concrete properties is incorporated in the mass density(w_c), the characteristic strength (f_{ck}) and the Young's modulus(E_c). These properties of concrete, are modelled as stochastic variables. Poisson's ratio of concrete is however considered as a deterministic variable. In order to derive the uncertainty in the material properties, experimental tests are performed. In the absence of experimental tests, one of the ways to derive the stochastic properties of concrete is from Probabilistic Model Code developed by Joint Committee on Structural Safety (JCSS) [44]. In this research, the concrete uncertainty is modelled based on the experimental research performed in Mexico by past researchers [53] (see Table 5.2). A comparison is drawn between the model parameters derived from experimental research and those derived from JCSS code (see Table 5.3).

5.7.1. Experimental Results

In this research, based on the based experimental tests the mean values and standard deviation of characteristic strength of concrete is computed. To calculate the mean value of concrete Young's modulus, formulae suggested by fib Model Code for Concrete Structures 2010[8] are used. The prescribed formulae are repeated in this section.

The mean value of Young's modulus of concrete, E_{cm} after 28 days is given in

$$E_{cm} = E_{c0} \cdot (\frac{f_{cm}}{10})^{1/3} \tag{5.23}$$

where

E_{c0} = 2.2E+04 Mpa

f_{cm} = mean concrete compressive strength in MPa

5.7.2. Calculation from Probabilistic Design code

The Probabilsitic Model Code (PMC) Part 3: Resistance models (JCSS 2001) provide formuale and guidelines for the calculation of concrete properties. Similar to the Eurocode, in PMC, the properties of concrete are based on the basic concrete compression strength, f_{c0}, which is the compressive strength of a standard test specimen (cylinder).

The in-situ compressive strength, f_c can be determined from f_{c0} factoring in concrete age at loading time, duration of loading and spatial variability. Further, the other properties of concrete can be calculated from f_c. For probabilistic analysis, further variability is also incorporated.

To calculate the elastic properties of concrete, first step is to compute the concrete compressive strength. In general, the distribution of concrete compressive strength is log normal, given that the parameters are derived from an ideal infinite sample. For practical purposes, a sufficiently high number of samples are also acceptable for log normal distribution. According to the model proposed in PMC [44], reference concrete strength distribution can be expressed as :

$$f_{co,ij} = exp(m'' + t_v s'' * (1 + 1/n'')^{0.5}) \tag{5.24}$$

where

$m", n", s", v"$ = Parameters,depend on the amount of specific information [44]

$f_{co,ij}$ = distribution of concrete compressive strength in MPa

t_v = Student's t-variate with v degrees of freedom

The distribution of $f_{co,ij}$ is expressed in terms of coefficients m'', n'', s'', v'' which are derived post testing (posterior information)

The coefficient n is interpreted as a "hypothetical number of observations" from which the mean value m was estimated.Further, v is denotes "degrees of freedom" and refers to the number of tests, which can either real or hypothetical, based on which the standard deviation s was determined (number of tests – 1). Usually, to analyse the test results $v = n - 1$.

If no prior information (that is tests) is available, then based on past research,[44],Table 5.1 gives the specific values.

Table 5.1: Prior parameters for concrete strength distribution (f_{co} in MPa) [44] [73]

Concrete Type	Concrete Grade	Parameters			
		m'	n'	s'	v
Ready Mix	C15	3.40	3.0	0.14	10
	C25	3.65	3.0	0.12	10
	C35	3.85	3.0	0.09	10
	C45	3.98	3.0	0.07	10
Pre-cast element	C25	3.80	3.0	0.09	10
	C35	3.95	3.0	0.08	10
	C45	4.08	4.0	0.07	10
	C55	4.15	4.0	0.05	10

The coefficients m', n', v', s' denote the information prior to the test (prior information).

According to [44], if $n'', v'' > 10$, a log-normal distribution for concrete strength probabilistic distribution is a good fit with mean m'' and standard deviation $s'' \frac{n''v''}{(n''-1)(v''-2)}$.

Other than the characteristic for determining the mean value of compressive strength, according to PMC, variability due to 'additional factors' like variation in curing, the concrete age, loading time and the duration of loading should also be incorporated.

In general, when no experimental measurements are available and the concrete type is known, stochastic values of concrete compressive strength can be derived as:

- Identify the concrete class, and select the coefficients m', n', s', v' from Table 5.1
- Using MATLAB, generate many samples, that is 100000 samples of lognormal distribution of mean m' and standard deviation $\sigma = s' \frac{n'v'}{(n'-1)(v'-2)}$
- Using the log normal distribution compute the mean and variance of the associated normal distribution
- Compute the characteristic value on the 5th percentile of the cummulative distribution

The derived values for C25, C30, and C35 are listed in Table 5.3. It is to be noted here that in these calculation spatial variability is not considered. When compared the results with those obtained from experimental results, we can observe that the obtained distribution of characteristic strength is different.

Table 5.2 lists the material properties that are used in this research. These properties are taken from the experiments performed in Mexico by past researchers [53].

Table 5.2: Properties of concrete properties (C25) for random variables and deterministic variables based on past experiments [53]

	Distribution Type	k	μ	σ	θ	$others$
Characteristic strength(f_{ck}) (Mpa)	Lognormal		3.4782	0.1098		
Youngs modulus (E_c)(Mpa)	Lognormal		10.3697	0.0025		
Density of concrete (kN/m^3)	Generalized pareto	-1.3015		1.5359	21.959	
Poisson's Ratio	Deterministic					0.15

Note:*this is calculated based on the formulae given in Table 2.1

Table 5.3: Properties of concrete properties (C25, C30 and C35) for random variables and deterministic variables based Probabilistic Model Code [44]

	C25	C30(interpolated)	C35
Mean (lognormal)	3.65	3.75	3.85
Standard deviation (lognormal)	0.1643	0.14375	0.1232
Mean (Mpa)	39	42.9	47.35
Standard deviation (Mpa)	6.45	6.20	5.86
Coefficient of variation	0.165	0.145	0.124
Characteristic value(Mpa) (fck)	29.36	33.61	38.37

5.7.3. Dependence between material properties

Based on Table 5.2, the marginal distribution of the material properties is obtained. However, to model the wc, fc, and Ec in NPBN, information about their partial dependence is required. Based on the experimental test, the Pearson's product moment correlation is known for the pairs (fc,Ec) and (wc,Ec). Hence to derive the correlation matrix, an assumption is taken in this research that is Ec and wc are conditionally independent which mathematically implies $\rho_{Ec,wc|fc} = 0$. The assumption is illustrated in Figure 5.4.

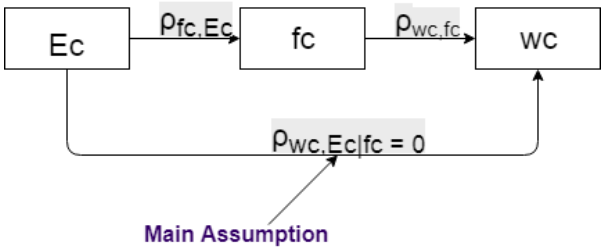

Figure 5.4: Model assumption for dependence between material properties

Further, using the Equation 5.9, the $\rho_{Ec,wc}$ can be estimated by Equation 5.26.

$$\rho_{Ec,wc} = \rho_{Ec,fc} \cdot \rho_{fc,wc} \tag{5.25}$$

where

$\rho_{Ec,fc} = 0.87101$

$\rho_{fc,wc} = 0.22144$

Hence,

$$\rho_{Ec,wc} = 0.1929 \tag{5.26}$$

The derived correlation matrix obtained is given in Equation 5.27.

$$\Sigma corr = \begin{matrix} \\ \text{Ec} \\ \text{fc} \\ \text{wc} \end{matrix} \begin{matrix} \begin{matrix} \text{Ec} & \text{fc} & \text{wc} \end{matrix} \\ \begin{pmatrix} 1 & 0.87 & 0.19 \\ 0.87 & 1 & 0.22 \\ 0.19 & 0.22 & 1 \end{pmatrix} \end{matrix} \tag{5.27}$$

5.8. Maximum Bending Moment and Shear Force

For each sample of axle load generated using Monte-Carlo simulation, finite element analysis is performed. That is, for each sample of the axle load, the load is treated as deterministic for the finite element analysis. As the time crosses the bridge, the bending moment and shear force at different nodes change for each sample distribution of axle loads. In order to estimate the probability of failure under shear, it is important to first determine the position of the train at which maximum shear force or maximum bending moment is observed. It is observed, that the maximum bending moment is observed at the midspan of the simply supported beam and maximum shear force is observed at the supports. This is similar to the case when the beam is loaded under uniformly distributed load. Hence the axle load behaves as distributed load on the beam with each axle carrying different load for each simulation.

It is observed that for almost simulations, the maximum shear force at support is observed at time = 1.822s for the train moving at 160km/h (given that the train enters the bridge at time=0s). Since the observed bending moment is also nearly maximum at the obtained position, the probabilistic assessment is carried out for the train position at time=1.822s.

Figure 5.5: Axle load position on the beam at t=1.822s

5.9. Non-Parametric Bayesian Network

To derive meaningful information from a database with a large number of variables is a complex procedure. Further, numerical ordering of variables in a multivariate set is important. In this research, marginal distributions of axle loads, properties of concrete, bending moment, shear force and displacement and their numerical ordering is used to obtain relevant information to compute probability of failure of the bridge. However, such an information is meaningless if the data is not represented adequately. One of the methods to model such a multivariate set is using a NPBN with Gaussian copula. An algorithm was introduced by Hanea [34] to learn the structure of a continuous NPBN with the Gaussian copula from multivariate dataset, containing a large number of variables and having no assumptions about the marginal distributions of these variables. The proposed algorithm is incorporated in the software UNINET [42] which is a standalone software for uncertainty analysis. It has a friendly user interface and performs fast simulations. In this research, all BN's are developed using UNINET.

Prior to the development of a NPBN with Gaussian copula, a diagnostic test is performed to verify that the joint normal copula is an adequate assumption for the given data. In order to do so, there are two tests that are applied in this research. The first is the semi-correlations approach. In the second

test, a model validation is performed by comparing the determinant of normal rank correlation with determinant of Bayesian belief network. These two tests are described in the following sections:

5.9.1. Semi-correlations approach

The semi-correlations approach is an approach suggested by Joe [47]. To compute the semi-correlations, the original variables are first transformed to standard normal distribution followed by computation of Pearson's product moment correlation in the upper half and lower half quadrants of the obtained normal distribution. Practically, given two variables (X, Y) and their standard normal transforms (Z_1, Z_2), the semi-correlation in the upper and lower quadrants can be expressed according to Equation 5.28 and Equation 5.29.

$$\rho_{ne} = \rho(Z_1, Z_2 | Z_1 > 0, Z_2 > 0) \tag{5.28}$$

$$\rho_{sw} = \rho(Z_1, Z_2 | Z_1 < 0, Z_2 < 0) \tag{5.29}$$

where

ρ_{ne} = semi-correlations in the upper right quadrant (NE)

ρ_{sw} = semi-correlations in the lower right quadrant (SW)

A positive correlation maybe expressed by ρ_{ne} and ρ_{sw}. For a negative correlation, semi-correlations in the upper left (NW) quadrant, ρ_{nw} and lower right quadrant (SE), ρ_{se} can be expressed by Equation 5.30 and Equation 5.31.

$$\rho_{nw} = \rho(Z_1, Z_2 | Z_1 > 0, Z_2 < 0) \tag{5.30}$$

$$\rho_{se} = \rho(Z_1, Z_2 | Z_1 < 0, Z_2 > 0) \tag{5.31}$$

where

ρ_{nw} = semi-correlations in the upper left quadrant (NW)

ρ_{se} = semi-correlations in the lower left quadrant (SE)

To describe the test using the semi-correlation, first the concept of **tail dependence** is introduced. Tail dependence is an important aspect of joint distributions. The upper tail dependence coefficient λ_U for two random variables X and Y is defined according to the equation Equation 5.32.

$$\lambda_U = \lim_{u \to 1} P(X > {F_X}^{-1}(u) | Y > {F_Y}^{-1}(u)) = \lim_{u \to 1} P(U > u | V > u) \tag{5.32}$$

$\lambda_U > 0$ indicates that it is likely (more than normal) to observe values of U greater than u given that V is greater than u for u almost close to 1. lower tail dependence is defined similar to upper tail dependence but for lower quadrant as expressed in Equation 5.33.

$$\lambda_U = \lim_{u \to 1} P(X < {F_X}^{-1}(u) | Y < {F_Y}^{-1}(u)) = \lim_{u \to 1} P(U < u | V < u) \tag{5.33}$$

For a Gaussian copula, no tail dependence is observed, that is, $\lambda_U = 0$. As a rule of thumb, tail dependence may be suggested if the larger absolute values of semi-correlations ($|\rho_{ne}|, |\rho_{sw}|, |\rho_{nw}|, |\rho_{se}|$) than the overall correlation are observed. As stated in earlier sections, Gaussian copula presents no tail dependence. Therefore, to verify that the Gaussian copula is an adequate assumption for the given data set, semi-correlation approach can be used.

5.9.2. Validation of the model

Model validation approach is used to verify the validity of joint normal copula for the given multivariate data. It is also used to validate the Bayesian network in terms of the accuracy of the results. In this method, the rank correlation matrices are used a tool to perform model validation. The determinant of a rank correlation matrix is 1 if all the variables are independent and, 0 if there exists a linear dependence between the variables transformed to standard normals [33]. In this approach, determinant of empirical rank correlation matrix (DER) and determinant of empirical normal rank correlation matrix (DNR) are computed. It is verified that the DER lies within the 90% confidence interval of the DNR. The detailed methodology on the statistical method is given as follows:

- Compute DER which is the determinant of the empirical rank correlation matrix. It is obtained by transforming the distribution of each variable to uniform distribution and then calculating the product moment correlation of the obtained transformed variables. The product moment correlation is further converted to rank correlation using Equation 5.17.
- Compute DNR which is the determinant of the empirical normal rank correlation matrix. This matrix is obtained by transforming the distribution of each variable to standard normal and then transforming the product moment correlation to rank correlation using Equation 5.17.
- Re-sample the data obtained from normal distribution to obtain the empirical distribution of DNR and obtain the 5^{th} and 95^{th} quantiles of this distribution
- Check if the DER obtained falls in the quantile obtained in the previous step. If yes, then the joint copula is valid else rejected.

In the past research [33], it is observed that for large data sets the above described statistical tests often fails. Hence, often the validation step is relaxed to favour better quantification of the model.

In this approach, a second step for validation entails constructing a skeletal NPBN and computing the determinant of rank correlation matrix of an NPBN (DBN) using the normal copula. The second step is described as follows:

- A skeletal NPBN is constructed
- Generate samples from the constructed BN to obtain the DBN
- Find the pairs of variables which don't have an arc between them in the DAG. From these pairs, choose the pair with the highest rank correlation. Add an arc between the obtained pair and recompute the DBN and its 90% confidence band.
- Check if the DNR is within the obtain 90% confidence band of DBN. If yes then the NPBN is validated else rejected and procedure from step 3 is repeated.

Complete automation of the procedure to build a NPBN is not there currently. This is because it is impossible to infer all directionality of influence from a multivariate data. Thus, it is possible that there are different NPBN structures which maybe equivalent or non-equivalent and may represent statistically acceptable models of a given multivariate data set. Generally, there is no definition of a 'best' model'. As far as the model represents the data to certain extent, provided it satisfies the above described tests, it can be an acceptable model for practice. Also, non-statistical reasoning may be used to build the arcs between nodes to represent directionality. In some cases, certain influences even though small may be included because the user wants to observe such influences.

5.9.3. Bayesian Network -I

This section describes the algorithm for learning a Bayesian network from data using a multivariate data set. The data set consists of the axle load obtained from Expert judgment studies and further sampled from Monte-Carlo simulations. Further, variables for concrete uncertainty are also included in the data set. Finally, the response of the bridge in the form of four variables- shear force at end supports, bending moment at mid span and displacement at mid span are incorporated in the multivariate data set. The data set contains 1000 samples forming the joint-distribution obtained from Monte-Carlo simulations. In the constructed Bayesian Network -I (BNI), the multivariate set is taken such that all cars of the train have the same distribution. It is assumed that every $n = 1 \ldots N$ car has $j = 1 \ldots 4$ axles, and distribution of every j^{th} axle of all N cars is exactly the same. The definition of the variables are listed in Table 5.4. The frequency histograms of the selected variable are plotted which is shown in Figure 5.6, Figure 5.7 and Figure 5.8 with values on the x axis and number of samples on y axis.

Table 5.4: Names and definitions of variables of BNI

Name of Variable	Units	Description
Axle 1	kN	Load in the first axle of each car
Axle 2	kN	Load in the second axle of each car
Axle 3	kN	Load in third axle of each car
Axle 4	kN	Load in fourth axle of each car
Ec	MPa	Young's modulus of concrete
wc	kg/m^3	Density of concrete
fc	Mpa	Characteristic strength of concrete
u	mm	Vertical displacement at mid span
BMn2	kN-m	Bending moment at mid span
SFn1	kN	Shear force at left support
SFn2	kN	Shear force at right support

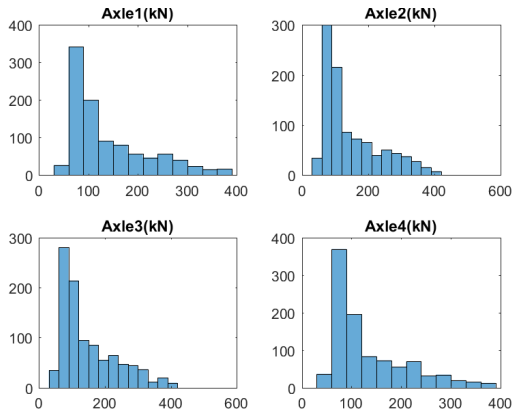

Figure 5.6: Histogram of Axle1, Axle2, Axle3 , Axle4

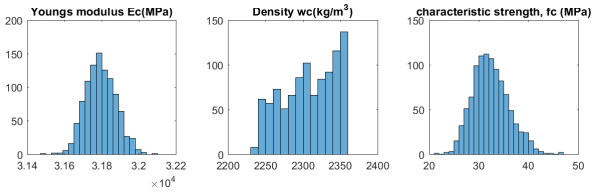

Figure 5.7: Histogram of Ec, wc, fc

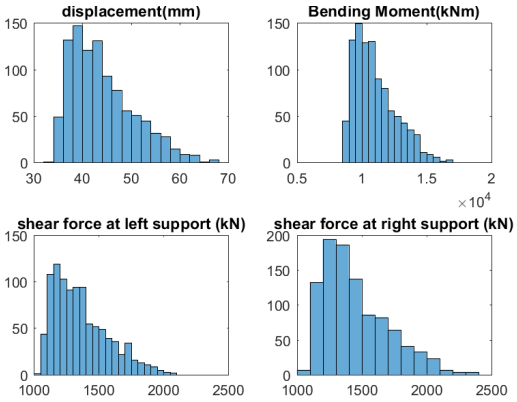

Figure 5.8: Histogram of u, BMn2, SFn1, SFn2

From Figure 5.6, it can be seen that the frequency of high magnitude of axle load is lower for all four axles and no value greater than 400kN is observed in the data set. In Figure 5.7, it can be observed that the Ec and fc behave consistently which may be because the value of mean Ec is derived from fc. In Figure 5.8, the response of the bridge in displacement, bending moment at mid span and shear force at end support are consistent with each other and also with the axle loads. It is observed that there is difference in the maximum observed shear force at the two supports, however most of the shear force in both supports is around 1200kN.

First the hypothesis that the dependence structure in the data is that of a joint normal copula can be tested by using semi-correlation approach, the theory of which is described above. The results of the semi-correlation test are listed in Table 5.5 and selected plots are shown in Figure 5.9,Figure 5.10, Figure 5.11, Figure 5.12 and Figure 5.13.

Table 5.5: Semi-correlations test for all pairs of variables (X,Y) used in the Bayesian network for bridge response

X	Y	ρ	ρ_{ne}	ρ_{sw}	ρ_{nw}	ρ_{se}
Axle1	Axle2	0.35	0.15	-0.01	0.08	0.12
Axle1	Sfn1	0.60	0.36	0.21	0.30	0.50
Axle1	BMn2	0.52	0.26	0.15	0.26	0.48
Axle1	SFn2	0.46	0.23	0.10	0.20	0.49
Axle1	u	0.55	0.30	0.18	0.29	0.51
Axle2	Axle3	0.59	0.32	0.35	0.12	0.07
Axle2	Sfn1	0.83	0.70	0.51	0.08	0.36
Axle2	BMn2	0.78	0.61	0.46	0.08	0.38
Axle2	SFn2	0.74	0.52	0.43	0.12	0.35
Axle2	u	0.79	0.62	0.47	0.11	0.42
Axle3	Axle4	0.55	0.28	0.33	0.11	0.10
Axle3	Sfn1	0.71	0.54	0.45	0.13	0.44
Axle3	BMn2	0.79	0.66	0.49	0.16	0.38
Axle3	SFn2	0.83	0.73	0.52	0.12	0.30
Axle3	u	0.77	0.61	0.48	0.17	0.34
Axle4	Sfn1	0.54	0.33	0.26	0.09	0.46
Axle4	BMn2	0.63	0.46	0.31	0.12	0.43
Axle4	SFn2	0.68	0.52	0.34	0.11	0.42
Axle4	u	0.61	0.43	0.29	0.08	0.45
Ec	fc	0.87	0.74	0.70	0.26	0.33
Ec	u	-0.04	-0.04	0.07	0.02	-0.06
wc	fc	0.23	0.04	0.09	0.00	0.17
wc	Sfn1	0.05	0.11	0.14	0.02	0.17
wc	BMn2	0.06	0.09	0.13	0.04	0.16
wc	u	0.05	0.09	0.11	0.02	0.16
SFn1	BMn2	0.99	0.95	0.98	0.46	0.65
SFn1	SFn2	0.96	0.87	0.93	0.36	0.58
SFn1	u	0.99	0.97	0.99	0.57	0.64
BMn2	SFn2	0.99	0.98	0.99	0.44	0.49
BMn2	u	1.00	0.99	1.00	0.61	0.43
SFn2	u	0.99	0.95	0.97	0.55	0.35

From Table 5.5, it is observed that 26 out of 31 pairs of variables verify the semi-correlation test. The absolute value of the correlation (ρ) of the whole model is greater than the absolute value of the semi-correlations for these pairs. For the correlation between Axle1 and SFn2, very slight lower tail dependence is indicated hence Gaussian copula is a valid assumption. This is also valid for the pair of Ec and u where a slight lower dependence is observed. For the pair of variables with one variable as wc, a high lower tail dependence is observed. However, to study the influence of the density on the bridge response, wc is included in the NPBN. It can be summarized that the Gaussian copula is a suitable assumption for most of the bivariate distribution in the Bayesian network developed for bridge response.

From Figure 5.9,Figure 5.10, Figure 5.11 and Figure 5.12, it is observed that the response of the bridge is positively correlated to the axle loads on the bridge. This observation follows the intuitive conclusion. It can be also observed that axle 2 and axle3 loads have a higher correlation with the shear force, bending moment and vertical displacement of the the bridge. In Figure 5.13, it is observed that the variables representing the bridge response that is, shear force, bending moment, and displacements have a very high positive correlation. This may be observed considering the linear elastic analysis performed in the model. Therefore in the model, either of these variables can be incorporated and the others can be removed since they provide almost the same information. However, in this research, all the variables are incorporated in the Bayesian network to study the influence on the bridge response in terms of individual components.

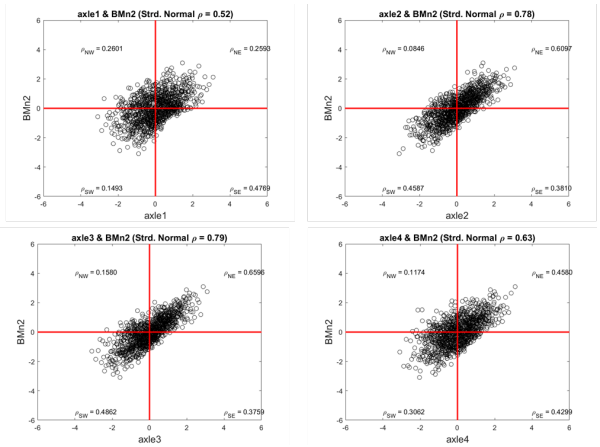

Figure 5.9: Graphs of Bending moment paired with axle loads in the Bayesian network. The values of the semi-correlation are indicated for each quadrant and for sample in the title

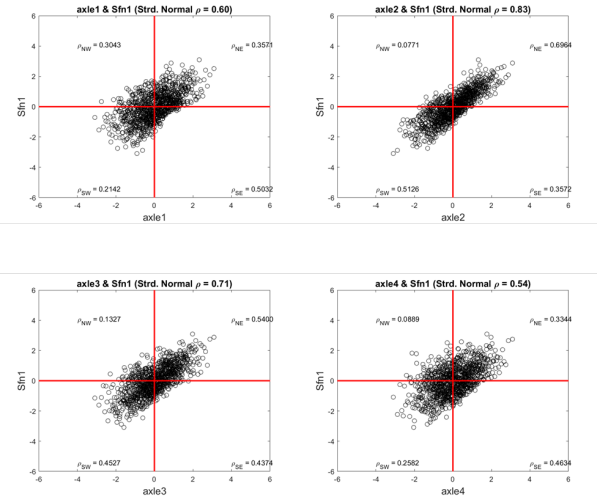

Figure 5.10: Graphs of SFn1 paired with axle loads in the Bayesian network. The values of the semi-correlation are indicated for each quadrant and for sample in the title

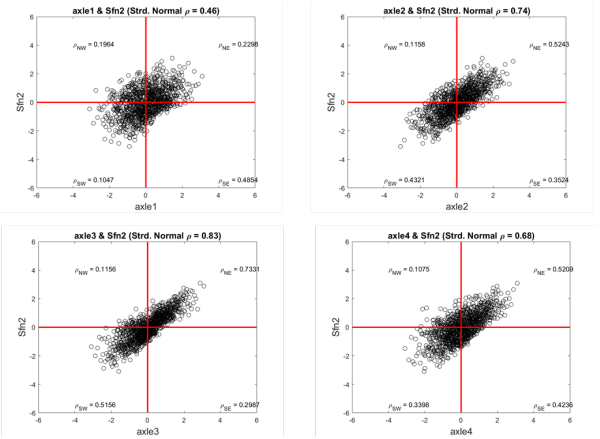

Figure 5.11: Graphs of SFn2 paired with axle loads in the Bayesian network. The values of the semi-correlation are indicated for each quadrant and for sample in the title

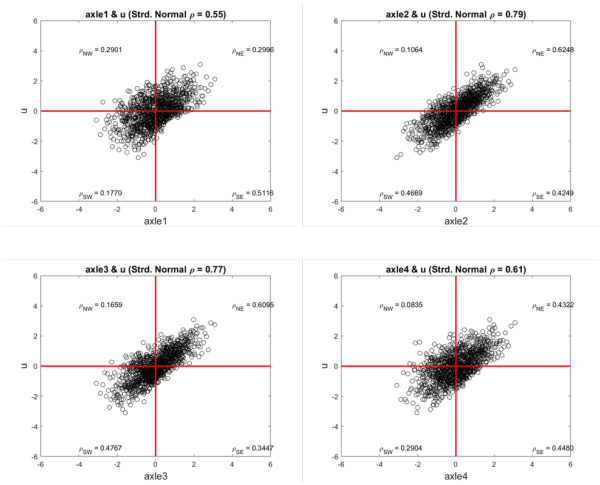

Figure 5.12: Graphs of u paired with axle loads in the Bayesian network. The values of the semi-correlation are indicated for each quadrant and for sample in the title

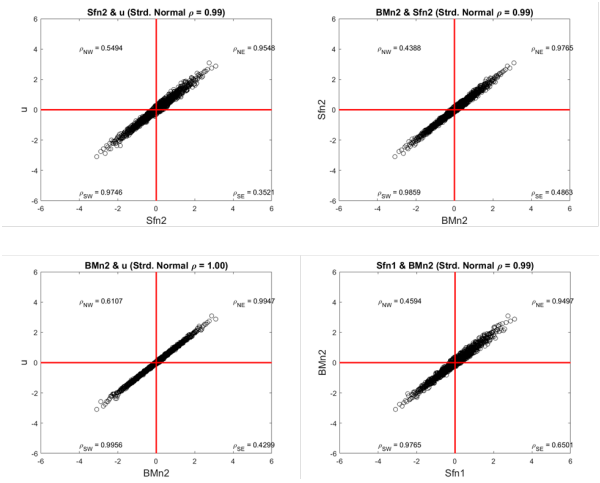

Figure 5.13: Graphs of selected pairs of responses in the Bayesian network. The values of the semi-correlation are indicated for each quadrant and for sample in the title

BN construction is done by first importing all the variables in UNINET as nodes. The BN with no arcs is shown in Figure 5.14. The corresponding empirical rank correlation matrix is shown in Figure 5.15.

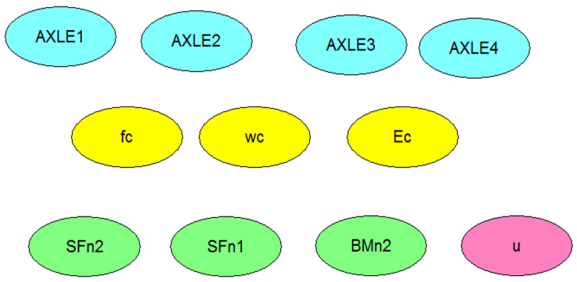

Figure 5.14: BN with no arcs

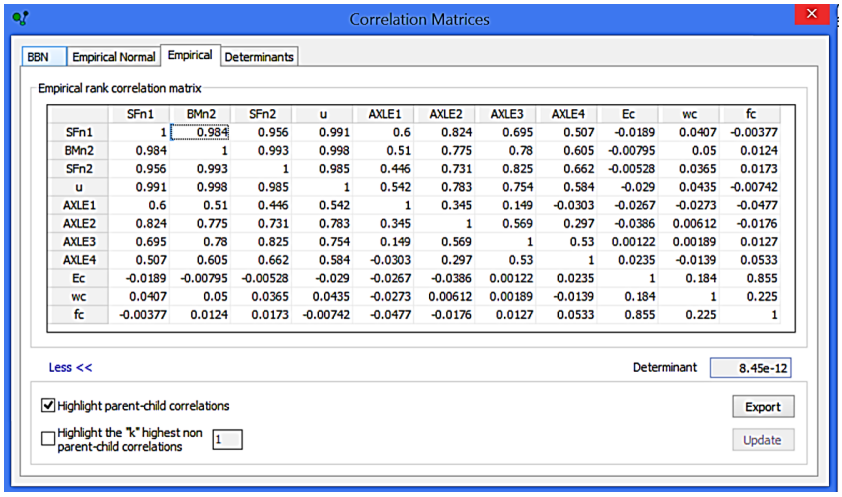

	SFn1	BMn2	SFn2	u	AXLE1	AXLE2	AXLE3	AXLE4	Ec	wc	fc
SFn1	1	0.984	0.956	0.991	0.6	0.824	0.695	0.507	-0.0189	0.0407	-0.00377
BMn2	0.984	1	0.993	0.998	0.51	0.775	0.78	0.605	-0.00795	0.05	0.0124
SFn2	0.956	0.993	1	0.985	0.446	0.731	0.825	0.662	-0.00528	0.0365	0.0173
u	0.991	0.998	0.985	1	0.542	0.783	0.754	0.584	-0.029	0.0435	-0.00742
AXLE1	0.6	0.51	0.446	0.542	1	0.345	0.149	-0.0303	-0.0267	-0.0273	-0.0477
AXLE2	0.824	0.775	0.731	0.783	0.345	1	0.569	0.297	-0.0386	0.00612	-0.0176
AXLE3	0.695	0.78	0.825	0.754	0.149	0.569	1	0.53	0.00122	0.00189	0.0127
AXLE4	0.507	0.605	0.662	0.584	-0.0303	0.297	0.53	1	0.0235	-0.0139	0.0533
Ec	-0.0189	-0.00795	-0.00528	-0.029	-0.0267	-0.0386	0.00122	0.0235	1	0.184	0.855
wc	0.0407	0.05	0.0365	0.0435	-0.0273	0.00612	0.00189	-0.0139	0.184	1	0.225
fc	-0.00377	0.0124	0.0173	-0.00742	-0.0477	-0.0176	0.0127	0.0533	0.855	0.225	1

Figure 5.15: Empirical correlation matrix of the BN with no arcs

As stated before, the correlation of bridge response is almost close to 1 and is also seen from the empirical rank correlation matrix. However, as stated before, all the bridge response variables are included in the NPBN to study the influence on them individually. First the arcs between the axle loads are constructed which are based on the dependence elicitation performed in expert judgment studies. Then, arcs between the material properties are constructed as explained in section 5.7. Then arcs between axle load variables, material variables and bridge response are constructed. Based on prior knowledge, it is known that the load values are independent of the material properties. Also, The bridge response is independent of the concrete strength however the displacement is dependent on the Young's modulus of concrete. UNINET calculates from the data the conditional (rank) correlations that are assigned to the arcs of the BN. The directionality of influence between the variables and the order of assigning arcs is important when constructing the NPBN. It can be seen in Figure 5.16, that model-1 and model-2 have different conditional (rank) correlation defined on the arcs given the order of the variables defined.

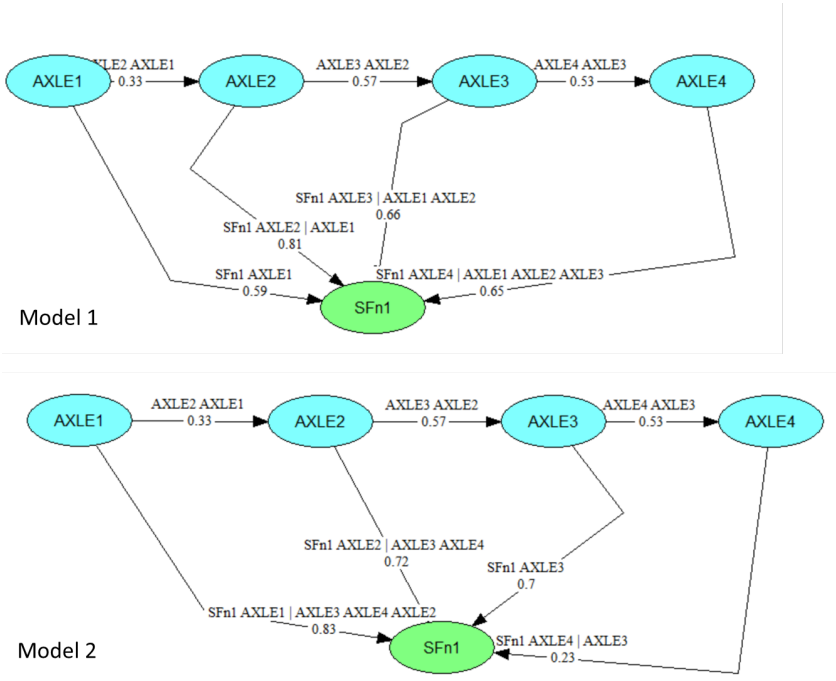

Figure 5.16: Example of difference in BN obtained by changing the order of the arcs

Following the BN model construction, the arcs are removed whose corresponding absolute conditional (rank) correlation is lower than a minimum threshold which is 0.1 in this research. The determinant of the DBN is calculated at each step to perform model validation test described in the earlier section.

The result of the model validation test for 100 and 1000 simulations in UNINET is shown in Figure 5.17. The determinant of the rank correlation matrix in the constructed BN has the 90% confidence interval [0.599E-10 1.889E-10] for 1000 iterations of sampling. The DNR is 6.931E-11 which lies in the 0.05 to 0.1 quantile of this distribution. For verification of Gaussian copula test, the DER does not lie in the 90% confidence interval of the DNR. However, for this research, the semi-correlation approach, explained above is relied upon.

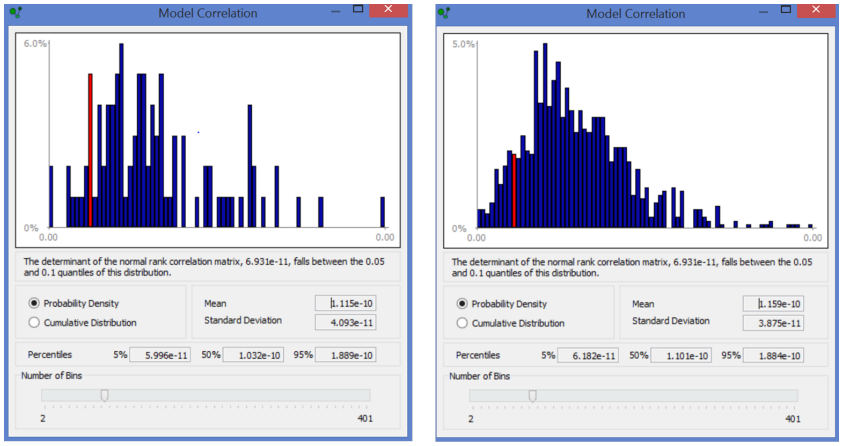

100 iterations 1000 iterations

Figure 5.17: Validation result of constructed BN of BN-I

The validated model is shown in Figure 5.18. It is to be noted that the BN structure, as shown in Figure 5.18, learned from the multivariate data set is not unique. By changing the order of the arcs, or by adding and deleting existing arcs from the BN, a different BN may be obtained. The correlation matrices of learned BN-I is given in Appendix E.

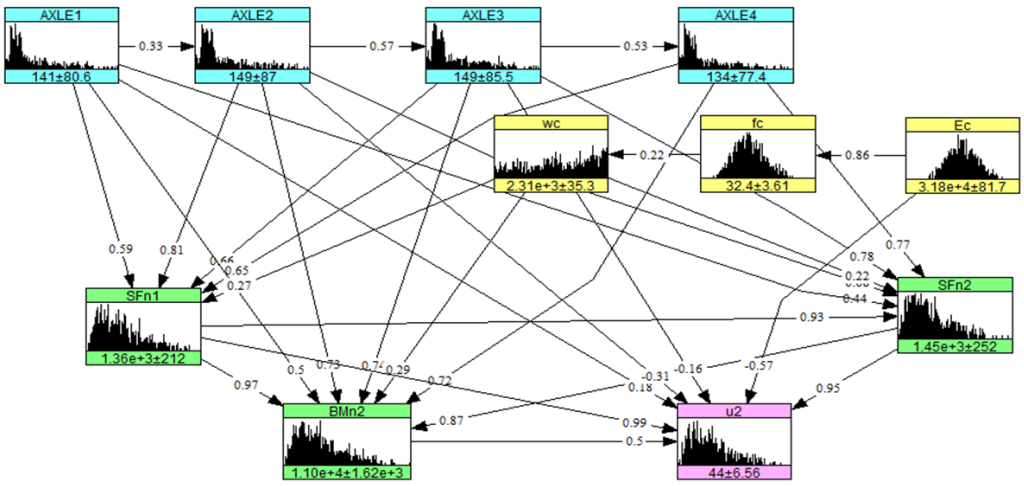

Figure 5.18: Continuous Non-Parametric Bayesian Network for BN-I

Conditional NPBN

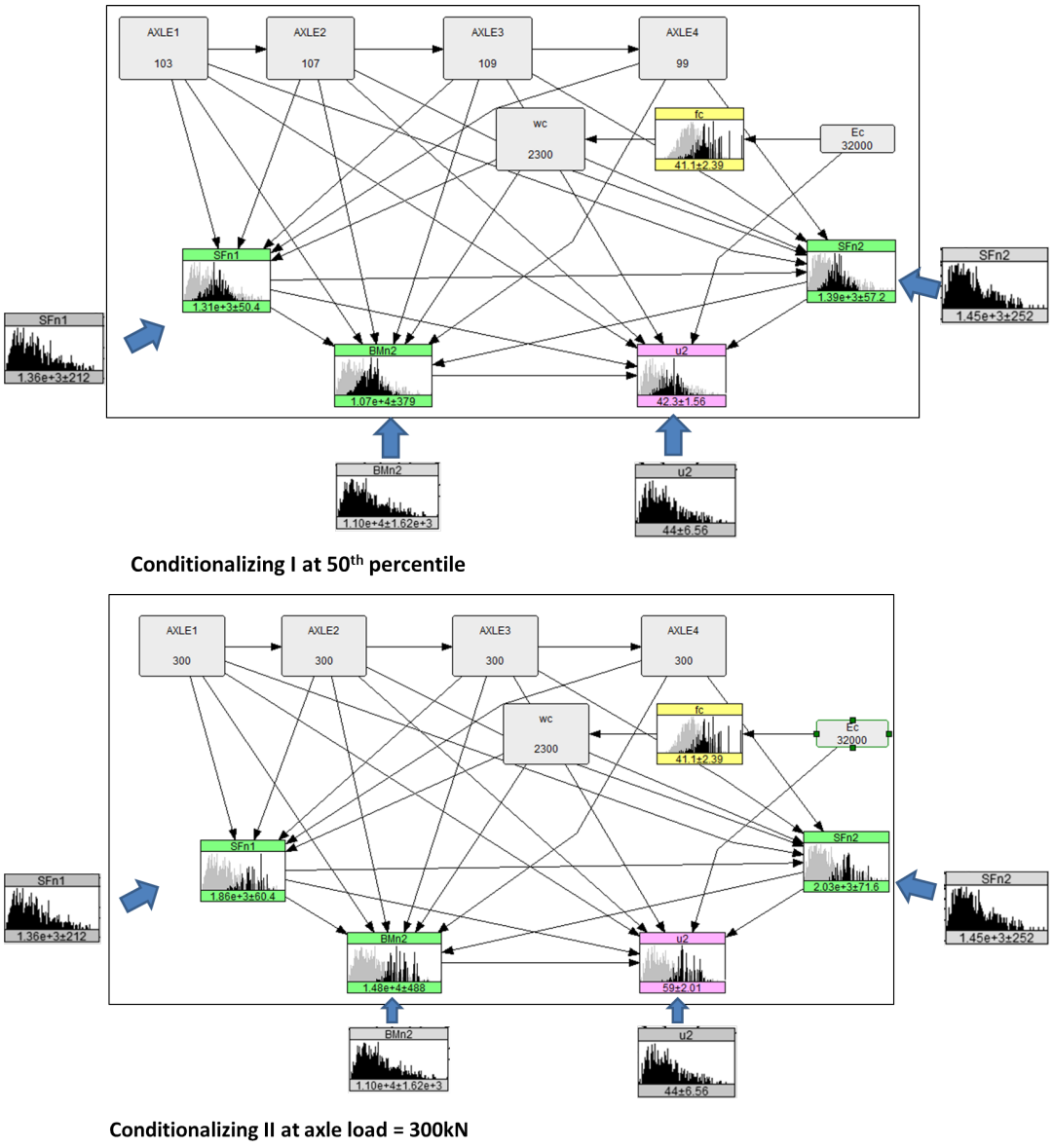

Figure 5.19: Conditional BN-1 with condition on the distribution at a point

One of the main advantages of the BNs is that once the BN is constructed and quantified, it can be updated when the evidence about the variables becomes known. In case of NPBN, application of normal copula assumption makes computing of influence between variables less complex. **This procedure of updating the BN on knowing the values of certain variables is referred to as conditionalization**. In this thesis, four example cases of conditionalization are described which are called conditionalizing-I, conditionalizing-II, conditionalizing-III and conditionalizing-IV. The former two examples consider the case when the variables are updated at a certain point in the distribution, as shown in Figure 5.19. The original baseline case histograms are shown in grey, whereas the updated belief (conditional distribution) is shown in black. The histogram of the bridge response prior to the conditionalising is shown outside the box in Figure 5.19. In conditionalizing-I, the values of the axle loads(Axle1, Axle2, Axle3 and Axle4) are updated at the 50th percentile that is the median value. The concrete density (wc) is also updated at a point close to the median, that is 2300kg/m^3. The Young's modulus is updated at 32000MPa. It can be observed that the mean of the variables SFn1, SFn2, BMn2 and u have slightly decreased, and the standard deviation is reduced significantly. In case of SFn1, SFn2,

and BMn2, the updated standard deviation is nearly $1/4th$ of the standard deviation prior to updating. In conditionalizing-II, the axle loads are updated at a high value that is 300kN, and the other variables wc and Ec are conditionalised at same point as in conditionalizing-I. It can be observed that the mean of SFn1, SFn2, BMn2 and u have increased significantly. Therefore, it can be seen that when the axle load increases from nearly 100kN to 300kN, the mean values of the maximum shear force, bending moment and vertical displacement all increase by nearly 40-50%.

The second type of conditionalization in BN is called interval conditioning. In this type of conditioning, the variables are updated for a range or interval of values in the given distribution. In this research, two intervals are defined, the low load interval when the axle loads are on [0 50] quantile of the given distribution. The conditionalization performed for this interval is called conditionalization-III. The high load interval is defined for [50 100] interval and similarly the corresponding conditionalization for this interval is called conditionalization-IV. The definition of conditional BN is shown in Figure 5.20. The results of the bridge response are shown as a cumulative distribution function in Figure 5.21 and Figure 5.22.

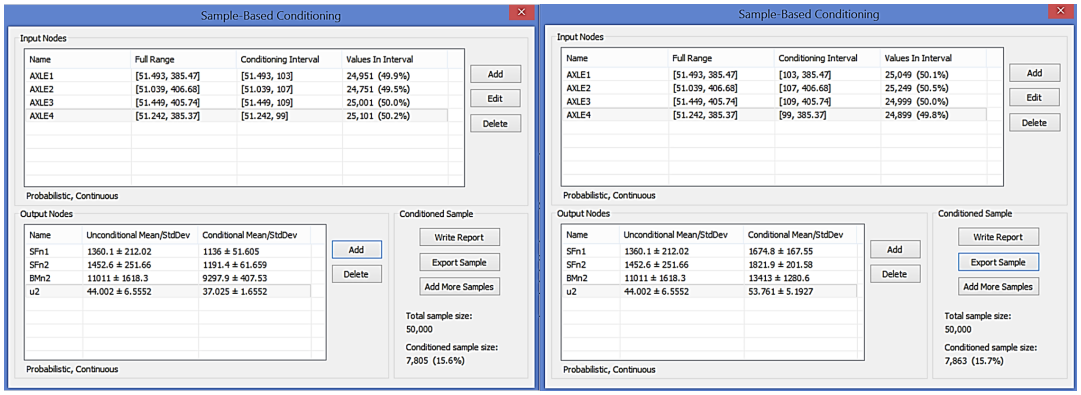

Figure 5.20: Definition of Conditional BN-1 (left: Conditionalising I;right:Conditionalising II) with interval conditioning

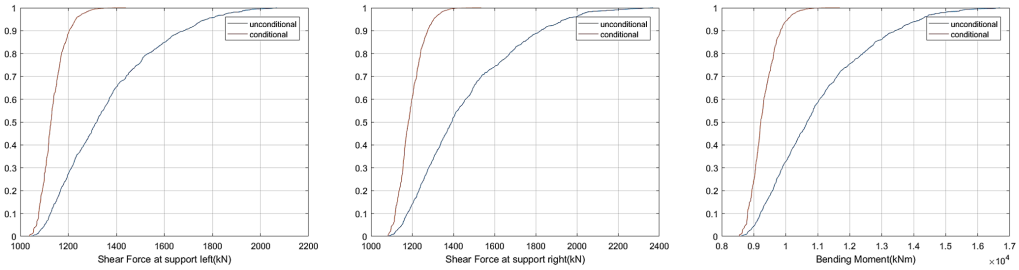

Figure 5.21: Conditionalizing III: response of bridge on conditionalising on axle loads in [0 50] quantile

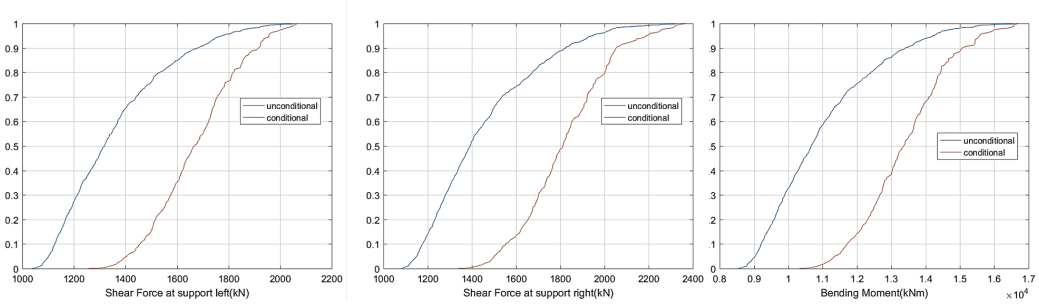

Figure 5.22: Conditionalizing IV: response of bridge on conditionalising on axle loads in [50 100] quantile

In conditionalising -III, when the axle loads are in low load interval, upper bound of the obtained cummulative distribution function is near to the median value of the unconditional bridge response for each of the variables SFn1, SFn2, and BMn2. This is also observed in conditionalising -IV, where the lower bound of the obtained cummulative distribution is near to the median value of the unconditional bridge response for each of the variables SFn1, SFn2, and BMn2

A situation is analyzed when higher loads are observed on axle 1 and axle 4 and lower loads are observed on axle 2 and axle 3, which may arise due to uneven distribution of passengers in the train car. To obtain the bridge response, the loads in axle 1 and axle are defined for [50 100] quantile and load in axle 2 and axle are defined for [0 50] quantile. The variable definition is shown in Figure 5.23. The results are shown in Figure 5.24. It can be seen that the lower bounds of SFn1, SFn2 and BMn2 after the interval conditioning is slightly higher than the unconditionalised BN, whereas the upper bound of conditional is lower than that of unconditional BN.

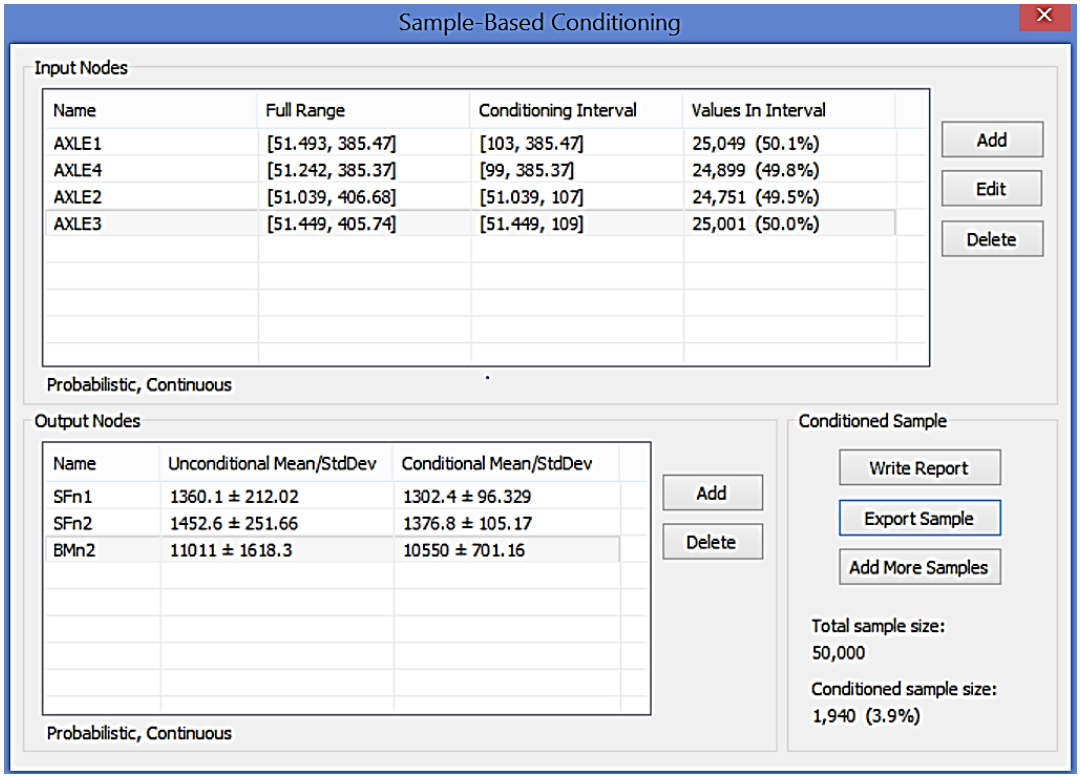

Figure 5.23: Definition of variable interval conditionition to analyse uneven distibution in axle load

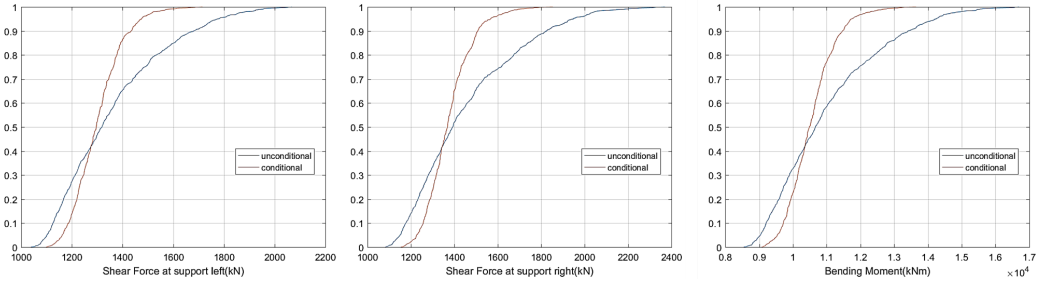

Figure 5.24: response of bridge on conditionalising on **axle 1 and axle 4 in [50 100]** and **axle 2 and axle 3 in [0 50]** quantile

The interval for axle loads are now reversed, that is axle 1 and axle 4 are defined in the interval [0 50] quantile and axle 2 and axle 3 are defined in the interval [50 100] (see Figure 5.25). The results are showin in Figure 5.26. It is observed that the lower bound of bridge response after conditionalising is higher by nearly 20% and the upper bound is nearly equivalent to that of unconditionalised BN. From Figure 5.24 and Figure 5.26, it can be inferred that the loads in axle 2 and axle 3 have a higher influence on the bridge response than axle 1 and axle4.

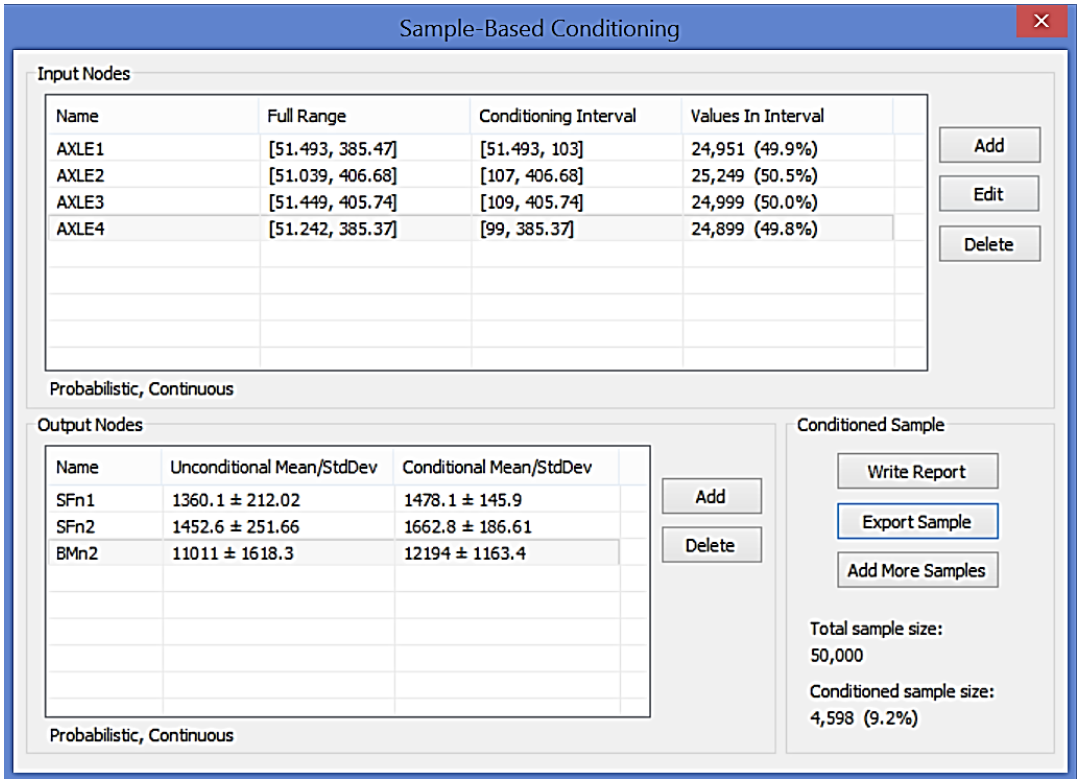

Figure 5.25: Definition of variable interval conditionition to analyse uneven distibution in axle load

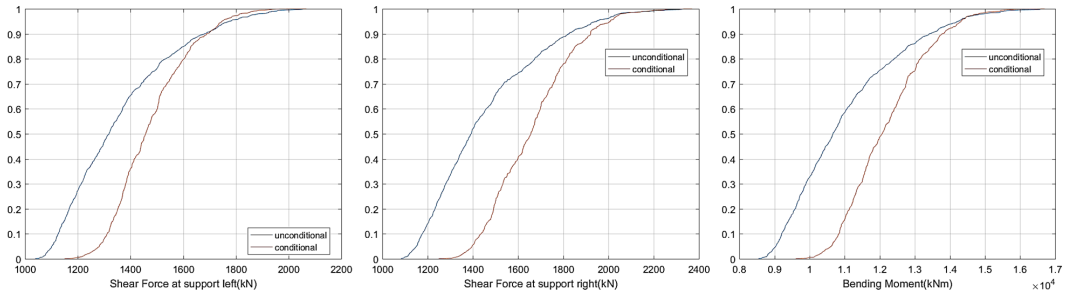

Figure 5.26: response of bridge on conditionalising on **axle 1 and axle 4 in [0 50]** and **axle 2 and axle 3 in [50 100]** quantile

5.9.4. Bayesian Network -II

As stated before, in BN-I, the distribution of axle load in each car is exactly the same. However, there is another approach to define the axle load distribution in each car. The multivariate set of axle load for each car may be derived from the same Gaussian copula however, for each car, a different sample (from Monte-Carlo simulations) can be obtained. In Bayesian network-II (BN-II), the multivariate set of axle loads obtained for $n = 1 \ldots 5$ car is different. The names and definition of the variables incorporated for BN-II are listed in Table 5.6.

Table 5.6: Names and definitions of variables of BNII

Name of Variable	Units	Description
Axle1_n	kN	Load in the first axle of n^{th}car
Axle2_n	kN	Load in the second axle of n^{th}car
Axle3_n	kN	Load in third axle of n^{th}car
Axle4_n	kN	Load in fourth axle of n^{th}car
Ec	MPa	Young's modulus of concrete
wc	kg/m^3	Density of concrete
fc	Mpa	Characteristic strength of concrete
u	mm	Vertical displacement at mid span
BMn2	kN-m	Bending moment at mid span
SFn1	kN	Shear force at left support
SFn2	kN	Shear force at right support

Similar to constructing BN-1, first the position of the train is identified when the maximum shear force is observed on the bridge. The maximum shear force for a simply supported beam is observed at the end supports. In this study, for BN-II, the maximum shear force is obtained at right support unlike in BN-I when maximum shear force is obtained at left support. For the particular position, the values of shear force at end supports, bending moment at mid span and vertical displacement at mid span is obtained for the 1000 simulations performed. The procedure for constructing the Bayesian network is similar to that of BN-I. The result of the model validation is shown in Figure 5.27. The learned BN-II is shown in Figure 5.30. The axle loads of car1 and car5 of the train are not included in the NPBN. This is because, the conditional(rank) correlation between the load in axle k for $Axlek_n$ for $k = 1 \cdots 4$ of car $n = 1, 5$ and SFn1, BMn2, SFn2 and u is below the minimum threshold (0.1) defined for this research. Axle 3 and Axle 4 of car 4 is also removed from the NPBN for the same reasoning.

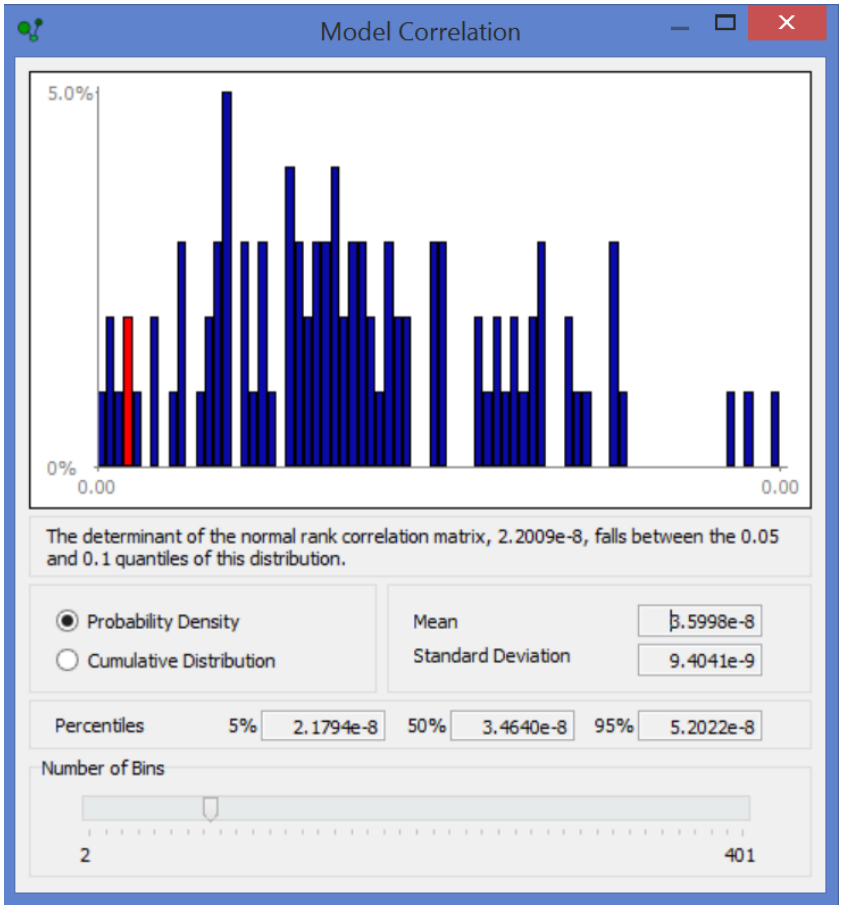

Figure 5.27: Validation result of constructed BN of BN-II

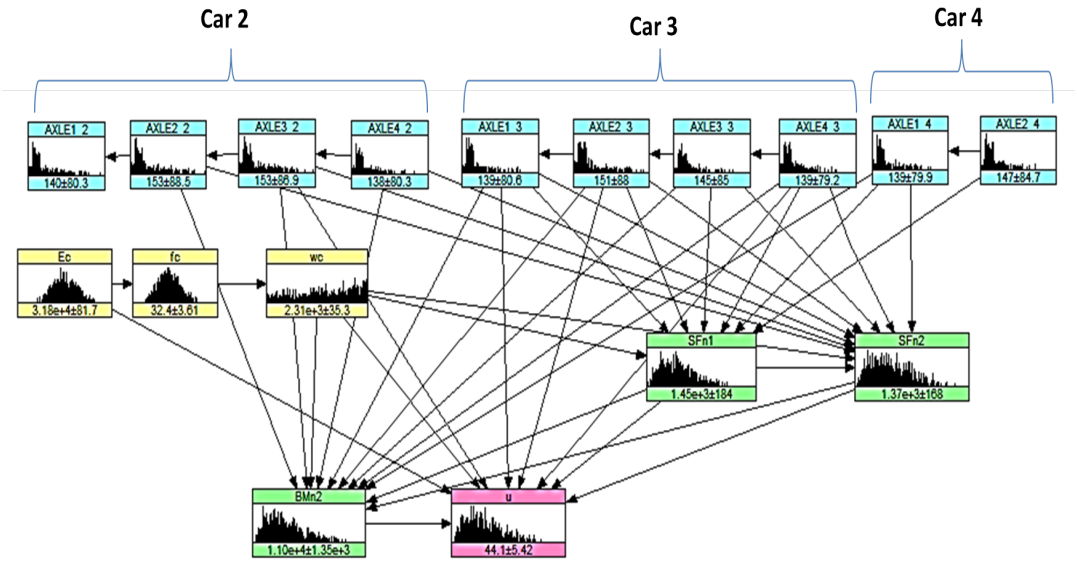

Figure 5.28: Continuous Non-Parametric Bayesian Network for BN-II

A comparison between BN-I and BN-II is drawn to study the influence of obtaining different samples for each car. It can be seen that the bending moment distribution is nearly the same for BN-I and BN-II. The observed difference in shear force at left and right support may be due to the maximum shear force

being observed at left support for BN-I and maximum shear force observed at right support for BN-II. The correlation matrices of learned BN-II is given in Appendix E.

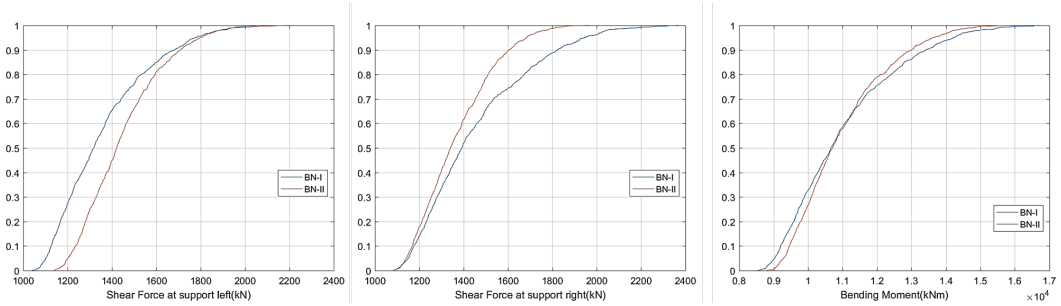

Figure 5.29: Comparison of Bridge response in BN-I vs BN-II

5.10. Probability of failure due to bending failure

With regard to the Ultimate Limite State requirements, its is essential to check that the structural resistance meets the bending moment resistance of the structure. The method for calculating the bending moment resistance of the section of a prestressed section is the same as for reinforced concrete section with the following difference:

- The stresses in steel and concrete are zero at the beginning of the loading in a reinforcement concrete beam. Whereas, for a structure with both reinforcing and prestressing steel, the initial stresses are not zero because the prestressing steel is pre-tensioned. To calculate the compatibility condition with respect to the deformation, the difference in strain between reinforcing steel and prestressing steel is accounted for.

- The loads due to prestressing are included in the applied loads. Thus, it is not allowed to use the full capacity of the prestressing steel while determining the moment resistance.

The calculation of bending moment capacity of the concrete girder is given in Appendix F.

The limit state function of bending moment Z_{bm} was assessed by considering the bending moment strength for the bridge of the mid span M_{Rd} and the maximum acting bending moment in the bridge, BM_{Max}(denoted by BMn1 in the Bayesian Network). The limit state function is given by Equation 5.34.

$$Z = M_{Rd} - BM_{Max} \tag{5.34}$$

For each simulation, the maximum bending moment of the cross section was calculated and stored and also the bending moment strength for each simulation was stored to evaluate the limit state function. To calculate the probability of failure, we evaluate the case when $Z_{bm} < 0$, that is the probability of Z_{bm} being less than 0 given by $P(Z_{bm} < 0)$. The Figure 5.30 shows the empirical cumulative distribution of Z_{bm} value the fitted the finite mixture models (for more details see [28]). Based on the obtained fitting, the probability of failure of the concrete girder due to bending is 1.388E-14. It is to be noted that the computed probability of failure is considering only the train axle loads and self weight of the concrete. The probability of failure of the bridge is expected to increase when earthquake loads are included. However, due to time limitation, such an analysis was not performed.

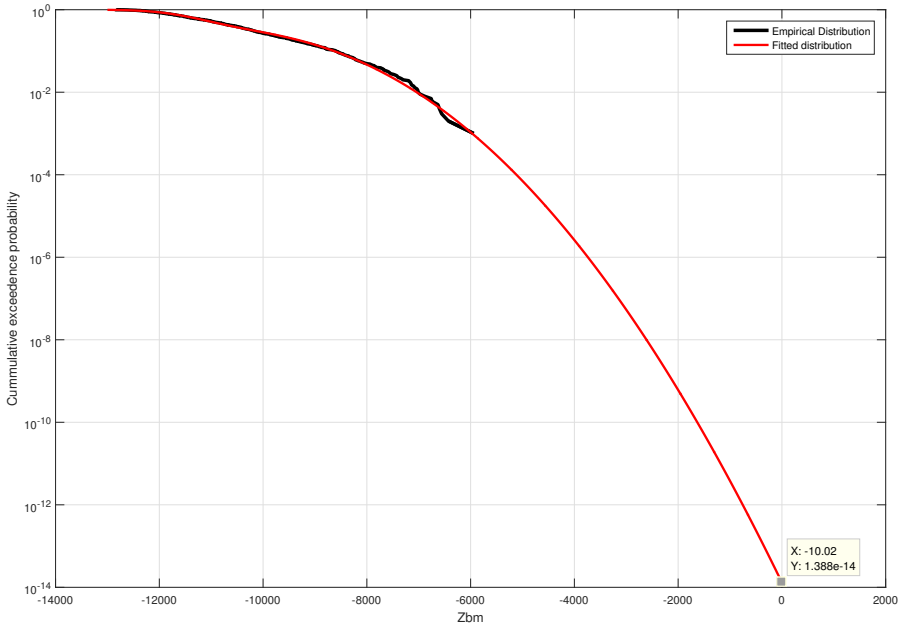

Figure 5.30: Probability of failure due to bending failure

To estimate the probability of failure, extreme value analysis could be performed. In order to do so, a period of 20 years can be considered, and considering all the trains for each year, the maximum bending moment of every year is derived. The probability of failure based on the obtained distribution is then calculated. This methodology is recommended for future research.

5.11. Conclusions

In this research, the marginal distribution and joint distribution obtained from the expert judgment elicitation (explained in the previous chapter) is used to obtain samples from Monte Carlo simulations. The material properties of the concrete are obtained from the past experimental tests and are compared with the prescribed values in the Probabilistic Model code. It is seen that the distributions obtained differ slightly however, experimental values are considered since the tests are conducted in the same location where the bridge is constructed. Therefore, the results of the experimental tests are closer to the actual concrete uncertainty.

Further, a probabilistic analysis is performed using Non-Parametric Bayesian Network. The main assumption in the NPBN is the application of Gaussian copula for joint distribution in a multivariate set. This assumption is verified with the semi-correlation approach in this chapter. For most of the pairs of variables, the Gaussian copula assumption is valid. Two Bayesian networks are developed : BN-I and BN-II. In BN-I, the distribution of axle load in each car is exactly the same, and in BN-II, the distribution of axle load in each car is different though obtained from same Gaussian copula. In BN-I, it is observed that loads in axle 2 and axle 3 have a higher influence on the bridge response variables which are shear force at end supports, bending moment and vertical displacement at mid span. On conditionalization of BN-I, it is also inferred that when the axle loads increase from nearly 100kN to 300kN, the mean values of the maximum shear force, bending moment and vertical displacement all increase by nearly 40-50%. Two situations are also analyzed in which the distribution in axle loads in uneven that is higher load in axle 1 and axle 4 and lower load in axle 2 and axle 3 and vice-verse. It is observed, that the bridge response is more influenced by the distribution in axle 2 and axle 3 than in axle 1 and axle 4. In BN-II it is observed that not all train cars have an influence on the maximum bridge response, when the train is at a particular position. This may be because of the linear elastic analysis and can be further commented upon using a non-linear analysis. The response of the bridge, however is close to that obtained in BN-I.

6

Conclusions and Recommendations

The objective of this research was to perform a probabilistic analysis of a concrete bridge under railway loading and uncertain concrete material properties by using expert judgment studies. Due to the unavailability of the measured data for axle loads in the location of the construction of the bridge, expert judgment elicitation was performed to derive uncertainty and dependence information on axle loads. The material uncertainty was quantified on the basis of past experimental work. The results of the experimental work were compared with the prescribed formulae in Probabilistic Model code. Further, to implement the load and material uncertainty and determine the bridge response, a finite element model of the bridge was developed. The bridge was modelled as a simply supported concrete girder and a moving axle load analysis was performed on the developed model. Finally, a Non-Parametric Bayesian Network was constructed incorporating the variables representing concrete material uncertainty, axle load uncertainty and uncertainty in the derived response. The resistance of the bridge was calculated analytically and then the probability of failure was computed.

6.1. Findings on the methodology

- The selection of experts is an important criteria in order to avoid over-conservatism and under-conservatism. Moreover, the clarity in calibration questions influences the experts' assessments significantly.
- The choice of modelling technique for reliability analysis depends on the level of accuracy desired by the risk analyst. Past researchers chapter 2, have classified the degree of accuracy into levels of assessment. For a level of assessment II (loA-II), which is chosen for this research, a linear finite element analysis is chosen. Furthermore, in loA-II, the bridge geometry can be modelled as 2D beam, or as a grillage model.
- To perform a reliability analysis using finite element modelling, there are two popular ways. The first is to manually program using a mathematical tool. OpenSees is popular with such an approach, since it has inbuilt packages to incorporate reliability analysis. The second approach is to use a FEA software, for example ABAQUS. However, in FE software, there are limited internal features to incorporate uncertainties and therefore the software has to be combined with a reliability platform.
- In a moving load analysis, position and magnitude of maximum bending moment and shear stress varies in time. For a reliability analysis, the maximum bending moment and shear force is a point of interest to estimate the probability of failure. Hence, it is important to identify the position of the train at which critical shear and bending stresses are observed.

6.2. Conclusions

- **Expert Judgment studies**

  - *What are the results of the expert judgment elicitation to estimate the axle load uncertainty and dependence in a train running at a velocity of 160km/h?*

    Expert judgment studies were performed for uncertainty and dependency separately. Based on the results obtained, it was reiterated that the same experts do not perform well in both dependence elicitation and uncertainty elicitation. For uncertainty elicitation, the score of the decision maker was maximized using equal weighing method, however this is not a general recommendation for all expert judgment elicitation. A broad range of uncertainty was observed when the expert assessment was combined using equal weighing. For dependence elicitation, global weight pooling method was used in order to maximize the d-calibration score. To arrive at the maximum d-calibration score, a minimum calibration threshold was chosen, on the basis of which only one expert contributed to the assessment pooling.

  - *What is the level of similarity between expert judgment elicitation performed in Mexico to the WiM measurements in the Netherlands*[1]*?*

    A comparison was drawn between the measured rail axle loads in Netherlands to the results from the expert judgment studies. It was observed that the expert assessment was conservative for the axle loads. The order of the values obtained from expert judgment elicitation was however similar to those of the measurements. Further, given the difference in the two loading conditions because of two different countries, the types of train, number of passengers at a given moment may be different due to which a difference in the assessment and measurement is observed.

- **Finite Element Modeling of the bridge**

  - *How to model a simply supported bridge in a finite element methodology to perform computationally efficient large number of simulations for reliability analysis?*

    A simply supported beam was modelled in ABAQUS CAE for a 2D response. To get computationally efficient model, a sufficiently accurate mesh size is obtained from mesh sensitivity analysis. In order to perform a moving axle load analysis, a static concentrated force approach was used in which the concentrated force was applied exactly at the nodal position. The position of the force was then varied in time. This approach could be incorporated in the future research for assessing reliability under moving load.

- **Probabilistic Analysis of the bridge**

  - *How to develop a Non-Parametric Bayesian Network(NPBN) for a simply supported bridge model with load and material uncertainty?*

    The proposed NPBN included the following variables : loads in train axles, density of concrete, characteristic strength of concrete, Young's modulus of concrete, maximum shear force at end supports, maximum bending moment at mid span, vertical displacement at mid span. By means of Expert judgment elicitation, experimental results and finite element modelling, these variables were quantified and using Monte Carlo simulations, samples representing the probability distributions were obtained. A Gaussian copula test and model validation was performed. Two Bayesian Networks were developed. In the first Bayesian Network (BN-I), the probabilistic distributions of axle loads in each car is exactly the same. In the second Bayesian Network (BN-II), different samples of the the probabilistic distribution of axle loads in each car is incorporated. In both BN-I and BN-II, a positive correlation is observed between the loading variables and the bridge response variables. Additionally, a high correlation (0.9) is observed between the bridge response variables. This is because of a linear elastic analysis performed in the research. The probability distribution in variables representing bridge response in BN-I and BN-II is similar though a slight variation is observed.

[1] The data on rail WiM measurement in the Netherlands was only available near the end of the thesis duration

– *What are the effects of conditionalization on the bridge response?*
  On conditionalisation of BN-I, it is observed that the when the axle loads increase from nearly 100kN to 300kN, the mean values of the maximum shear force, bending moment and vertical displacement all increase by nearly 40-50%. Further, it is also observed that the bridge response (maximum shear force and maximum bending moment) is more influenced by loads in axle 2 and axle 3.
– *What is the probability of failure of the bridge?* The probability of failure in flexure is computed in the thesis. Considering a span of 33m, simply supported single bridge girder, the probability of failure of the concrete girder due to bending failure is computed as 1.388E-14. Considering the bridge is constructed in a location which is earthquake, it is expected that the probability of failure will increase when earthquake loading is included in the model.

6.3. Recommendations

In this section, recommendations for future research and development related to the work in this thesis are discussed.

Non-Linear Analysis

The finite element model incorporated in this research is based on the linear elastic behaviour of the materials. However, in order to increase the level of accuracy of the risk assessment, a non-linear finite element model of the bridge is recommended.

Earthquake Loading

Assessment of infrastructure for earthquake loading in earthquake prone areas is important. Since the bridge is being built in Mexico, which has a history of witnessing high magnitude earthquakes, it is recommended to perform reliability assessment for earthquake loads. Due to the time limitation for this research, the given analysis could not be performed.

Copula Assumption

The NPBN is constructed with the assumption of Gaussian copula for the joint distribution the the given multivariate data set. This assumption however, is questionable for some pairs of variables. Therefore, it is recommended to explore the validity of other copula, for example, Gumbel, Clayton copula, etc.

3D Finite Element Model

For the ease of computation, the bridge response was studied in 2-dimensions. However, to study the influence of torsion, and incorporate the influence of stress distribution on bridge slabs, developing a 3D finite element model is advised. It may also be challenging computationally to perform the reliability analysis on a 3D non-linear model.

Modelling with measured WiM data

Since, the data measured in Netherlands for rail WiM*(referred to as Quo-Vadis)*, only became available towards the end of the duration of the thesis, detailed analysis of risk assessment with measured data was not done. Also, the comparison between the expert judgment elicitation and measured data may be of interest for further research.

A

Basic Reliability Theory

In this chapter, general aspects of reliability, of which explanations were deliberately omitted in the main report, are briefed upon. Within the field of probabilistic calculations, four levels are normally distinguished:

- **Level 0** Formally, this is used to denote a deterministic calculation methodology, where uncertainties and variations are not taken into account.
- **Level I** Semi-probabilistic calculations: uncertainties are taken into account by means of safety factors (for example the partial safety factors in the Eurocode).
- **Level II** Fully probabilistic, i.e. all uncertainties are quantified or estimated, and taken into account. The reliability however is obtained by approximation techniques (in this report: FORM, see section section A.5).
- **Level III** Fully probabilistic, where the reliability is determined using exact methods or methods which are exact in nature (in this report: Monte Carlo analysis, see section A.4).

A.1. General concepts

Random variable

Random variables are variables, which can, with a certain probability, take on a set of possible values. They are also denoted as stochastic variables. Random variables can be either continuous or discrete: the former can take on any number in an interval (can be unbounded), while the latter is limited to only a finite set of distinct values. In this thesis, all stochastic variables are continuous. Probability density functions (abbreviated with 'pdf') assign a certain chance to each value a random variable can take on. Because, in the continuous case, the number of possible realizations of a random variable is infinite, the probability of taking on one single value is zero. Probability distribution functions therefore define the chance of taking on a value in a relative way. The probability of taking on a value within an interval however, is determined by integrating the pdf over this interval. Closely related to this, is the cumulative distribution function ('cdf'). It expresses the probability of non-exceedance as a function of a 'dummy variable' expressing the range. The cdf can therefore be expressed in terms of the pdf:

$$F_X(x) = P(X < x) = \int_{-\infty}^{x} f_X(x)dx \tag{A.1}$$

where

X = random variable,

x = dummy variable, used for describing the range of possible outcomes

F_X = cumulative distribution function (cdf) of X

$f_X(x)$ = probability density function (pdf) of X

$P(X < x)$ = probability of X being smaller than x, i.e. the probability of non-exceedance

Therefore, the pdf can also be defined as the derivative of the cdf:

$$f_X(x) = \frac{dF_X(x)}{dx} \tag{A.2}$$

Expectation
The expectation of a random variable is the best estimator for it's outcome, and is determined by weighing possible realizations of this random variable with corresponding probabilities of attainment. For discrete random variables, this is a summation over all possible outcomes:

$$E[X] = \sum x_i P(X = x_i) \tag{A.3}$$

where

$E[\dot{]}$ = expected value,
X = random variable, in this case discrete
x_i = the i'th possible outcome of X
$P(X = x_i)$ = probability of X being equal to x_i

Analogously, for continuous distributions the expectation is defined as the first moment (commonly denoted by μ_X):

$$E[X] = \int_{-\infty}^{\infty} x f_X(x) dx = \mu_X \tag{A.4}$$

Variance
The variance of a random variable is a measure of its spread around its expectation. Numerically, the variance is equal to the expected squared distance between its possible outcomes and its mean, weighed by the outcome's probabilities. For discrete random variables:

$$Var(X) = E[(X - \mu_X)^2] = \sum_{i=1}^{n} (x_i - \mu_X)^2 P(X = x_i) \tag{A.5}$$

For continuous random variables:

$$Var(X) = \int_{-\infty}^{\infty} (x - \mu_X)^2 f_X(x) dx = \int_{-\infty}^{\infty} (x)^2 f_X(x) dx - {\mu_X}^2 = {\sigma_X}^2 \tag{A.6}$$

From these, the coefficient of variation is defined as a measure of variations relative to the mean value:

$$c_{v,X} = \frac{\sigma_X}{\mu_X} \tag{A.7}$$

Risk
Risk is defined as the product of expected consequences and their associated probability of occurrence:

$$risk = P * C \tag{A.8}$$

where

P = probability of event occurring,
C = consequences associated to this event

It is thus closely related to the expectation. In other words, risk may be interpreted as the expected costs from an adverse event (e.g. structural failure). In case of multiple possible events, risks should be summed, as is the case with expectations. Risk can be used to objectively weigh the probability that some adverse event may occur, against e.g. the costs of improving strength.

Probability of failure
The probability of failure is denoted with P_F , and quantifies the likelihood of failure occurring. It should always be related to a time-frame, for example the probability that a bridge will fail during the coming 50 years. The reliability (L) is the complement of the failure probability, i.e.:

$$L = 1 - P_F \tag{A.9}$$

where
P_F = probability of failure,
L = reliability

Therefore, reliability and probability of failure are completely dependent .

Reliability index
The reliability index, denoted with β, is frequently used to express the reliability of, among others, structures. It is defined as:

$$\beta = \Phi^{-1}(1 - P_F) = \Phi^{-1}(L) \tag{A.10}$$

where
β = reliability index,
Φ = standard normal distribution cdf ($\mu = 0; \sigma = 1$),
Φ^{-1} = inverse standard normal distribution cdf,

and therefore,

$$P_F = \Phi(-\beta) \tag{A.11}$$

Thus reliability index is fully replaceable by its corresponding probability of failure.

A.2. Probability distributions used in work

Some of the probability distributions which were deemed as ‘generally known’, were not elaborated in the main text. To provide all the information necessary for the reader, however, these have been included in this chapter.

Normal distribution
Probability density function (pdf):

$$f_X(x) = \frac{1}{\sigma\sqrt{2\pi}} \exp -\frac{(x-\mu)^2}{2\sigma^2} \tag{A.12}$$

Cumulative distribution function (cdf):

$$F_X(x) = \int_{-\infty}^{x} f_X(x)dx \tag{A.13}$$

Mean value (expectation):

$$\mu_X = \mu \tag{A.14}$$

Variance:

$$\sigma_X{}^2 = \sigma^2 \tag{A.15}$$

Stochasts which are normally distributed are symbolized by ‘‘$X(\mu X, \sigma X)$’.

Lognormal distribution
Probability density function (pdf):

$$f_X(x) = \frac{1}{x\sigma\sqrt{2\pi}} \exp -\frac{(\ln x - \mu)^2}{2\sigma^2} \tag{A.16}$$

Cumulative distribution function (cdf):

$$F_X(x) = \int_{-\infty}^{x} f_X(x)dx \tag{A.17}$$

Mean value (expectation):

$$\mu_X = e^{\mu+\sigma^2/2} \tag{A.18}$$

Variance:

$${\sigma_X}^2 = (e^{\sigma^2} - 1)e^{2\mu+\sigma^2} \tag{A.19}$$

Stochasts which are normally distributed are symbolized by ''$XLN(\mu X, \sigma X)$'.

A.3. Solving the reliability integral

This section, along with sections A.4 and A.5, is based on Probabilities in Civil Engineering (CUR-committee E10, 1997). The 'reliability equation' or 'limit state function' is written in such a way, that negative values of the safety margin Z correspond to failure. The reliability equation has the general form[1]:

$$Z = R - S \tag{A.20}$$

where

Z = safety margin,
R = resistance to failure
S = load

The probability of failure can then be expressed in terms of the reliability equation as

$$P_F = P(Z \leq 0) = P(R \leq S) \tag{A.21}$$

where P_F is the probability of failure. Calculating the failure probability comes down to determining the probability of Z being smaller than zero. This probability is calculated by integration of the probability density function of Z over the (hyper)space of variables, for those combinations where $Z \leq 0$. This may seem more clear if 'integration' is replaced with 'summation'. First, imagine a *n*-dimensional hyperspace (for $n > 3$), where n is the number of (random) variables. Assume now that the probability density functions are known for each variable, and that variables are independent. The probability density at any point in the hyperspace, can then be determined from the product of probabilities that each variable attains the value corresponding to this point in the hyperspace. The probability of failure is determined from the probability density function defined on the hyperspace, only concerning those points where $Z = g(X_1, X_2, ..., X_n)$ is less than or equal to zero, and is obtained from summation of probabilities related to all those possible combinations which lead to failure.

Back to the formulation using the integrals: the failure probability is expressed as

$$P_F = \iint_{Z \leq 0} f(R,S)\, dR\, dS \tag{A.22}$$

with

$$Z = g(X_1, X_2, ..., X_n) \tag{A.23}$$

This means that the failure probability can be calculated with the integral

$$P_F = \int \cdots \int_{Z \leq 0} x_1, ..., x_n\, dX_1 \ldots dX_n \tag{A.24}$$

[1]Any form is possible, as long as it is accompanied by a clear definition failure and survival

from which it is clear that integration is performed over all variables, thus representing the aforementioned hyperspace. The integral in equation Equation A.24 proves quite hard to solve for the failure probability, even to the extent that analytical solutions are an exception. Therefore, the integration is generally done using numerical routines (section A.4) or the reliability is determined using approximation techniques (section A.5).

A.4. Monte Carlo method

The Monte Carlo method is a 'brute force' approach to the solution of the reliability integral. Starting from known distributions for all stochastic variables, a random realization of each variable is drawn. From this, the safety margin (Z) is determined by substitution in the reliability equation. Then it is checked whether $Z \leq 0$ (failure) or $Z \geq 0$ (survival). This process is repeated a large number of times, from which the failure frequency is calculated. This serves as an estimate for the failure probability, i.e.

$$P_F = \frac{n_f}{n} \tag{A.25}$$

where

n_f = number of simulated failures,

n = number of simulations

Equation A.25 converges to the true solution of the integral Equation A.24 for increasing n. The accuracy of the Monte Carlo is dictated by the number of simulations. Usually, the number of simulations required for acceptable accuracy is rather high which can make the method computationally expensive. As a general rule, for crude Monte Carlo, the number of simulations for 95% accuracy is in the order of $400/P_f$, which shows that it it increasingly difficult to achieve a stable and accurate solution for a decreasing failure probability.

A.5. First order reliability method

In this section an approximate method for solving the reliability integral using first order linearization is explained. In case all variables in the reliability equation are normally distributed, and the reliability equation is some linear function of these variables, then the reliability function itself will also be normally distributed. If so, the probability that of *Z* being equal to or smaller than zero can be directly calculated from

$$P_F = P(Z < 0) = \Phi(-\frac{\mu_z}{\sigma_z}) \tag{A.26}$$

to which the reliability index β owes its alternate definition:

$$\beta = \frac{\mu_z}{\sigma_z} \tag{A.27}$$

B

Expert Judgment questionnaire

Elicitation of Uncertainty distributions for Passenger loads in the Mexico – Toluca Railway

B.1. Introductionn

This questionnaire focuses on the elicitation of uncertainty distributions over passenger loads in the soon to be operational Mexico – Toluca railway.This questionnaire is a part of an Expert Judgment Exercise for the purpose of a Master Thesis Project at TU Delft. This approach has been developed at TU Delft and has been used in numerous studies. Description of the variables of interest is provided in the subsequent section. It is followed by a set of questions in order to elicit uncertainty over these variables of interest. Your personal details will not be used in the open literature to associate individual answers to individual experts. They are necessary however to warranty the accountability and duplicatable of this workshop as a scientific exercise.
Name

Current Position

Email

B.2. Data of Interest

A new interurban passenger train system from Toluca to Mexico City is being constructed. It has an approximate 57.7 kilometer high-speed rail line linking the cities of Toluca and Mexico City. Service will be provided to six stations: 1) Observatorio in Mexico City; 2) Santa Fe, 3) Lerma, 4) Metepec (near the Toluca International Airport), the 5) Toluca Bus Station and 6) Zinacantepec. The train will carry an estimated 300,000 passengers daily and travel at a top speed of 160 kilometers-per-hour, making the trip from Toluca to Mexico City in about 39 minutes. As expressed before, we are interested in the weight distribution in a single wagon as measured by a hypothetical WIM system if available. WIM is a weight in motion measurement done using instruments installed on tracks. It records the moving vehicular weight which includes the dead weight of the locomotive and the additional load being carried in the form of passengers/cargo. In other words we will ask estimates of your uncertainty over the weight observed in each of the 4 axles of a single wagon of the train briefly described above (However excluding the dead load of the train). These questions are divided into two time segments. The train that will be running is manufactured by CAF. The distribution of the axles in the wagons is shown in the Figure B.2. There are four axles in each of the wagons.

B.3. Procedure

The first part of the questionnaire will ask you to provide your estimates for the Variables of Interest (whose value is unknown to the researcher). The second part asks you to elicit dependence between

Characteristics of Train	
Type	Electric Motorised Unit
Number of cars	5 (can be doubled in peak hours)
Total Passenger Capacity of train	711
Maximum Speed	160km/hr
Total train length (For upto 5 cars)	98.97m

Figure B.1: (left) Plan view of proposed route of Mexico-Toluca Train (right)Characteristics of train)

Figure B.2: Representative drawing of the train for Mexico-Toluca bridge

these variables of interest in the form of conditional probabilities of exceedance. The third, fourth and fifth part of the questionnaire will ask your estimates for calibration variables. These calibration variables are used for empirical control of the data collected in this questionnaire. Your contribution will help us quantify the unknown data. You are asked to quantify 3 percentiles of your subjective uncertainty distribution per variable:
1. 5% quantile : in 5% of the cases true value will be lower than your estimate
2. 50% quantile : in 50% of the cases the true value will be lower/higher than your estimate
3. 95% quantile: in 95% of the cases the true value will be lower than your estimate.
To illustrate, one example is given below based on expert judgment on the average monthly temperature distribution in Mexico from 1991-2015

Table B.1: Expert Judgment question on the average monthly temperature distribution in Mexico from 1991-2015

5% quantile (Degree Celsius)	50% quantile (Degree Celsius)	95% quantile (Degree Celsius)
12	20	24

The above data can be interpreted as : According to the expert, in 95% of the of the cases average monthly temperature (from 1991-2015) is greater than 12° Celsius, in 50% of the cases higher/lower than 20° Celsius and 95 of the cases it is lower than 24° Celsius.

B.4. Questionnaire

B.4.1. Variables of Interest (Uncertainty)

Please provide the 5th 50th and 95th percentiles of your uncertainty distribution over the weight in a single car in tons that would be measured by a WIM system in (see Table B.2):

Table B.2: For Elicitation of Uncertainty of Variable of Interest

	5th quantile	50th quantile	95th quantile	
Axle 1				ton
Axle 2				ton
Axle 3				ton
Axle 4				ton

B.4.2. Variables of Interest (Dependence)

Description: This question segment, asks the expert to determine the dependency between the load distribution in different axles.

Consider Table Table B.2. Consider a sample of 200000 cars with the characteristics listed above. For each row in Table B.3 there will be 100000 cars for which load in Y1 will be larger than the 50th quantile value that you provided in Table above. Consider the samples of Y2 corresponding to the 100000 samples of Y1 described above. On how many of them will the value of Y2 will be larger than the median value of Y2 you provided in Table above? In other words what is P(Y2>its median | Y1>its median)? (Refer to the Appendix for relation between correlation and Probability)

Table B.3: For Elicitation of Dependence of Variable of Interest

Y1	Y2	Probability (%)
Axle 1	Axle 2	
Axle 2	Axle 3	
Axle 3	Axle 4	
Axle 4	Axle 1	

B.4.3. Calibration Variables-1 (Uncertainty)

This section refers to data collected by the WIM system of the Netherlands from 1st of April 2008 to 30 of April 2008. We will discuss data concerning vehicles with 4 axles (35,057 vehicles in total). The total number of 4 axle vehicles are 35,057 on Left Lane of A15 Highway in The Netherlands

Please provide the 5th 50th and 95th percentiles of your uncertainty distribution over the maximum weight in tons that would be measured by the WIM system in the data described (Table B.4).

Table B.4: Maximum weight in tons that would be measured by the WIM system

	5th quantile	50th quantile	95th quantile	
Axle 1				ton
Axle 2				ton
Axle 3				ton
Axle 4				ton

B.4.4. Calibration Variables-1 (Dependence)

Description: This question segment, asks the expert to determine the dependency between the load distribution in different axles in 5 axle vehicle.

Consider a sample of 35057 vehicles with 4 axles (See Figure below). For each row in Table B.5 there will be ‘x’ number of vehicles (out of 35057 vehicles) for which load in Y1 will be larger than the 50th quantile value. Consider the samples of Y2 corresponding to the ‘x’ samples of Y1 described above. On how many of them will the value of Y2 will be larger than the median value of Y2 you provided in Table above?

In other words what is P(Y2>its median | Y1>its median)?

Table B.5: For Elicitation of Dependence of Calibration variables

Y1	Y2	Probability (%)
Axle 1	Axle 2	
Axle 2	Axle 3	
Axle 3	Axle 4	
Axle 4	Axle 1	

B.4.5. Calibration Variables - 2 (Uncertainty)

This section refers to data collected by the Rail WIM system of the Netherlands . The measurements are recorded using the 'Gotcha / Quo Vadis' system.

The system classifies as 'weigh-in-motion' (WIM), as measurements are obtained from moving trains. The installations consist of four glass-fiber sensors mounted on the underside of the tracks (two on each side). Also, an antenna is placed which reads RF-tags on trains, which can be used for identification. The system produces optic signals, i.e. when a train passes the sensors, the tracks bend slightly. This causes a disturbance in the optic signal, which is translated to a static weight and dynamic forces. The system is calibrated frequently (order of magnitude is daily), using vehicles with known weights (preferably dedicated locomotives).

Information regarding the available data is summarized in table 4-4 and the overview of the corresponding measured sites are given in Figure 4-1, Figure 4-2, Figure 4-, Figure 4-4 and Figure 4-5

DetectorID	km	GeoCode	GeoDetailDescription	TrackName	Latitude	Longtitude
11	51.72	104	Voorschoten I	LF	52.12324	4.42896
12	51.72	104	Voorschoten I	KF	52.12324	4.42896
18	51.72	104	Voorschoten II	MF	52.12291	4.42958
19	51.72	104	Voorschoten II	NF	52.12291	4.42958
111	24.801	513	Tricht	GU	51.89117	5.26765
114	24.801	513	Tricht	GJ	51.89117	5.26765
163	75.059	112	Schiedam	CF	51.95656	4.38279
164	75.059	112	Schiedam	DF	51.95656	4.38279
363	50.759	035	Zeist	AF	52.06595	5.31602
364	50.759	035	Zeist	AT	52.06595	5.31602

Figure B.3: (left) Plan view of proposed route of Mexico-Toluca Train (right)Characteristics of train)

Figure B.4: Map of The Netherlands with marked locations of WiM installations

Voorschoten lies between The Hague and Leiden. Detectors 12 and 19 were subjected to axle loads of larger magnitudes than detectors 11 and 18 (Refer Figure 4-6)

Tricht The tracks near Tricht are used extensively for freight transports. Interestingly, the most frequent occurrence of large axle loads is measured at detector 111, i.e. track GU. Figure 4-3 suggests that,

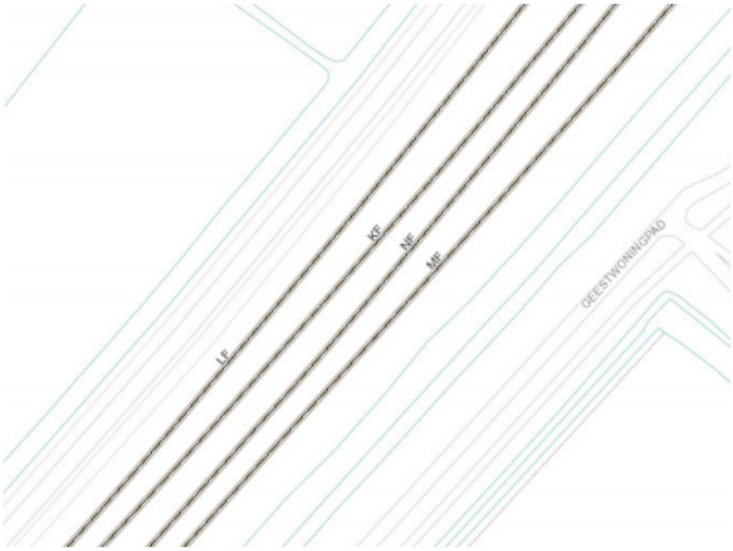

Figure B.5: Overview of tracks near Voorschoten (Geocode 104)

given the assumption that most of the traffic on the Dutch railways is right-driving, this track is mainly used for inland transportation of freight, or export eastwards (e.g. Germany).
Schiedam : The station is close to Rotterdam and most trains come from and go to Rotterdam.
Zeist lies close to Utrecht. It is noted that Freight is transported primarily from Utrecht towards the eastern part of the country.

Figure B.6: Overview of tracks near Tricht (Geocode 513)

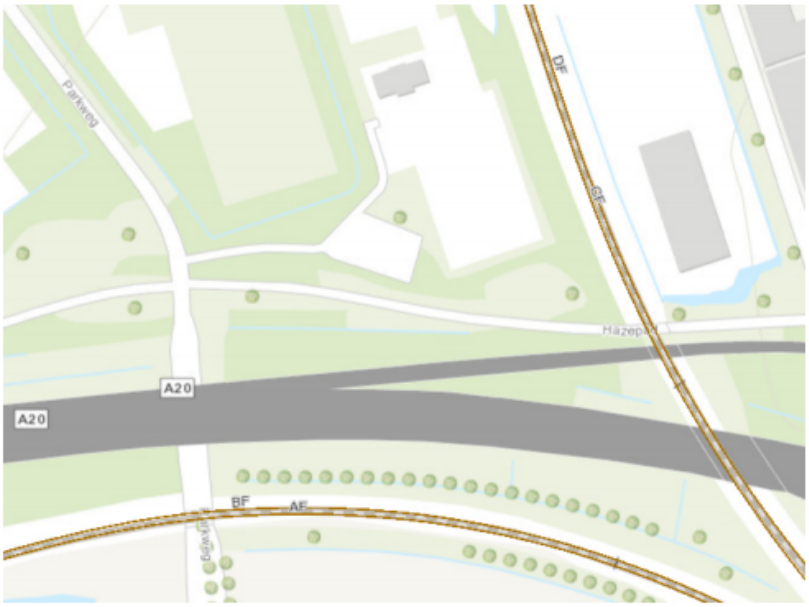

Figure B.7: Overview of tracks near Schiedam (Geocode 112)

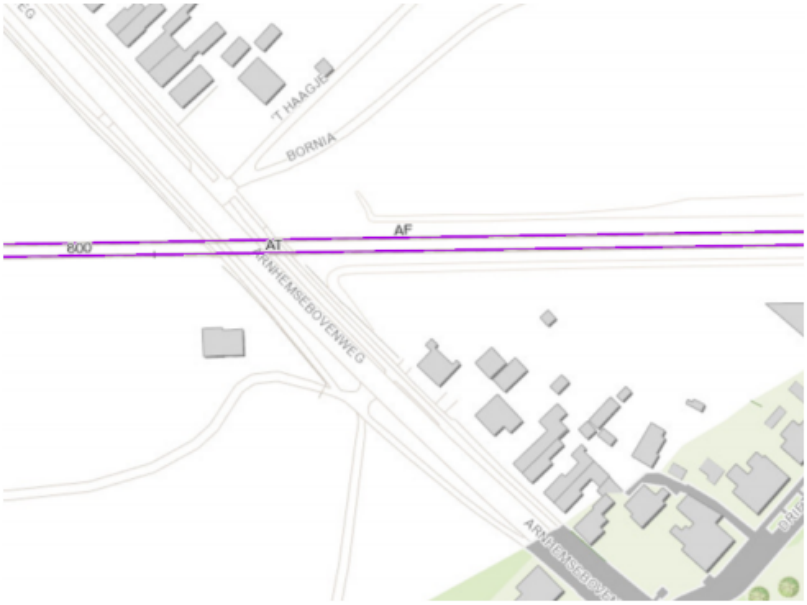

Figure B.8: Overview of tracks near Zeist (Geocode 035)

Histograms for axle loads (in kN) are plotted for a pair of detectors at Voorschoten and Tricht below:

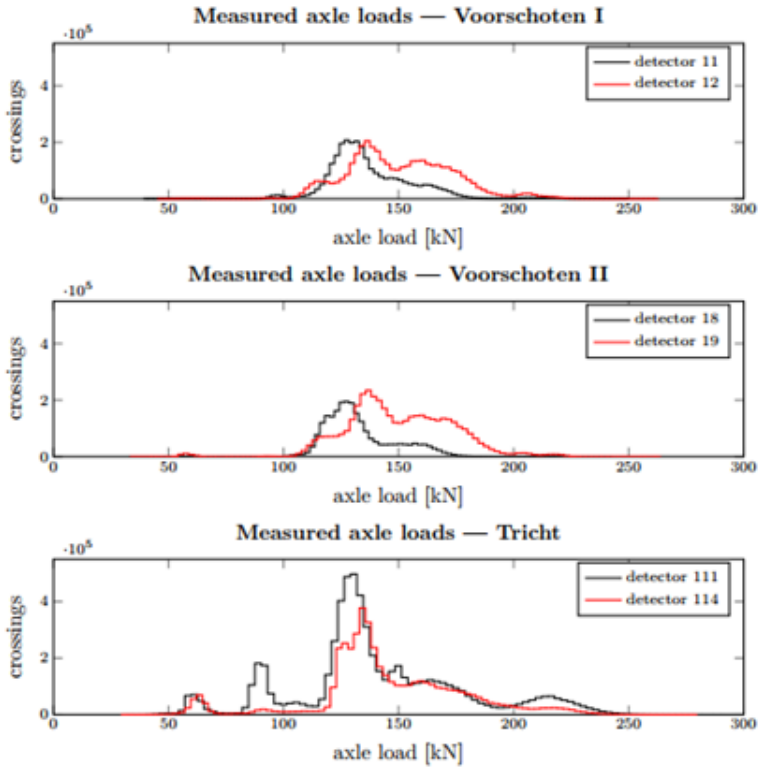

Figure B.9: Histograms for axle loads (in kN) for a pair of detectors at Voorschoten and Tricht

We are interested in the uncertainty in Axle loads for sites at Schiedam and Zeist. The following questions are therefore based on these sites

Q1. Please provide the 5th 50th and 95th percentiles of your uncertainty distribution over the mean weight in tons across all axles that would be measured by the WIM system at Schiedam in the data described by detector 163

Table B.6: For Elicitation of Uncertainty of mean axle load at Schiedam

	5th quantile	50th quantile	95th quantile	
Mean Axle Load at Schiedam				Ton

Q2. Please provide the 5th 50th and 95th percentiles of your uncertainty distribution over the mean weight in tons across all axles that would be measured by the WIM system at Zeist in the data described by detector 363

Table B.7: For Elicitation of Uncertainty of mean axle load at Zeist

	5th quantile	50th quantile	95th quantile	
Mean Axle Load at Zeist				Ton

Q3. Please provide the 5th 50th and 95th percentiles of your uncertainty distribution over the maximum weight in tons across all axles that would be measured by the WIM system at Schiedam in the data described by detector 163

Table B.8: For Elicitation of Uncertainty of maximum axle load at Schiedam

	5th quantile	50th quantile	95th quantile	
Maximum Axle Load at Schiedam				Ton

Q4. Please provide the 5th 50th and 95th percentiles of your uncertainty distribution over the maximum weight in tons across all axles that would be measured by the WIM system at Zeist in the data described by detector 363

Table B.9: For Elicitation of Uncertainty of maximum axle load at Zeist

	5th quantile	50th quantile	95th quantile	
Maximum Axle Load at Zeist				Ton

B.4.6. APPENDIX

The following graph illustrates the probability vs correlation behaviour. The graph can be utilised to answer questions in Section II and Section IV.

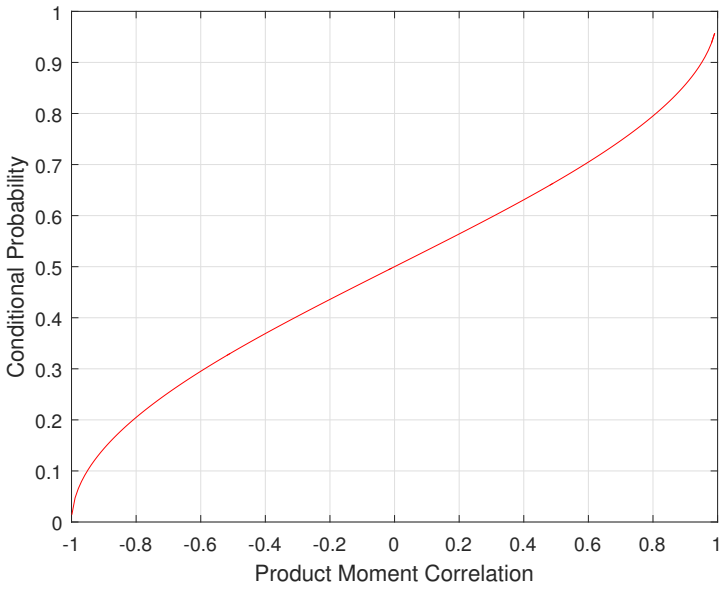

Figure B.10: Probability vs correlation behaviour

C

Finite Element Modelling

This appendix describes the modelling details used in this thesis. The following section briefs about the basic concepts of Finite Element Analysis (FEA), element type and analysis types.

C.1. Basic Concepts of FEA

In structural mechanics, a dominant discretization technique is the finite element method (FEM). The physical interpretation of the FEM is done by subdivision of the mathematical model into non-overlapping components of simple geometry, which are elements for short or finite elements. A finite number of degrees of freedom are used to express the response of each element. These are characterized, at a set of nodal points, as the value of an unknown function (or functions). The discrete model obtained by connecting or assembling the collection of all elements is used to approximate the response of the mathematical model. The natural occurrence of the disconnection-assembly concept takes place during the examination of many artificial and natural systems. For example, visualization of an engine, bridge, building, airplane, or skeleton as made from simpler components is easy .

One of the most useful tools to solve partial differential equations is FEM. The solution to these equations on complex geometries is particularly easy to find using this model. The ability to automatize it makes highly suitable for computer implementation, which is efficient. Hence, the result is that we get matrices, over very large, which are easily solvable using a computer. The basis of finite element is variational formulations, which differentiates it from the more popular finite difference method. The concepts of virtual work and energy are taken well into account, while solving problems in solid and structural mechanics.

An energy functional is minimized to obtain the stresses, temperatures, flows, or other desired unknown parameters in the finite element model. All energies related to the particular FEM are part of the energy functional. The finite element energy functional must be zero, as per the law of conservation of energy. By minimizing the energy functional, the correct solution is obtained for any FEM. The derivative of the functional with respect to the unknown grid point is set to zero and that helps us find the minimum of the functional.

Thus, the basic equation for finite element analysis is :

$$\frac{\partial F}{\partial p} = 0 \tag{C.1}$$

where

$F =$ energy functional,

$p =$ In mechanics, the potential is displacement

This is based on the principle of virtual work, which states that if a particle is under equilibrium, under a set of a system of forces, then for any displacement, the virtual work is zero. Each finite element will have its own unique energy functional.As an example, in stress analysis, the governing equations for

a continuous rigid body can be obtained by minimizing the total potential energy of the system. The total potential energy Γ can be expressed as:

$$\Pi = \frac{1}{2}\int_{\Omega} \sigma^T \epsilon dV - \int_{\Omega} d^T b dV - \int_{\Gamma} d^T q dS \tag{C.2}$$

where

σ = stress,

ϵ = strain,

d = vector of displacement,

b = vector of body force components per unit volume,

q = vector of applied surface traction components at any surface point,

Γ = boundary of the body Ω,

Ω = region of structure

The first term on the right hand side of this equation represents the internal strain energy and the second and third terms are, respectively, the potential energy contributions of the body force loads and distributed surface loads.

In the finite element displacement method, the displacement is assumed to have unknown values only at the nodal points, so that the variation within the element is described in terms of the nodal values by means of interpolation functions. Thus, within any one element,

$$d = Nu \tag{C.3}$$

where

N = matrix of interpolation functions termed shape functions,

u = vector of unknown nodal displacements

The strains within the element can be expressed in terms of the element nodal displacements as

$$\epsilon = Bu \tag{C.4}$$

where

B = the strain displacement matrix

The stresses may be related to the strains by use of an elasticity matrix (e.g. Young's modulus E)

$$\sigma = E\epsilon \tag{C.5}$$

The total potential energy of the discretized structure will be the sum of the energy contributions of each individual element. Thus,

$$\Pi = \sum_{e} \Pi_e \tag{C.6}$$

where

Π_e = total potential energy of an individual element

$$\Pi_e = \frac{1}{2}\int_{\Omega_e} u^T (B^T E B)^T u dV - \int_{\Omega_e} u^T N^T p dV - \int_{\Gamma} u^T N^T q dS = 0 \tag{C.7}$$

Taking the derivative,

$$\frac{\partial \Pi_e}{\partial u} = \frac{1}{2}\int_{\Omega_e} (B^T E B)^T u dV - \int_{\Omega_e} N^T p dV - \int_{\Gamma} N^T q dS = 0 \tag{C.8}$$

resulting equation is,

$$f = \int_{\Omega_e} N^T u dV + \int_{\Gamma} N^T q dS = 0 \tag{C.9}$$

where

f = force vector

Equation C.10 is of the form $ku - f = 0$ where

$$k = \int_{\Omega_e} (B^T E B) u dV \tag{C.10}$$

where

k = element stiffness matrix

C.2. Elements

A finite element model is composed of elements, which generally consist of connected nodes. The elements mentioned in this report will be briefly discussed in the following sections.

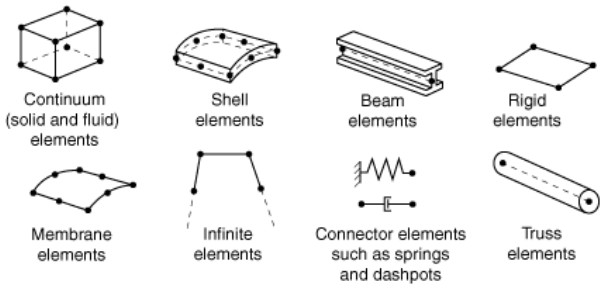

(a) Different families of element type in ABAQUS Hibbett et al.

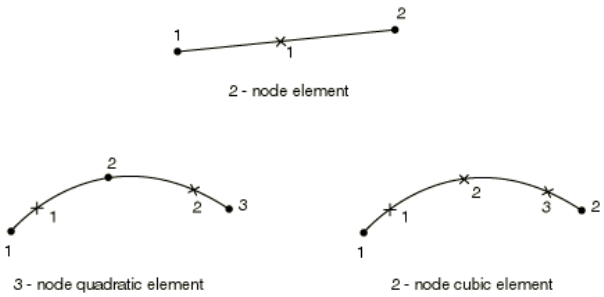

(b) 2 noded beam elements Hibbett et al.

Figure C.1: Element Types in ABAQUS

B21/B31- Beam Elements

B21 beam elements and B31 beam element follow Timoshenko beam theory, thus allowing transverse shear deformation. Slender, as well as thick(”stout”) beams allow the usage of these elements . There are beams, that are entirely made of an uniform material. In such cases, useful results can be provided for cross-sectional dimensions up to the wavelength of the highest natural mode, contributing significantly to the response or 1/8th of typical axial distance. The behavior, transverse shear, of Timoshenko beams is assumed by Abaqus to be linear elastic with a fixed modulus. Hence, it is independent of the response of the beam section to bending and also axial stretch. B21 is a 2-noded linear beam element with 3 degrees of freedom (2 translational in plane - x, y, and 1 rotational ϕ_z;,while B31 is a 2-noded linear beam element with six degrees of freedom (along $x, y, z, \phi_x, \phi_y, \phi_z$).The beam cross sectional properties are given in the section properties for the element, from which the area and moment of inertia are calculated, to compute the beam response to stretching, bending, shear and torsion.

C.3. Analysis type

In Abaqus, It is possible to use different analysis types when modelling. The analysis types used are described in this section

Static Analysis
A static structural analysis determines the displacements, stresses, strains, and forces in structures or components caused by loads that do not induce significant inertia and damping effects. Steady loading and response conditions are assumed; that is, the loads and the structure's response are assumed to vary slowly with respect to time.

Modal Analysis
A modal analysis determines the vibration characteristics (natural frequencies and mode shapes) of a structure

Dynamic Analysis
A Dynamic analysis accounts for the mass and inertia effect of the system with respect to time. Eurocode 1, elaborates on the criteria to decide whether a dynamic analysis is required or not.

C.4. Time Integration method

To increment the time in discrete steps Δt, schemes are involved by time stepping algorithms. Given the values of $a_n, \dot{a}_n$and $\ddot{a}_n$ at time t_n (and perhaps also at earlier times steps), the values $a_{n+1}, \dot{a}_{n+1}$and $\ddot{a}_{n+1}$ at time t_{n+1} = t_n + Δt are needed.A time stepping scheme is essential to perform this. Until the desired time is reach, time is continuously incremented. There are two types of time stepping schemes: 1. Implicit and 2. Explicit

C.4.1. Implicit/ABAQUS Standard

The dependency of implicit schemes is on information at various steps. This can be at time step n+1, and also information at time step n and steps prior to that. Therefore, a system of equations must be solved for implicit schemes. Linear and nonlinear response options are both provided by Abaqus/Standard. Linear analysis, at the time when the procedure is introduced, is considered as linear perturbation analysis, as the program is truly integrated. General application of linear analysis is allowed by linear perturbation approach, especially in particular case. This case is when the linear response is dependent on either of the two factors: 1. Pre-Loading 2. Nonlinear response history of the model. A convergent solution is needed to be obtained at the lowest possible cost in nonlinear problems. Two approaches are offered to this by nonlinear procedures in Abaqus/Standard. In one of the choices, the user specifies the increment scheme. This is the direct user control of increment size. In the other choice, the user needs to define the step and also specify tolerances or error measures. Post which, Abaqus/Standard automatically selects the increments as responses develop in the step. The user cannot foresee the response before time and this makes the entire approach usually more efficient. In this research study, ABAQUS Standard is used with automatic time stepping.

Explicit
In the explicit form of analysis, the preceding step places a very crucial role. The result in each step is dependent on the quantities obtained in the previous step. To compute the solution at the time step n+1, integrators, explicit, rely on information at timestep n or even earlier(such as n-1).

D

Measurement of WiM Data

The Dutch railway network is equipped with measurement systems for measuring the weights of moving trains which is referred to as Quo Vadis. The information given in this chapter is obtained from the Quo-Vadis information guide provided by ProRail unless stated otherwise.

Quo Vadis measures the rail deflection using optical sensors Figure D.1.

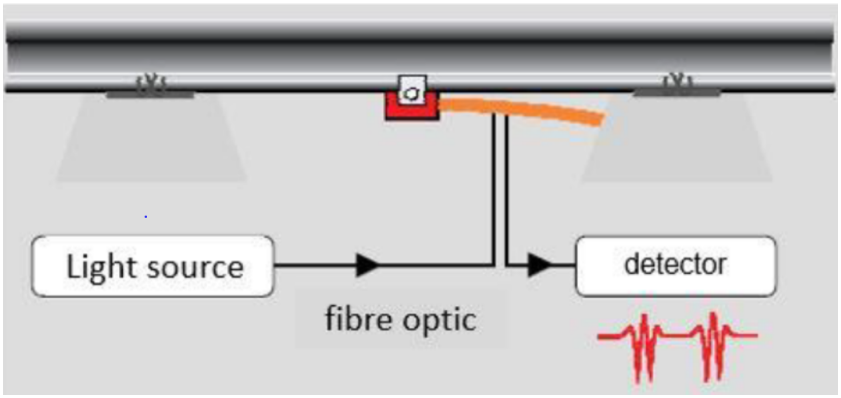

Figure D.1: Quovadissensor

The following information is derived from the sensors:

- weight of axle
- wheel-load differences
- weight ratio between wheels diagonally opposite each other on the bogie
- uneven load

45 sites throughout Dutch rail network has installed Quo Vadis systems. The reliability of the weight reading taken with Quo Vadis is +/- 3%. This depends on sufficient calibrations, valid sensors, track layout and track quality. Quo Vadis measures weight using 12 sensors (6 per rail). The axle load is reported in tonnes. Measurements from Quo Vadis and HotBox detection are forwarded to ProRail's central server (the central Gotcha server). This server controls active signalling. The measurements are then forwarded to the Quo Vadis application.

For this research, the WiM data is used for trains whose speeds are lesser than 200km/h for the period of one year from August 2017-September 2018, for 15th day of each month.

E

Correlation Matrix

In this chapter, the correlation matrices of the Bayesian Network-I and Bayesian Network-II are presented.

E.1. Bayesian Network - I

In Figure E.1, Figure E.2, and Figure E.3, the correlation matrices of Bayesian Network, BN-I explained in chapter 5 are shown.

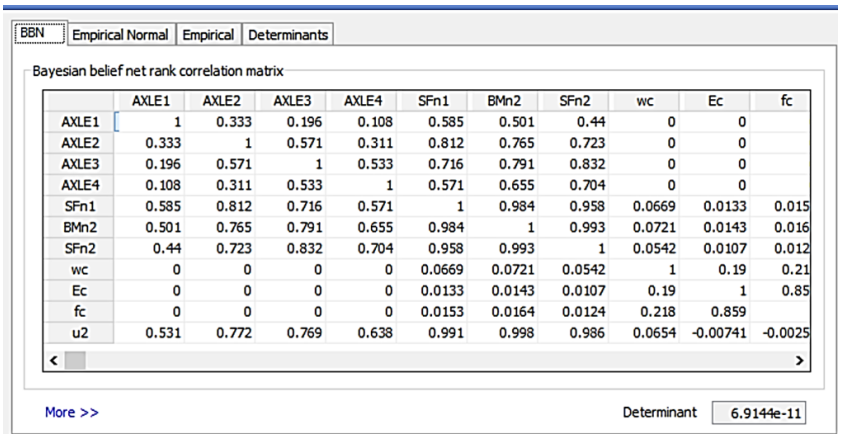

	AXLE1	AXLE2	AXLE3	AXLE4	SFn1	BMn2	SFn2	wc	Ec	fc
AXLE1	1	0.333	0.196	0.108	0.585	0.501	0.44	0	0	
AXLE2	0.333	1	0.571	0.311	0.812	0.765	0.723	0	0	
AXLE3	0.196	0.571	1	0.533	0.716	0.791	0.832	0	0	
AXLE4	0.108	0.311	0.533	1	0.571	0.655	0.704	0	0	
SFn1	0.585	0.812	0.716	0.571	1	0.984	0.958	0.0669	0.0133	0.015
BMn2	0.501	0.765	0.791	0.655	0.984	1	0.993	0.0721	0.0143	0.016
SFn2	0.44	0.723	0.832	0.704	0.958	0.993	1	0.0542	0.0107	0.012
wc	0	0	0	0	0.0669	0.0721	0.0542	1	0.19	0.21
Ec	0	0	0	0	0.0133	0.0143	0.0107	0.19	1	0.85
fc	0	0	0	0	0.0153	0.0164	0.0124	0.218	0.859	
u2	0.531	0.772	0.769	0.638	0.991	0.998	0.986	0.0654	-0.00741	-0.0025

Figure E.1: Correlation Matrix of Bayesian belief network of BN-I

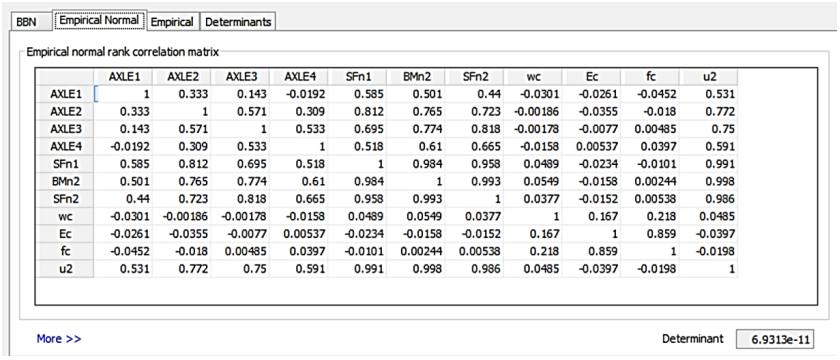

	AXLE1	AXLE2	AXLE3	AXLE4	SFn1	BMn2	SFn2	wc	Ec	fc	u2
AXLE1	1	0.333	0.143	-0.0192	0.585	0.501	0.44	-0.0301	-0.0261	-0.0452	0.531
AXLE2	0.333	1	0.571	0.309	0.812	0.765	0.723	-0.00186	-0.0355	-0.018	0.772
AXLE3	0.143	0.571	1	0.533	0.695	0.774	0.818	-0.00178	-0.0077	0.00485	0.75
AXLE4	-0.0192	0.309	0.533	1	0.518	0.61	0.665	-0.0158	0.00537	0.0397	0.591
SFn1	0.585	0.812	0.695	0.518	1	0.984	0.958	0.0489	-0.0234	-0.0101	0.991
BMn2	0.501	0.765	0.774	0.61	0.984	1	0.993	0.0549	-0.0158	0.00244	0.998
SFn2	0.44	0.723	0.818	0.665	0.958	0.993	1	0.0377	-0.0152	0.00538	0.986
wc	-0.0301	-0.00186	-0.00178	-0.0158	0.0489	0.0549	0.0377	1	0.167	0.218	0.0485
Ec	-0.0261	-0.0355	-0.0077	0.00537	-0.0234	-0.0158	-0.0152	0.167	1	0.859	-0.0397
fc	-0.0452	-0.018	0.00485	0.0397	-0.0101	0.00244	0.00538	0.218	0.859	1	-0.0198
u2	0.531	0.772	0.75	0.591	0.991	0.998	0.986	0.0485	-0.0397	-0.0198	1

Figure E.2: Correlation Matrix of Empirical Normal distribution of BN-I

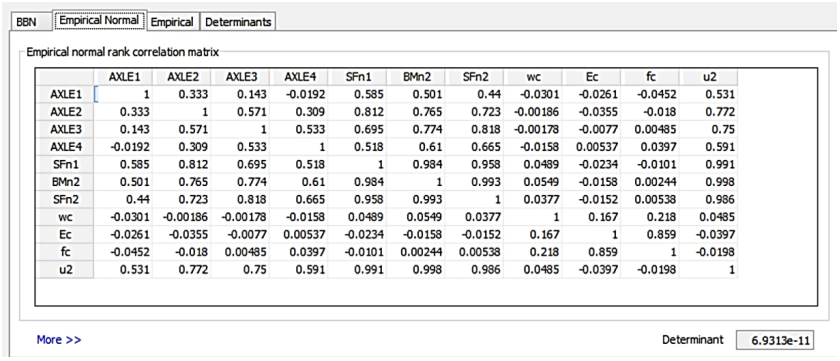

	AXLE1	AXLE2	AXLE3	AXLE4	SFn1	BMn2	SFn2	wc	Ec	fc	u2
AXLE1	1	0.333	0.143	-0.0192	0.585	0.501	0.44	-0.0301	-0.0261	-0.0452	0.531
AXLE2	0.333	1	0.571	0.309	0.812	0.765	0.723	-0.00186	-0.0355	-0.018	0.772
AXLE3	0.143	0.571	1	0.533	0.695	0.774	0.818	-0.00178	-0.0077	0.00485	0.75
AXLE4	-0.0192	0.309	0.533	1	0.518	0.61	0.665	-0.0158	0.00537	0.0397	0.591
SFn1	0.585	0.812	0.695	0.518	1	0.984	0.958	0.0489	-0.0234	-0.0101	0.991
BMn2	0.501	0.765	0.774	0.61	0.984	1	0.993	0.0549	-0.0158	0.00244	0.998
SFn2	0.44	0.723	0.818	0.665	0.958	0.993	1	0.0377	-0.0152	0.00538	0.986
wc	-0.0301	-0.00186	-0.00178	-0.0158	0.0489	0.0549	0.0377	1	0.167	0.218	0.0485
Ec	-0.0261	-0.0355	-0.0077	0.00537	-0.0234	-0.0158	-0.0152	0.167	1	0.859	-0.0397
fc	-0.0452	-0.018	0.00485	0.0397	-0.0101	0.00244	0.00538	0.218	0.859	1	-0.0198
u2	0.531	0.772	0.75	0.591	0.991	0.998	0.986	0.0485	-0.0397	-0.0198	1

Figure E.3: Correlation Matrix of Empirical Normal distribution of BN-I

E.2. Bayesian Network - II

In Figure E.4, Figure E.5, and Figure E.6, the correlation matrices of Bayesian Network, BN-II explained in chapter 5 are shown.

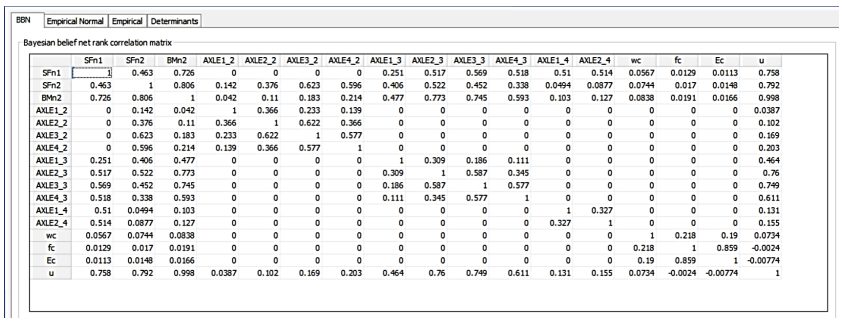

	SFn1	SFn2	BMn2	AXLE1_2	AXLE2_2	AXLE3_2	AXLE4_2	AXLE1_3	AXLE2_3	AXLE3_3	AXLE4_3	AXLE1_4	AXLE2_4	wc	fc	Ec	u
SFn1	1	0.463	0.726	0	0	0	0	0.251	0.517	0.569	0.518	0.51	0.514	0.0567	0.0129	0.0113	0.758
SFn2	0.463	1	0.806	0.142	0.376	0.623	0.596	0.406	0.522	0.452	0.338	0.0494	0.0877	0.0744	0.017	0.0148	0.792
BMn2	0.726	0.806	1	0.042	0.11	0.183	0.214	0.477	0.773	0.745	0.593	0.103	0.127	0.0838	0.0191	0.0166	0.998
AXLE1_2	0	0.142	0.042	1	0.366	0.233	0.139	0	0	0	0	0	0	0	0	0	0.0387
AXLE2_2	0	0.376	0.11	0.366	1	0.622	0.366	0	0	0	0	0	0	0	0	0	0.102
AXLE3_2	0	0.623	0.183	0.233	0.622	1	0.577	0	0	0	0	0	0	0	0	0	0.169
AXLE4_2	0	0.596	0.214	0.139	0.366	0.577	1	0	0	0	0	0	0	0	0	0	0.203
AXLE1_3	0.251	0.406	0.477	0	0	0	0	1	0.309	0.186	0.111	0	0	0	0	0	0.464
AXLE2_3	0.517	0.522	0.773	0	0	0	0	0.309	1	0.587	0.345	0	0	0	0	0	0.76
AXLE3_3	0.569	0.452	0.745	0	0	0	0	0.186	0.587	1	0.577	0	0	0	0	0	0.749
AXLE4_3	0.518	0.338	0.593	0	0	0	0	0.111	0.345	0.577	1	0	0	0	0	0	0.611
AXLE1_4	0.51	0.0494	0.103	0	0	0	0	0	0	0	0	1	0.327	0	0	0	0.131
AXLE2_4	0.514	0.0877	0.127	0	0	0	0	0	0	0	0	0.327	1	0	0	0	0.155
wc	0.0567	0.0744	0.0838	0	0	0	0	0	0	0	0	0	0	1	0.218	0.19	0.0734
fc	0.0129	0.017	0.0191	0	0	0	0	0	0	0	0	0	0	0.218	1	0.859	-0.0024
Ec	0.0113	0.0148	0.0166	0	0	0	0	0	0	0	0	0	0	0.19	0.859	1	-0.00774
u	0.758	0.792	0.998	0.0387	0.102	0.169	0.203	0.464	0.76	0.749	0.611	0.131	0.155	0.0734	-0.0024	-0.00774	1

Figure E.4: Correlation Matrix of Bayesian belief network of BN-II

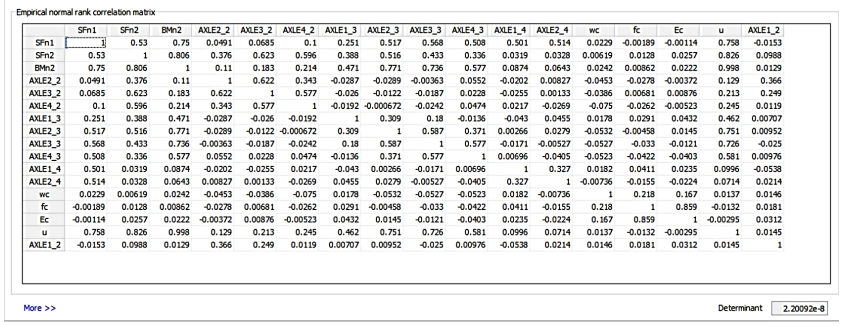

	SFn1	SFn2	BMn2	AXLE2_2	AXLE3_2	AXLE4_2	AXLE1_3	AXLE2_3	AXLE3_3	AXLE4_3	AXLE1_4	AXLE2_4	wc	fc	Ec	u	AXLE1_2
SFn1	1	0.53	0.75	0.0491	0.0685	0.1	0.251	0.517	0.568	0.508	0.501	0.514	0.0229	-0.00189	-0.00114	0.758	-0.0153
SFn2	0.53	1	0.806	0.376	0.623	0.596	0.388	0.516	0.433	0.336	0.0319	0.0328	0.00619	0.0128	0.0257	0.826	0.0988
BMn2	0.75	0.806	1	0.11	0.183	0.214	0.471	0.771	0.736	0.577	0.0874	0.0643	0.0242	0.00862	0.0222	0.998	0.0129
AXLE2_2	0.0491	0.376	0.11	1	0.622	0.343	-0.0287	-0.0289	-0.00363	0.0552	-0.0202	0.00827	-0.0453	-0.0278	-0.00372	0.129	0.366
AXLE3_2	0.0685	0.623	0.183	0.622	1	0.577	-0.026	-0.0122	-0.0187	0.0228	-0.0255	0.00133	-0.0386	0.00681	0.00876	0.213	0.249
AXLE4_2	0.1	0.596	0.214	0.343	0.577	1	-0.0192	-0.000672	-0.0242	0.0474	0.0217	-0.0269	-0.075	-0.0262	-0.00523	0.245	0.0119
AXLE1_3	0.251	0.388	0.471	-0.0287	-0.026	-0.0192	1	0.309	0.18	-0.0136	-0.043	0.0455	0.0178	0.0291	0.0432	0.462	0.00707
AXLE2_3	0.517	0.516	0.771	-0.0289	-0.0122	-0.000672	0.309	1	0.587	0.371	0.00266	0.0279	-0.0532	-0.00458	0.0145	0.751	0.00952
AXLE3_3	0.568	0.433	0.736	-0.00363	-0.0187	-0.0242	0.18	0.587	1	0.577	-0.0171	-0.00527	-0.0527	-0.033	-0.0121	0.726	-0.025
AXLE4_3	0.508	0.336	0.577	0.0552	0.0228	0.0474	-0.0136	0.371	0.577	1	0.00696	-0.0405	-0.0523	-0.0422	-0.0403	0.581	0.00976
AXLE1_4	0.501	0.0319	0.0874	-0.0202	-0.0255	0.0217	-0.043	0.00266	-0.0171	0.00696	1	0.327	0.0182	0.0411	0.0235	0.0996	-0.0538
AXLE2_4	0.514	0.0328	0.0643	0.00827	0.00133	-0.0269	0.0455	0.0279	-0.00527	-0.0405	0.327	1	-0.00736	-0.0155	-0.0224	0.0714	0.0214
wc	0.0229	0.00619	0.0242	-0.0453	-0.0386	-0.075	0.0178	-0.0532	-0.0527	-0.0523	0.0182	-0.00736	1	0.218	0.167	0.0137	0.0146
fc	-0.00189	0.0128	0.00862	-0.0278	0.00681	-0.0262	0.0291	-0.00458	-0.033	-0.0422	0.0411	-0.0155	0.218	1	0.859	-0.0132	0.0181
Ec	-0.00114	0.0257	0.0222	-0.00372	0.00876	-0.00523	0.0432	0.0145	-0.0121	-0.0403	0.0235	-0.0224	0.167	0.859	1	-0.00295	0.0312
u	0.758	0.826	0.998	0.129	0.213	0.245	0.462	0.751	0.726	0.581	0.0996	0.0714	0.0137	-0.0132	-0.00295	1	0.0145
AXLE1_2	-0.0153	0.0988	0.0129	0.366	0.249	0.0119	0.00707	0.00952	-0.025	0.00976	-0.0538	0.0214	0.0146	0.0181	0.0312	0.0145	1

Figure E.5: Correlation Matrix of Empirical Normal distribution of BN-II

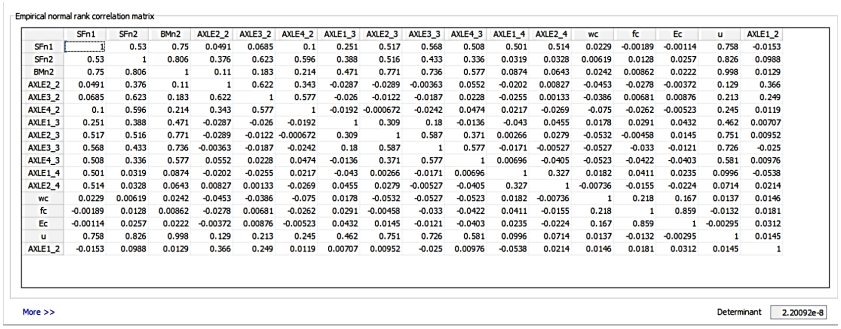

Empirical normal rank correlation matrix

	SFn1	SFn2	BMn2	AXLE2_2	AXLE3_2	AXLE4_2	AXLE1_3	AXLE2_3	AXLE3_3	AXLE4_3	AXLE1_4	AXLE2_4	wc	fc	Ec	u	AXLE1_2
SFn1	1	0.53	0.75	0.0491	0.0685	0.1	0.251	0.517	0.568	0.508	0.501	0.514	0.0229	-0.00189	-0.00114	0.758	-0.0153
SFn2	0.53	1	0.806	0.376	0.623	0.596	0.388	0.516	0.433	0.336	0.0319	0.0328	0.00619	0.0128	0.0257	0.826	0.0988
BMn2	0.75	0.806	1	0.11	0.183	0.214	0.471	0.771	0.736	0.577	0.0874	0.0643	0.0242	0.00862	0.0222	0.998	0.0129
AXLE2_2	0.0491	0.376	0.11	1	0.622	0.343	-0.0287	-0.0289	-0.00363	0.0552	-0.0202	0.00827	-0.0453	-0.0278	-0.00372	0.129	0.366
AXLE3_2	0.0685	0.623	0.183	0.622	1	0.577	-0.026	-0.0122	-0.0187	0.0228	-0.0255	0.00133	-0.0386	0.00681	0.00876	0.213	0.249
AXLE4_2	0.1	0.596	0.214	0.343	0.577	1	-0.0192	-0.000672	-0.0242	0.0474	0.0217	-0.0269	-0.075	-0.0262	-0.00523	0.245	0.0119
AXLE1_3	0.251	0.388	0.471	-0.0287	-0.026	-0.0192	1	0.309	0.18	-0.0136	-0.043	0.0455	0.0178	0.0291	0.0432	0.462	0.00707
AXLE2_3	0.517	0.516	0.771	-0.0289	-0.0122	-0.000672	0.309	1	0.587	0.371	0.00266	0.0279	-0.0532	-0.00458	0.0145	0.751	0.00952
AXLE3_3	0.568	0.433	0.736	-0.00363	-0.0187	-0.0242	0.18	0.587	1	0.577	-0.0171	-0.00527	-0.0527	-0.033	-0.0121	0.726	-0.025
AXLE4_3	0.508	0.336	0.577	0.0552	0.0228	0.0474	-0.0136	0.371	0.577	1	0.00696	-0.0405	-0.0523	-0.0422	-0.0403	0.581	0.00976
AXLE1_4	0.501	0.0319	0.0874	-0.0202	-0.0255	0.0217	-0.043	0.00266	-0.0171	0.00696	1	0.327	0.0182	0.0411	0.0235	0.0996	-0.0538
AXLE2_4	0.514	0.0328	0.0643	0.00827	0.00133	-0.0269	0.0455	0.0279	-0.00527	-0.0405	0.327	1	-0.00736	-0.0155	-0.0224	0.0714	0.0214
wc	0.0229	0.00619	0.0242	-0.0453	-0.0386	-0.075	0.0178	-0.0532	-0.0527	-0.0523	0.0182	-0.00736	1	0.218	0.167	0.0137	0.0146
fc	-0.00189	0.0128	0.00862	-0.0278	0.00681	-0.0262	0.0291	-0.00458	-0.033	-0.0422	0.0411	-0.0155	0.218	1	0.859	-0.0132	0.0181
Ec	-0.00114	0.0257	0.0222	-0.00372	0.00876	-0.00523	0.0432	0.0145	-0.0121	-0.0403	0.0235	-0.0224	0.167	0.859	1	-0.00295	0.0312
u	0.758	0.826	0.998	0.129	0.213	0.245	0.462	0.751	0.726	0.581	0.0996	0.0714	0.0137	-0.0132	-0.00295	1	0.0145
AXLE1_2	-0.0153	0.0988	0.0129	0.366	0.249	0.0119	0.00707	0.00952	-0.025	0.00976	-0.0538	0.0214	0.0146	0.0181	0.0312	0.0145	1

More >>

Determinant 2.20092e-8

Figure E.6: Correlation Matrix of Empirical Normal distribution -of BN-II

F

Bending Moment Capacity

The calculation of the bending moment resistance MRd is discussed step by step. This methodology is taken from TU Delft reader *CIE3150/4160, Prestressed concrete* unless stated otherwise.

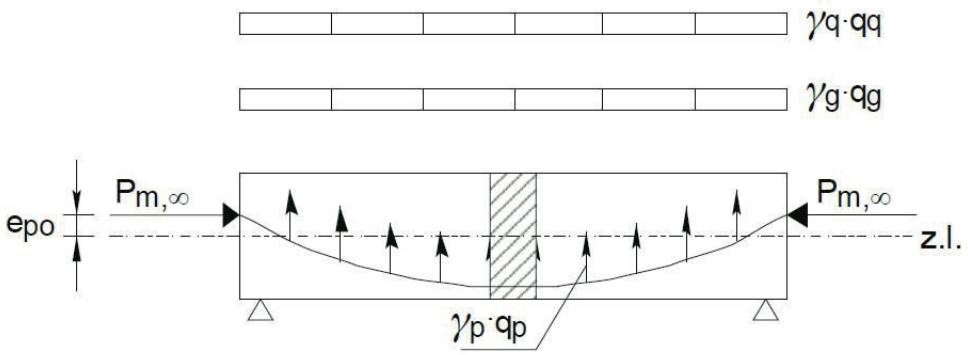

Figure F.1: (Beam subjected to permanent load, variable load and prestressing load

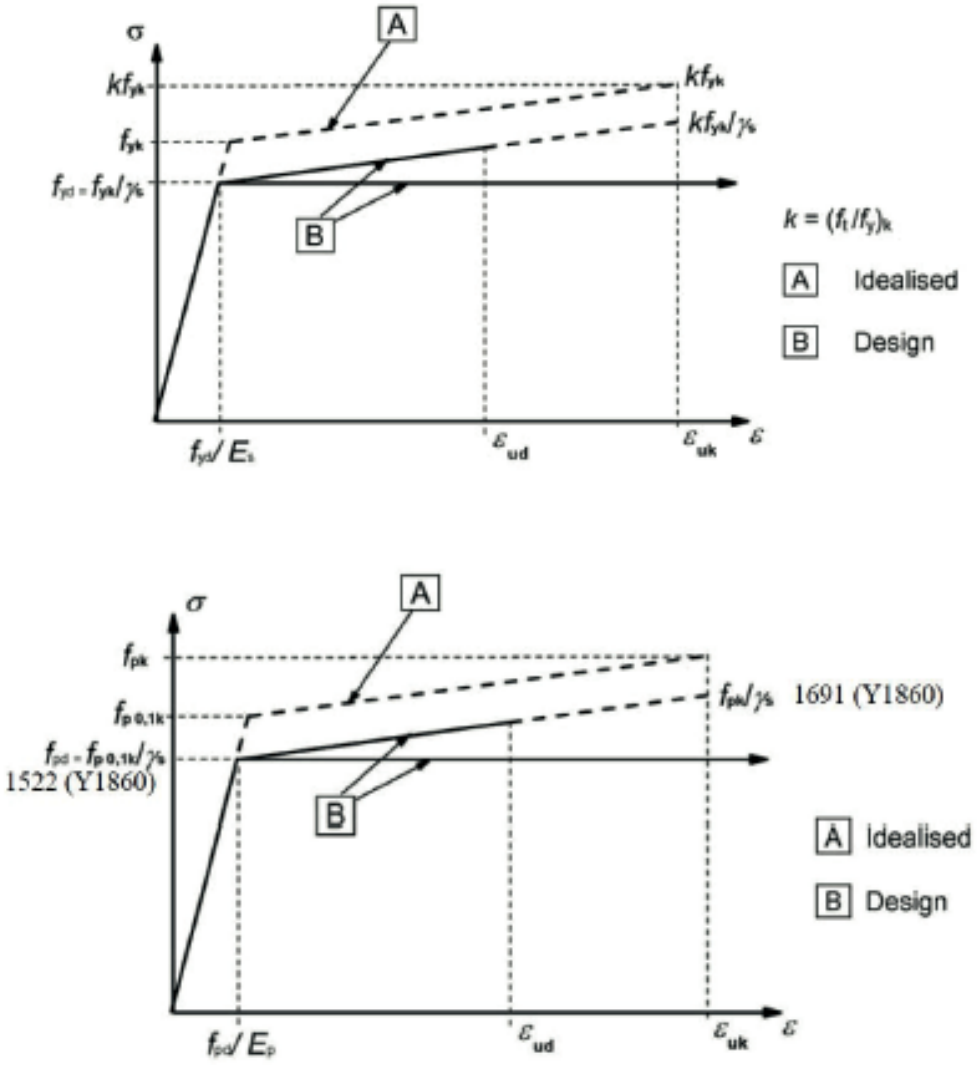

Figure F.2: (Top) Stress-strain relationship of reinforcing steel in ULS ; (Bottom) Stress-strain relationship of prestressing steel in ULS

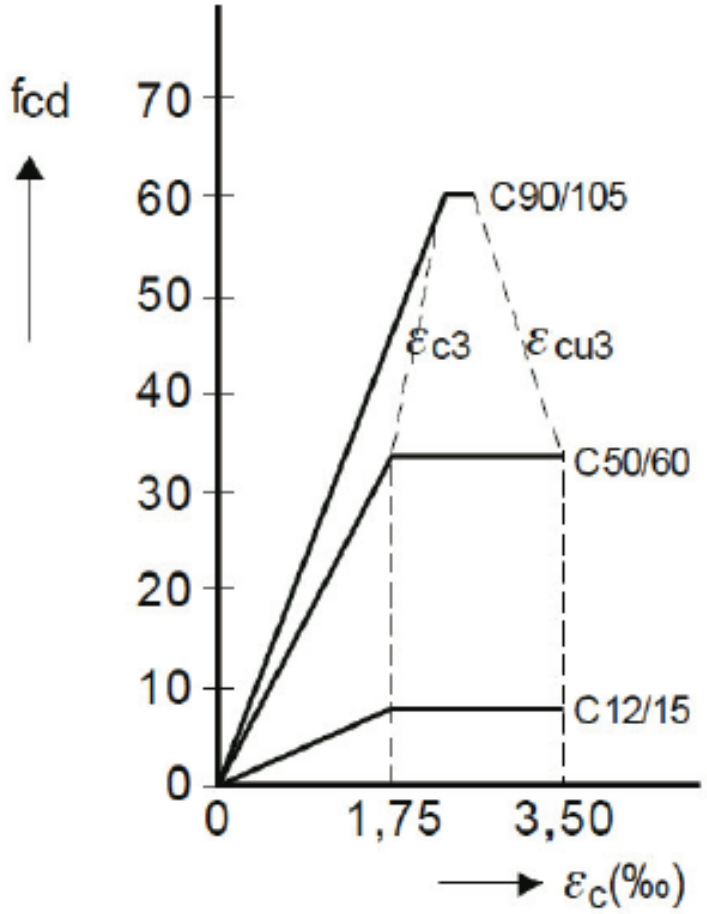

Figure F.3: Stress-strain relationship of concrete in compression in ULS

- First, the height of the compressive zone is estimated. For that purpose the compressive forces are determined. When the reinforcing steel yields (using the horizontal branch from Figure F.3 in the calculation), the total force in this steel is $Asfyd$.When the prestressing steel is in the plastic state (using the horizontal branch from Figure F.2), its total force is $Apfpd$. Since equilibrium of horizontal forces is required, it should hold (see Figure F.4):

$$N_c = P_{m,\infty} + \Delta N_p + N_s = A_p\sigma_{m/\infty} + A_p(f_p d - \sigma_{p,\infty} + A_s f_{yd} \quad \text{(F.1)}$$

$N_c = \alpha b x_u f_c d$in case of a rectangular compressive zone cross-section (F.2)

For a rectangular compressive zone cross-section, a concrete strength class < C50/60 , and a bi-linear stress-strain relationship (EN 1992-1-1 fig. 3.4) α= 0.75. From this first approximation the height xu of the compressive zone is obtained. In case of a rectangular concrete compressive zone cross-section it reads:

$$x_u = A_s f_{yd} + A_p(f_p d - \sigma_{p,\infty} + P_{m,\infty}/\alpha b f_{cd} \quad \text{(F.3)}$$

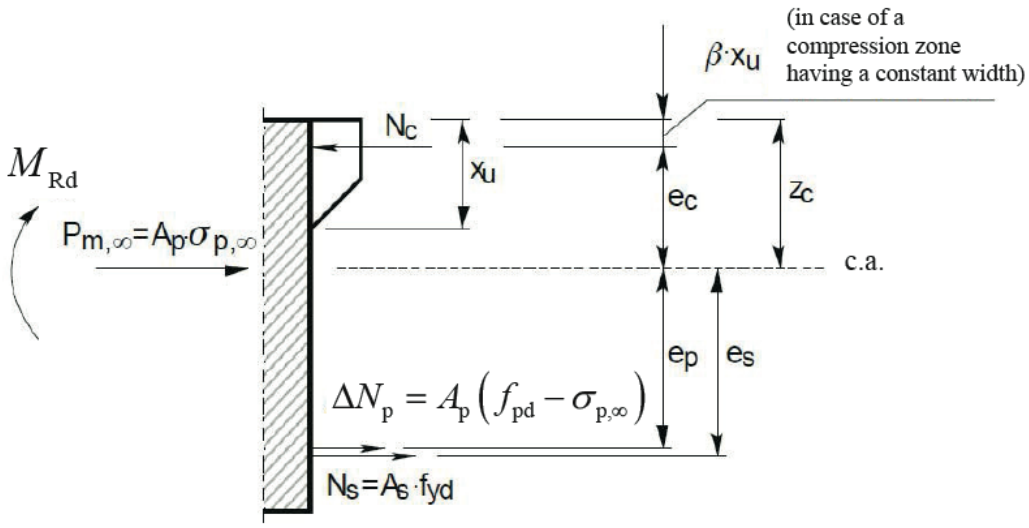

Figure F.4: Equilibrium between external and internal forces

- Check whether the height xu of the compressive zone meets the requirement with regard to the maximum height of the compressive zone according to the Dutch National Annex to EN 1992-1-1 cl. 5.5:

$$\delta = \frac{f}{500 + f} + \frac{x_u}{d} \text{for } f_{ck} \leq 50 N/mm2 \tag{F.4}$$

  and where δ is the ratio of the redistributed moment to the elastic bending moment (according to the linear theory of elasticity).

- With the obtained height xu of the compressive zone, the concrete and prestressing steel strains can be determined (Figure F.5).

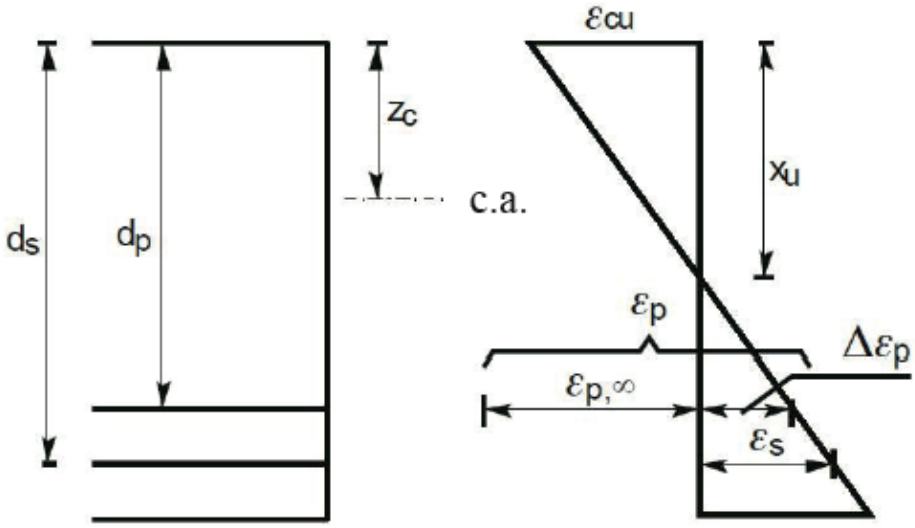

Figure F.5: Determination of the strains in concrete and prestressing steel for a certain height of the compressive zone x_u

The strain ϵ_s in the reinforcing steel follows from:

$$\frac{\epsilon_{cu}}{x_u} = \frac{\epsilon_{cu} + \epsilon_s}{d_s} \tag{F.5}$$

The increase of the strain in the prestressing steel n be determined in a similar way:

$$\frac{\epsilon_{cu}}{x_u} = \frac{\epsilon_{cu} + \Delta\epsilon_p}{d_p} \tag{F.6}$$

The total strain in the prestressing steel is $\epsilon_p = \epsilon_{p,\infty} + \Delta\epsilon_p$

- With these strains ϵ_s and $\Delta\epsilon_p$ the stresses in the reinforcing and prestressing steel σ_{su} and σ_{pu}can be calculated. From these strains the force in the reinforcing steel and the increase of the force in the prestressing steel are obtained:

$$N = N_s + \Delta N_p \tag{F.7}$$

- Next it should be checked whether the following condition is satisfied:

$$N + P_{m,\infty} = N_c (= \alpha b x_u f_c d) \tag{F.8}$$

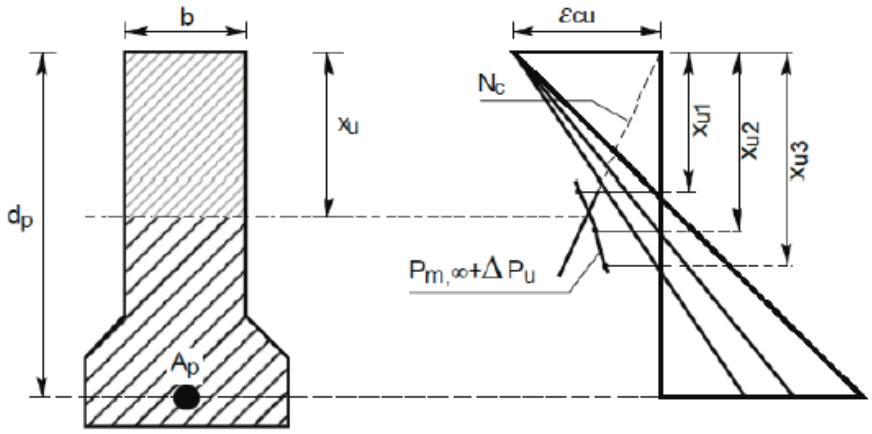

Figure F.6: Graphical representation of the iteration process for the determination of the height of the concrete compressive zone x_u

Figure F shows a graphical representation of the iteration process. For the first assumed compressive zone height xu, the magnitude of the concrete compressive force Nc and the steel force $N + P_{m,\infty}$ are presented in horizontal direction, using the solid vertical line from the strain diagram as axis. If $N + P_{m,\infty}$ is larger than Nc, as is the case in the first iteration step shown in , the compression zone height is too small and the calculation has to be repeated using a larger xu. So, with graphical support as shown in the figure, the correct value for xu can be found for which axial equilibrium is satisfied.

- With the correct height xu of the concrete compressive zone, the magnitude of the bending moment resistance MRd can be determined. This follows from (also see Figure F.7

$$M_{Rd} = A_s \sigma_{su}(d_s - y) + A_p(\sigma_{pu} - \sigma_{p,\infty})(d_p - y) + P_{m,\infty}(z_c - y) \tag{F.9}$$

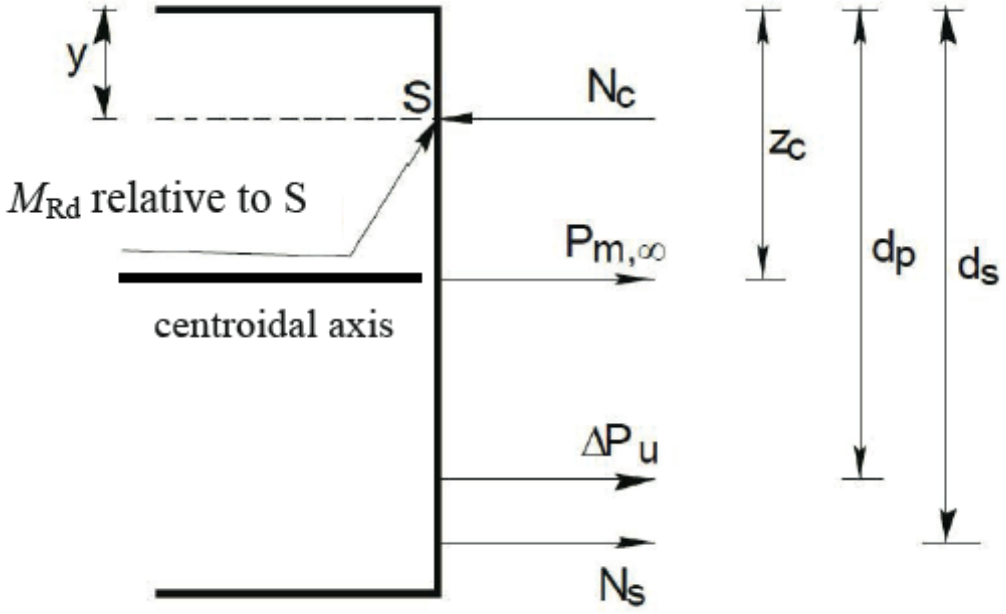

Figure F.7: Determination of the bending moment resistance M_{Rd}

The calculation performed in this thesis is as follows:

Centroid from middle of bottom edge $x_{centroid} := 0.0094m$ $y_{centroid} := 1.3149m$

Depth of beam $d_{beam} := 2.4m$

Concrete C25 $A_c := 3.4m^2$ $f_c := f_c MPa$

Prestressing steel Y1860S7 $f_{cd} := \frac{f_c}{1.5}$

$E_p := 195 \cdot 10^3 MPa$

$\sigma_{pinf} := 1080MPa$

Area of 1 bar $A_{p1} := 140mm^2$

Number of wires in 1 tendon $n := 1$

Number of tendons in beam $n_{tendon} := 80$

Area of prestressing steel $A_p := A_{p1} \cdot n \cdot n_{tendon}$

$A_p = 0.011\ m^2$

$f_{pk} := \frac{1860}{1.1} MPa = 1.691 \times 10^9\ Pa$

$\Delta N_p := A_p \cdot \left(0.95 \cdot \frac{1860}{1.1} MPa - \sigma_{pinf} \right) = 5.895 \times 10^6 N$

$P_{minf} := \sigma_{pinf} \cdot A_p = 1.21 \times 10^7 N$

Reinforcing steel Area of 1 steel bar $A_{s1} := 200mm^2$

number of steel bars $n_s := 44$

Total area of steel $A_s := n_s \cdot A_{s1} = 8.8 \times 10^{-3} m^2$

$E_s := 200 \cdot 10^3 MPa$

$f_{yd} := 435MPa$

Geometry

width of top flange $b := 6.9m$

height of top flange $h_{fl} := 0.25m$

Total width of web $b_{web} := 0.4m$

Calculating concrete compression zone using rectangular stress block:

$$x_u := \frac{A_s \cdot f_{yd} + A_p \cdot 0.95 \cdot \frac{f_{pk}}{1.1}}{\alpha \cdot b \cdot f_{cd}}$$

$x_u < h_{fl}$ Yes

Hence, on computing moment equilibrium at the bottom of the beam cross cross section:

$$M_{Rd} := P_{minf} \cdot (y_{centroid}) - x_u \cdot b \cdot f_{cd} \cdot \left(d_{beam} - \frac{x_u}{2} \right) + \Delta N_p \cdot (0.08m) + A_s \cdot f_{yd} \cdot (0.08m)$$

Given, the uncertainty in fc, the distribution of Xu and then Mrd can be computed

Bibliography

[1] Code Committee 351001. Assessement of structural safety of an existing structure at repair or unfit for use–basic requirements, nen 8700: 2011 (in dutch), 2011.

[2] LRFD Aashto. Bridge design specifications, 1998.

[3] T AASHTO. 307 (2003) determining the resilient modulus of soils and aggregate materials. *American Association of State Highway and Transportation Officials, Washington, DC*, 2003.

[4] Karim T Abou-Moustafa, Fernando De La Torre, and Frank P Ferrie. Designing a metric for the difference between gaussian densities. In *Brain, Body and Machine*, pages 57–70. Springer, 2010.

[5] W Aspinall. Expert judgment elicitation using the classical model and excalibur. *Seventh Session of the Statistics and Risk Assessment Section's International Expert Advisory Group on Risk Modeling: Iterative Risk Assessment Processes for Policy Development Under Conditions of Uncertainty I Emerging Infectious Diseases: Round IV*, pages 1–22, 2008.

[6] Georgios Balomenos. Probabilistic finite element analysis of structures using the multiplicative dimensional reduction method. 2015.

[7] Paul J Barr, Marc O Eberhard, and John F Stanton. Live-load distribution factors in prestressed concrete girder bridges. *Journal of Bridge Engineering*, 6(5):298–306, 2001.

[8] Paul Beverly. *fib model code for concrete structures 2010*. Ernst & Sohn, 2013.

[9] R Michael Biggs, Furman W Barton, Jose P Gomez, Peter J Massarelli, and Wallace T McKeel Jr. Finite element modeling and analysis of reinforced-concrete bridge decks. Technical report, 2000.

[10] Thomas Braml, Alexander Taffe, Sascha Feistkorn, and Otto Wurzer. Assessment of existing structures using probabilistic analysis methods in combination with nondestructive testing methods. *Structural Engineering International*, 23(4):376–385, 2013.

[11] Sustainable Bridges. URL `http://www.sustainablebridges.net/`.

[12] Daniel Cantero, Eugene J OBrien, Arturo González, Bernard Enright, and Cillian Rowley. Highway bridge assessment for dynamic interaction with critical vehicles. 2009.

[13] Daniel Cantero, Therese Arvidsson, Eugene OBrien, and Raid Karoumi. Train–track–bridge modelling and review of parameters. *Structure and Infrastructure Engineering*, 12(9):1051–1064, 2016.

[14] JR Casas, DF Wisniewski, J Cervenka, and M Plos. Safety and probabilistic modelling: background document d4. 4. *Sustainable Bridges–VI Framework Program: Brussels, Belgium*, 2007.

[15] Robby Caspeele. From quality control to structural reliability: where bayesian statistics meets risk analysis. *Heron*, 59(2-3):79–100, 2014.

[16] CHBDC. Canadian highway bridge design code, can/csa-s6-00, 2000.

[17] Robert T Clemen and Robert L Winkler. Combining probability distributions from experts in risk analysis. *Risk analysis*, 19(2):187–203, 1999.

[18] Abigail R Colson and Roger M Cooke. Cross validation for the classical model of structured expert judgment. *Reliability Engineering & System Safety*, 163:109–120, 2017.

[19] Nuclear Regulatory Commission et al. Reactor safety study. an assessment of accident risks in us commercial nuclear power plants. appendices iii and iv. Technical report, Nuclear Regulatory Commission, 1975.

[20] Goossens L.H.J. Cooke, R.M. Procedures guide for structured expert judgement, 2000.

[21] R. M. Cooke. *Experts in uncertainty: Opinion and subjective probability in science*. 1991.

[22] Roger M Cooke and Louis HJ Goossens. Expert judgement elicitation for risk assessments of critical infrastructures. *Journal of risk research*, 7(6):643–656, 2004.

[23] Ove Ditlevsen and Henrik O Madsen. *Structural reliability methods*, volume 178. Wiley New York, 1996.

[24] Justin W Eggstaff, Thomas A Mazzuchi, and Shahram Sarkani. The effect of the number of seed variables on the performance of cooke′ s classical model. *Reliability Engineering & System Safety*, 121:72–82, 2014.

[25] I Enevoldsen, M Sloth, and J Lauridsen. Danish guideline for probability based assessment of bridges. *Proc. IABMAS'04*, 2004.

[26] Morten Engen, Max AN Hendriks, Jochen Köhler, Jan Arve Øverli, and Erik Åldstedt. A quantification of the modelling uncertainty of non-linear finite element analyses of large concrete structures. *Structural Safety*, 64:1–8, 2017.

[27] CEN (European Committee for Standardization). Basis of structural design, 2002.

[28] DP Geoffrey McLachlan. Finite mixture models hoboken, 2000.

[29] Arturo Gonzalez. Development of a bridge weigh-in-motion system. *Korean Society of Civil Engineers*, 62(1):91–91, 2014.

[30] LHJ Goossens and GN Kelly. Expert judgement and accident consequence uncertainty analysis (cosyma), 2000.

[31] Louis HJ Goossens, RM Cooke, Andrew R Hale, and Lj Rodić-Wiersma. Fifteen years of expert judgement at tudelft. *Safety Science*, 46(2):234–244, 2008.

[32] Edmund C Hambly. *Bridge deck behaviour*. CRC Press, 2014.

[33] Anca Hanea, Oswaldo Morales Napoles, and Dan Ababei. Non-parametric bayesian networks: Improving theory and reviewing applications. *Reliability Engineering & System Safety*, 144:265–284, 2015.

[34] Anca M Hanea, Dorota Kurowicka, and Roger M Cooke. Hybrid method for quantifying and analyzing bayesian belief nets. *Quality and Reliability Engineering International*, 22(6):709–729, 2006.

[35] Terje Haukaas and Armen Der Kiureghian. *Finite element reliability and sensitivity methods for performance-based earthquake engineering*. Number 14. Pacific Earthquake Engineering Research Center, College of Engineering, University of California, Berkeley, 2004.

[36] Terje Haukaas and Armen Der Kiureghian. Strategies for finding the design point in non-linear finite element reliability analysis. *Probabilistic Engineering Mechanics*, 21(2):133–147, 2006.

[37] Terje Haukaas and Armen Der Kiureghian. Methods and object-oriented software for fe reliability and sensitivity analysis with application to a bridge structure. *Journal of Computing in Civil Engineering*, 21(3):151–163, 2007.

[38] K Henchi, M Fafard, M Talbot, and G Dhatt. An efficient algorithm for dynamic analysis of bridges under moving vehicles using a coupled modal and physical components approach. *Journal of sound and Vibration*, 212(4):663–683, 1998.

[39] Hibbett, Karlsson, and Sorensen. *ABAQUS/standard: User's Manual*, volume 1. Hibbitt, Karlsson & Sorensen, 1998.

[40] Christopher Higgins, Theresa K Daniels, David V Rosowsky, Thomas H Miller, and Solomon C Yim. Assessment and risk ranking of conventionally reinforced concrete bridges for shear. *Transportation research record*, 1928(1):110–117, 2005.

[41] Robin M Hogarth. *Judgement and choice: The psychology of decision*. Number Sirsi) i9780471914792. 1987.

[42] http://www.lighttwist.net/wp/uninet. Uninet « lighttwist software – cutting edge scientific software.

[43] British Standards Institution. *Eurocode 1: Actions on Structures. Traffic Loads on Bridges*. BSI, 2004.

[44] JCSS JCSS. Probabilistic model code. *Joint Committee on Structural Safety*, 2001.

[45] Uwe Jensen. Probabilistic risk analysis: foundations and methods, 2002.

[46] Jong-Su Jeon, Abdollah Shafieezadeh, Do Hyung Lee, Eunsoo Choi, and Reginald DesRoches. Damage assessment of older highway bridges subjected to three-dimensional ground motions: characterization of shear–axial force interaction on seismic fragilities. *Engineering Structures*, 87: 47–57, 2015.

[47] H Joe. Dependence modeling with copulas, chapman hall, crc. *Published June/July*, 2014.

[48] Poul Henning Kirkegaard, Søren RK Nielsen, and Ib Enevoldsen. Heavy vehicles on minor highway bridges: dynamic modelling of vehicles and bridges. 1997.

[49] Eva OL Lantsoght, Cor van der Veen, Ane de Boer, and Joost Walraven. Proposal for the extension of the eurocode shear formula for one-way slabs under concentrated loads. *Engineering Structures*, 95:16–24, 2015.

[50] Eva OL Lantsoght, Cor van der Veen, Ane de Boer, and Dick A Hordijk. Probabilistic prediction of the failure mode of the ruytenschildt bridge. *Engineering Structures*, 127:549–558, 2016.

[51] Georgios Leontaris and Oswaldo Morales-Nápoles. Anduril—a matlab toolbox for analysis and decisions with uncertainty: Learning from expert judgments. *SoftwareX*, 7:313–317, 2018.

[52] E Lightfoot and F Sawko. Structural frame analysis by electronic computer: grid frameworks resolved by generalized slope deflection. *Engineering*, 187(1):18–20, 1959.

[53] Miguel Angel Mendoza Lugo. Reliability analysis in reinforced concrete vehicle bridges columns using nonparemetric bayesian networks, case study, 2017.

[54] Larry W Mays. *Hydraulic design handbook*. McGraw-Hill Professional Publishing, 1999.

[55] Sher Ali Mirza, James G MacGregor, and Michael Hatzinikolas. Statistical descriptions of strength of concrete. *Journal of the Structural Division*, 105(6):1021–1037, 1979.

[56] O Morales, Dorota Kurowicka, and A Roelen. Eliciting conditional and unconditional rank correlations from conditional probabilities. *Reliability Engineering & System Safety*, 93(5):699–710, 2008.

[57] O Morales-Nápoles and DTH Worm. Hypothesis testing of multidimensional probability distributions. *WP4 GAMES2R TNO Report*, (0100003764), 2013.

[58] O Morales-Nápoles, AM Hanea, and DTH Worm. Experimental results about the assessments of conditional rank correlations by experts: Example with air pollution estimates. In *ESREL 2013: Proceedings of the 22nd European Safety and Reliability Conference" Safety, Reliability and Risk Analysis: Beyond the Horizon", Amsterdam, The Netherlands, 29 september-2 oktober 2013*. CRC Press/Balkema-Taylor & Francis Group, 2013.

[59] Oswaldo Morales-Nápoles. Calibration and combination of experts' dependence estimates. *Manuscript submitted for publication*.

[60] Oswaldo Morales-Nápoles and Raphaël DJM Steenbergen. Analysis of axle and vehicle load properties through bayesian networks based on weigh-in-motion data. *Reliability Engineering & System Safety*, 125:153–164, 2014.

[61] Oswaldo Morales-Nápoles, David Joaquín Delgado-Hernández, David De-León-Escobedo, and Juan Carlos Arteaga-Arcos. A continuous bayesian network for earth dams' risk assessment: methodology and quantification. *Structure and Infrastructure Engineering*, 10(5):589–603, 2014.

[62] M Granger Morgan and M Henrion. Uncertainty: a guide to dealing with uncertainty in quantitative risk and policy analysis cambridge university press. *New York, New York, USA*, 1990.

[63] Aurelio Muttoni and Miguel Fernández Ruiz. The levels-of-approximation approach in mc 2010: application to punching shear provisions. *Structural Concrete*, 13(1):32–41, 2012.

[64] NKB. Structure for building regulations, 1978.

[65] Andrzej S Nowak and Maria M Szerszen. Bridge load and resistance models. *Engineering structures*, 20(11):985–990, 1998.

[66] Transportation Officials. *AASHTO LRFD Bridge Design Specifications: Customary US Units*. American Association of State highway and transportation officials, 1994.

[67] M Olsson. Finite element, modal co-ordinate analysis of structures subjected to moving loads. *Journal of Sound and Vibration*, 99(1):1–12, 1985.

[68] Fumika Ouchi. A literature review on the use of expert opinion in probabilistic risk analysis. 2004.

[69] Keogh DamienL O'Brien EugeneJ. Bridge deck analysis. *E & FN Spon*, 1999.

[70] Judea Pearl. *Probabilistic reasoning in intelligent systems: networks of plausible inference*. Elsevier, 2014.

[71] Mário Pimentel, Eugen Brühwiler, and Joaquim Figueiras. Safety examination of existing concrete structures using the global resistance safety factor concept. *Engineering Structures*, 70:130–143, 2014.

[72] G. James E. Bruwhiler A. Herwig F. Carlsson R. Karoumi, A. Liljencranz. Loads and dynamic effects: background document d4. 3. *Sustainable Bridges–VI Framework Program: Brussels, Belgium*, 2007.

[73] Rüdiger Rackwitz. Predictive distribution of strength under control. *Matériaux et Construction*, 16 (4):259–267, 1983.

[74] SB-LRA. Guideline for load and resistance assessment of existing european railway bridges, 2007.

[75] Hendrik Schlune, Mario Plos, and Kent Gylltoft. Safety formats for nonlinear analysis tested on concrete beams subjected to shear forces and bending moments. *Engineering structures*, 33(8): 2350–2356, 2011.

[76] Raphael DJM Steenbergen and ACWM Vrouwenvelder. Safety philosophy for existing structures and partial factors for traffic loads on bridges. *Heron, 55 (2), 2010*, 2010.

[77] RDJM Steenbergen, Ane De Boer, and Cornelis Van Der Veen. Safety assessment of existing concrete slab bridges for shear capacity. *Proceedings of Applications of Statistics and Probability in Civil Engineering*, 2011.

[78] George Stefanou. The stochastic finite element method: past, present and future. *Computer Methods in Applied Mechanics and Engineering*, 198(9-12):1031–1051, 2009.

[79] O Tugrul Turan, Christopher Higgins, and David V Rosowsky. Statistical modeling of coupled shear-moment resistance for rc bridge girders. *Journal of Bridge Engineering*, 13(4):351–361, 2008.

[80] ACWM Vrouwenvelder. Developments towards full probabilistic design codes. *Structural safety*, 24(2-4):417–432, 2002.

[81] Christoph Werner, Tim Bedford, Roger M Cooke, Anca M Hanea, and Oswaldo Morales-Nápoles. Expert judgement for dependence in probabilistic modelling: a systematic literature review and future research directions. *European Journal of Operational Research*, 258(3):801–819, 2017.

[82] Christoph Werner, Tim Bedford, and John Quigley. Sequential refined partitioning for probabilistic dependence assessment. *Risk Analysis*, 2018.

[83] Robert West. C&ca/ciria-recommendations on the use of grillage analysis for slab and pseudo-slab bridge decks. 1973.

[84] Dawid F Wiśniewski, Paulo JS Cruz, A Abel R Henriques, and Rui AD Simões. Probabilistic models for mechanical properties of concrete, reinforcing steel and pre-stressing steel. *Structure and Infrastructure Engineering*, 8(2):111–123, 2012.

[85] XQ Zhu and SS Law. Dynamic load on continuous multi-lane bridge deck from moving vehicles. *Journal of Sound and Vibration*, 251(4):697–716, 2002.